EVOLUTION OF THE TETHYAN SEAWAY DURING THE OLIGOCENE AND MIOCENE: CONSTRAINTS FROM FORAMINIFERAL FAUNAS OF THE QOM FORMATION, IRAN

Dissertation zur Erlangung des Doktorgrades
an der

Fakultät für Mathematik, Informatik und Naturwissenschaften
Fachbereich Geowissenschaften
der Universität Hamburg

vorgelegt von

Fatemeh Dabaghi Sadr
aus dem Iran

Hamburg
2017

University of Hamburg
Department of Earth Sciences
PhD thesis
Supervisor: Prof. Dr. Gerhard Schmiedl

Eidesstattliche Versicherung
Declaration on oath

Hiermit erkläre ich an Eides statt, dass ich die vorliegende Dissertationsschrift selbst verfasst und keine anderen als die angegebenen Quellen und Hilfsmittel benutzt habe.

> *I hereby declare, on oath, that I have written the present dissertation by my own and have not used other than the acknowledged resources and aids.*

Hamburg,

KURZFASSUNG

Der Übergang vom Treibhaus- zum Eishausklima im Känozoikum ging mit paläogeographischen Veränderungen im Bereich der Tethys einher. Durch die Schließung des Tethys-Korridors mit seinen Meeresverbindungen im Iran während des späten Paläogen und frühen Neogen, zwischen etwa 28 und 18 Millionen Jahren vor heute, wurde der latitudinale Wassermassen- und Wärmeaustausch eingeschränkt. Dieser Prozess ist in Sedimentabfolgen der Qom-Formation im Iran dokumentiert. Die räumliche und zeitliche Variabilität der Sedimentationsprozesse während der Bildung der Qom-Formation ist allerdings noch weitgehend unverstanden. Entsprechend wenige Informationen existieren über die regionale Meeresspiegelentwicklung und den Einfluss von tektonischen Prozessen und Klimaveränderungen auf die marinen Ökosysteme und Ablagerungsräume im Iran. Die vorliegende Doktorarbeit befasst sich mit der Lithostratigraphie, Biostratigraphie, Paläoökologie und Paläoumwelt-Entwicklung der Iranischen Meeresverbindungen während des späten Oligozän und frühen Miozän. Hierzu wurde die Foraminiferenfauna und Karbonatfazies an ausgewählten Sedimentabfolgen des Qom-Beckens untersucht. Die Qom-Formation wurde während des Oligozän und Miozän in einem Backarc-Becken im zentralen Iran abgelagert. Die faunistischen und sedimentologischen Untersuchungen wurden an insgesamt 191 Proben aus zwei repräsentativen Abfolgen der Qom-Formation durchgeführt. Das Molkabad-Profil liegt nordwestlich des Molkabad-Gebirges und südwestlich von Garmsar. Die 760 m mächtige Sedimentabfolge besteht aus Kalksteinen, Kalk-Mergeln und Gips-führenden Mergeln. Die Molkabad-Abfolge liegt diskordant über Sedimenten des Eozän und besteht aus folgenden lithostratigraphischen Einheiten (vom Liegenden zum Hangenden): Lithothamnium-Kalkstein, Unterer Mergel-Kalkstein, Bryozoen-Kalkstein und Obere Mergel-Gruppe. Die Molkabad-Störung trennt die Qom-Formation von den überlagernden Sedimenten der „Oberen Rot-Formation". Die zweite untersuchte Sedimentabfolge liegt im Bereich der Navab-Antikline. Die Sedimentabfolge der Navab-Antikline besteht überwiegend aus Kalksteinen, Mergeln und Gipslagen mit einer Gesamtmächtigkeit von 318 m. Die Sedimente überlagern diskordant Sedimente des Eozän. Ökologische Informationen rezenter Foraminiferen-Faunen des Persischen Golfes wurden genutzt um Änderungen in der Wassertiefe und im Salzgehalt während der Ablagerung der Qom-Formation abzuschätzen. Aufbauend auf diesen Daten konnten glazioeustatische Signale von regionalen tektonischen Ereignissen getrennt werden. Diese Daten tragen dazu bei, die Auswirkungen der Schließung des Tethys-Korridors auf die großräumige Paläozeanographie und Paläoklima des Känozoikums besser zu verstehen.

ABSTRACT

The Cenozoic climate transition from greenhouse to icehouse conditions was associated with major paleogeographic changes in the Tethyan realm. The closure of the Tethyan Seaway and its Iranian gateways during the terminal Paleogene and early Neogene, between approximately 28 and 18 million years, influenced the latitudinal exchange of water masses and energy and is documented in sediment successions of the Qom formation in central Iran. Little is known on the spatial expression and the exact depositional histories of the Qom Formation on orbital time-scales, including a lack of quantitative sea-level reconstructions and studies on the impact of climatic and tectonic changes on marine ecosystems and sedimentation processes. The PhD project focuses on the investigation of lithostratigraphy, biostratigraphy, paleoecology and paleoenvironmental evolution of the Iranian gateways based on late Oligocene to early Miocene foraminiferal faunas and carbonate facies from selected sediment sections of the Qom Basin. The Qom Formation was deposited in the Central Iranian back-arc basin during the Oligocene-Miocene. In this study foraminiferal faunas and carbonate microfacies were studied based on a total of 191 samples from two sections of the Qom Formation. One of them is the Molkabad section, which is located northwest of the Molkabad Mountains, southeast of Garmsar. The section mainly consists of limestones, calcareous marls, and gypsum-bearing marls with a total thickness of 760 meters. The Qom Formation at Molkabad section overlies Eocene rocks with an unconformity and consists of the following lithostratigraphic units (from the lower to upper part): Lithothamnium Limestone, Lower Marl Limestone, Bryozoa Limestone, and Upper Marl Group. The Molkabad fault separates the Qom Formation from the overlying Upper Red Formation. The other section is located at Navab anticline. The section mainly consists of limestones, marls, and gypsum with a total thickness of 318 meters. The Navab anticline section overlies Eocene rocks with an unconformity. In a novel approach, ecological information from recent faunas of the Persian Gulf were applied to the assessment of changes in paleo-water depth and paleo-salinity. Based on these data, global glacio-eustatic signals will be separated from regional tectonic events. This information can be used to better assess potential impacts of the closure of the Tethyan Seaway on Cenozoic paleooceanography and paleoclimate.

TABLE OF CONTENTS

1 CHAPTER: INTRODUCTION

1.1 GENERAL INTRODUCTION

The Cenozoic era experienced the transition from “greenhouse” to “icehouse” conditions,

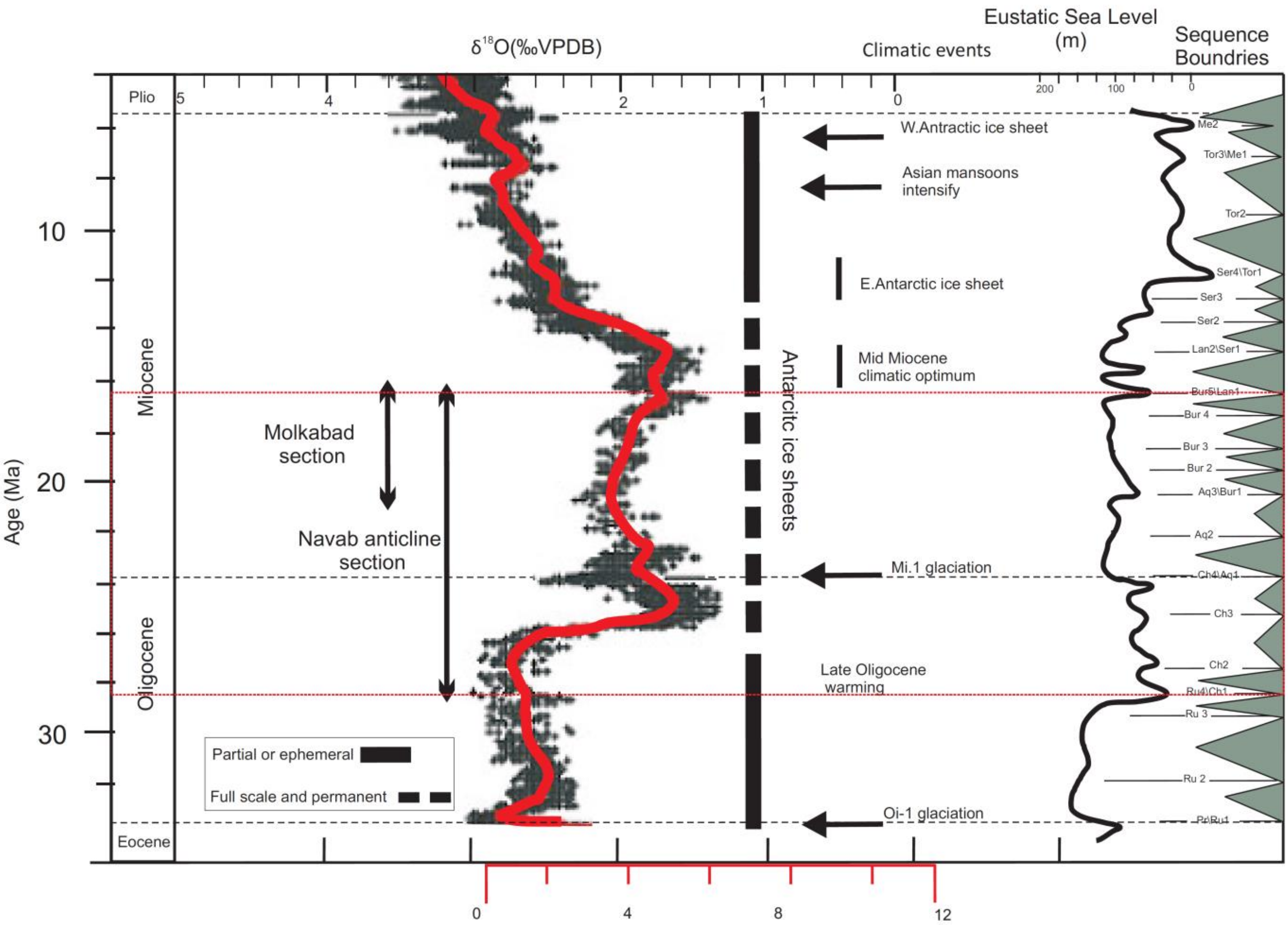

Figure 1.1: Climate record for the past 65-milion years as reflected by a stacked deep-sea benthic foraminiferal stable isotope record (after Zachos *et al.* 2001a, 2008). The Qom formation was deposited during the late Oligocene through early Miocene, following the first major expansion of Antarctic ice sheets. The isotope record during this time interval reflects both changes in temperature and ice volume.

including various transient climatic events that have been accompanied by the expansion of Antarctic ice sheets and a global sea-level decline (Haq *et al.*, 1987, Zachos *et al.*, 2001a, 2008, Miller *et al.* 2005) (Fig. 1.1). This climate deterioration has been related to major paleogeographic changes, including the separation of Antarctica and the closure of the Tethyan Ocean, resulting in the reorganization of ocean circulation and heat transport. The first major cooling and ice-sheet expansion occurred at the Eocene-Oligocene boundary. Subsequently, the closure of the Tethyan Seaway occurred during the Oligocene and early Miocene, between approximately 28 and 18 million years, a time when Antarctica was either ice free or only partially glaciated (Zachos *et al.*, 2001a). These ice-sheet fluctuations resulted in pronounced glacio-eustatic sea-level changes in the order of several tens of meters (Abreu and Anderson 1998, Hardenbol *et al.* 1998, Miller *et al.* 2005). High-resolution deep sea benthic oxygen isotope records suggest a closer relation of these climate and glaciations changes to orbital forcing, including a transient glaciation at the Oligocene-Miocene boundary (Zachos *et al.*, 2001b). Evolution of the Tethyan realm at the late Paleogene and Neogene and its seaways to the Atlantic and Indian oceans is related with both tectonic and climatic

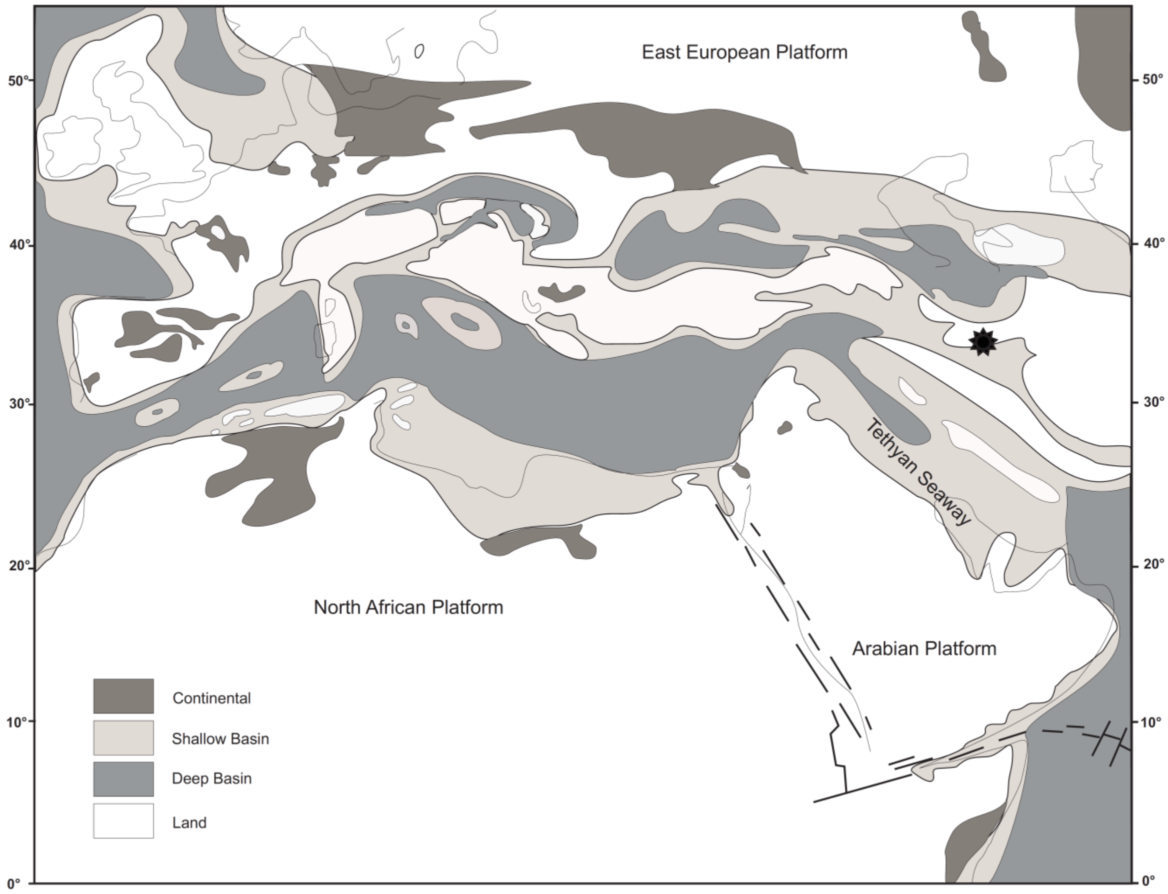

Figure. 1.2: Schematic paleogeographic map for the early Miocene (early Burdigalian), showing continental basins, shallow and deep marine basins and environments (from Meulenkamp and Sissingh 2003). The Asterisk indicates the position of the Qom Basin as part of the Iranian gateways.

changes. The northward drift and rotation of the Arabian Peninsula and African continent at the Eocene-Oligocene boundary derive in separation of the Tethys Ocean into the Mediterranean Sea and the Eurasian intercontinental Paratethys Basin, while the Tethyan Seaway continued until the early Neogene (Steininger and Wessely 2000) (Fig. 1.2).

The closure of the Tethyan Seaway is best documented in the Oligocene-Miocene Qom Formation that represented the last marine transgression in Central Iran and has been deposited on extensive mixed carbonate-siliciclastic ramps in the Central Esfehan-Sirjan Basin that are separated by an island arc complex (Reuter *et al.*, 2009) (Figs. 1.2, 1.3). The Esfehan-Sirjan Basin represents the for-arc, the Qom Basin the back-arc depositional environments. Furre and Soder (1955) established the type locality near the town of Qom and subdivided the Qom Formation deposits into six members, from bottom to top including a (basal limestone), b (sandy marls), c (alternating marls and limestone), d (evaporates), e (green marls) and f (top limestone).

The Qom Formation is up to 1.200 m thick and includes seven to nine stratigraphic sequences that can be related to the Ru 3 to Bur 2 third order sea-level fluctuations of Hardenbol *et al.*, (1998) (Reuter *et al.* 2009, Sabouhi *et al.*, 2010) (Fig. 1.4). During the so-called Terminal Tethyan Event, the Tethyan Seaway was closed due to the collision of the African/Arabian and Iranian/Eurasian plates. Facies analyses of sediments from Molkabad section and Navab anticline section indicate paleoenvironments ranging from terrestrial to open marine setting,

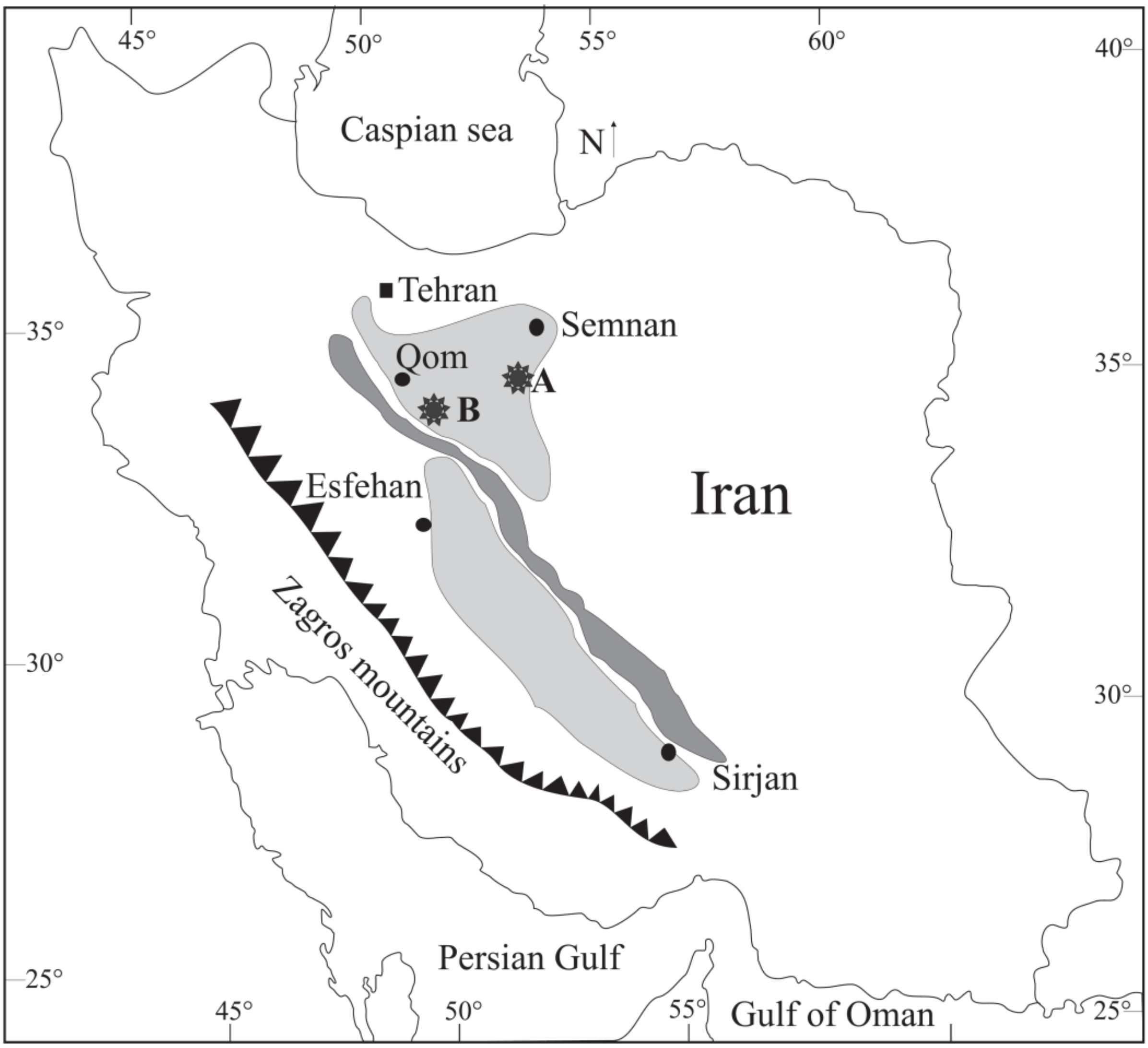

Figure 1.3: Overview map of Iran with location of the target sections (A) Navab anticline and (B) Molkabad sections. Location of the Qom and Esfehan-Sirjan basins with light gray, volcanic arc with dark gray is indicated according to the Reuter et al. (2009). The triangles line represents the Zagros thrust fault.

including tidal flat, semi-restricted lagoon, lagoon, patch reef and open marine environments.

The Qom Formation is one of the most important gas and oil reservoirs of Central Iran, analogous to the Asmari Formation of Southwest Iran (Vaziri-Moghaddam *et al.* 2006). Organic geochemical analysis indicated that the hydrocarbons migrated from deeper source rock, likely of Jurassic age (Sabouhi *et al.*, 2010). Marine sediments of the Qom Formation contain rich foraminiferal faunas that have not yet been studied in detail. In addition, little is known on the interplay between climate and regional tectonic changes on paleoenvironments and marine ecosystems of the Iranian gateways. Foraminifers are extensively used for biostratigraphy of marine sediments and in paleoenvironmental studies. Shallow water habitats can be influenced by gradients in light, temperature, salinity, substrate, as well as velocity and turbulence of surface waters currents (Culver *et al.*, 1996, Sen Gupta, 1999). Shallow-water faunas often present high foraminiferal numbers, variable diversity and are dominated by epifaunal and shallow infaunal taxa (Murray, 2006).

1.2 RESEARCH QUESTIONS AND OBJECTIVES

The overarching objective of this PhD thesis is the reconstruction of paleoenvironments in the Tethyan Seaway and its Iranian gateways during the late Oligocene and early Miocene. This objective will be pursued by quantitative evaluation of foraminiferal faunas and sediment facies of selected sediment successions from central Iran. In addition, ecological information from Recent faunas of the Persian Gulf will be applied to the assessment of paleo-water depth and paleo-salinities. These data will improve our knowledge of potential impacts of the closure of the Tethyan Seaway on late Paleogene to early Neogene ocean circulation and climate. The major scientific questions are:

How did the foraminiferal faunas change during deposition of the Qom Formation and do the faunas provide biostratigraphic and paleoenvironmental information?

Which factors controlled the environmental evolution of the Qom Basin during the closure of the Tethyan Seaway? Is it possible to quantify the relative sea-level history and to separate global from regional climatic and tectonic processes?

What controls the distribution of recent benthic foraminifers in shelf environments of the Persian Gulf and do these faunas represent modern equivalents for the Oligocene and Miocene faunas of the Qom Basin?

1.3 THESIS OUTLINE

The results of this thesis are presented in three topical chapters, which are briefly introduced below.

In chapter 2 based on field observation and foraminifera faunas. This chapter presents new information on the biostratigraphy and lithostratigraphy of the Oligocene-Miocene Qom Formation at the Molkabad and Navab anticline sections of Central Iran.

The Qom Formation at the Molkabad and Navab sections based on benthic foraminifera was studied in chapter 3 in order to determine its microfacies and depositional environment. Based on the faunal and sedimentological results, the paleoenvironmental evolution of the Oligocene-Miocene deposits of the Tethyan Seaway is evaluated in chapter 4.

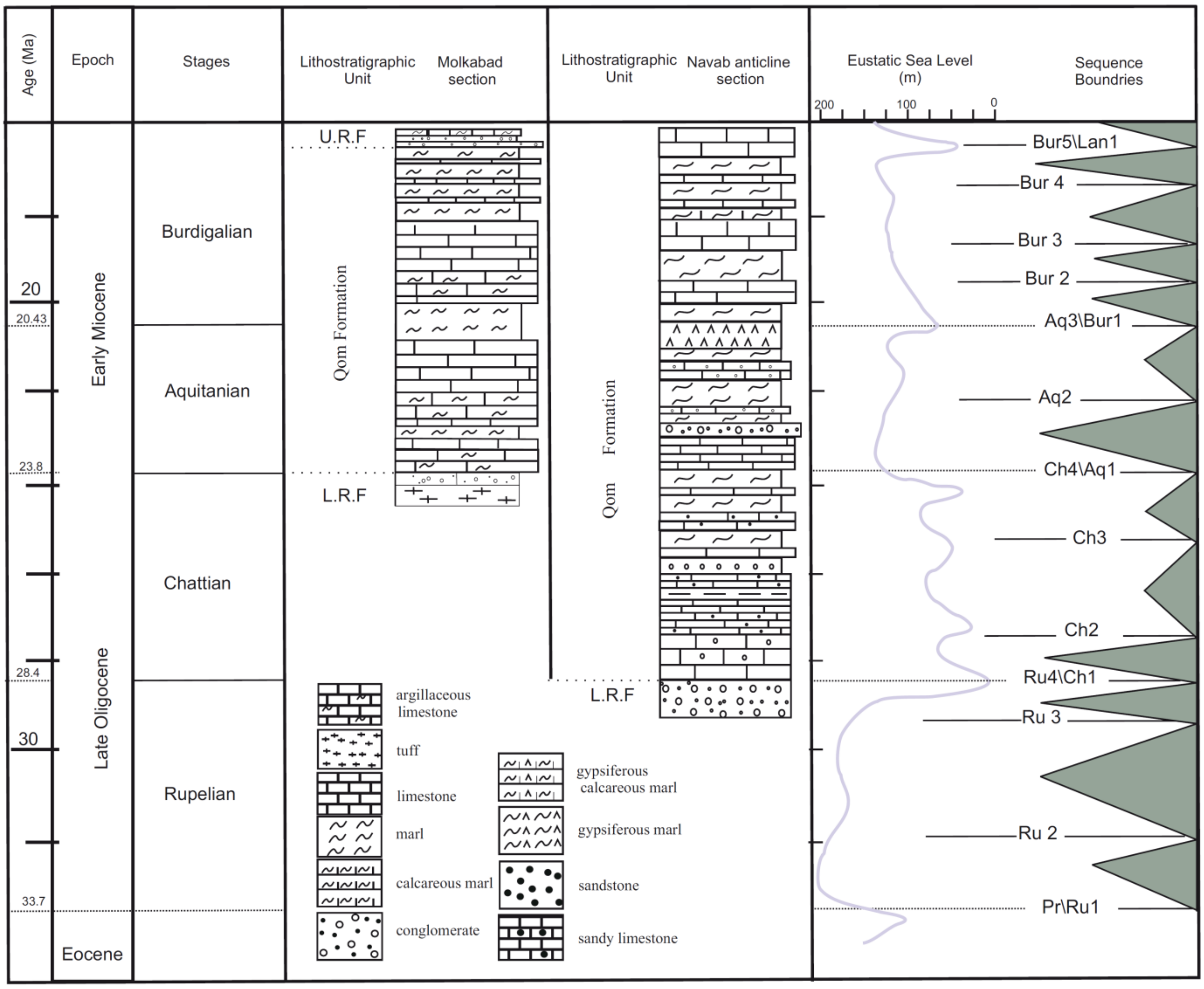

Figure. 1.4: Generalized lithology and sequence-stratigraphy concept of the Qom Formation in the Qom basin of central Iran (after Reuter et al., 2009). The inferred sediment sequences are correlated with global sea level curve of Hardenbol *et al.* (1998). L.R.F.= Lower Red Formation, U.R.F.= Upper Red Formation.

2 CHAPTER: LITHOSTRATIGRAPHY AND BIOSTRATIGRAPHY OF OLIGOCENE-MIOCENE DEPOSITS (QOM FORMATION) FROM CENTRAL IRAN

ABSTRACT

The Qom Formation was deposited in the central Iranian back-arc basin during the Oligocene-Miocene and documents the closure of the Tethyan Seaway. In this study, foraminiferal faunas were studied based on a total of 146 samples from the Molkabad section, which is located northwest of Molkabad Mountains, southeast of Garmsar, and the Navab Anticline section, which is located south of Kashan. The Molkabad section mainly consists of limestones, calcareous marls, and gypsum-bearing marls with a total thickness of 760 meters. The Navab anticline section with a total thickness of 318 meter consists of sandstones, red shales, gypsum-bearing marls and conglomerates. The Qom Formation at both sections overlies Eocene rocks with an unconformity. The studied sediments contain a variety of red algae, bryozoans, benthic and planktonic foraminifers. The distribution of index larger benthic foraminifers at the Molkabad section suggests an early Miocene (Aquitanian-Burdigalian) age, comprising the *Miolepidocyclina-Miogypsinoides* and *Borelis melo curdica-Meandropsina iranica-schlumbergerina* assemblage zones. At the Navab anticline section the distribution of the index larger benthic foraminifers indicates a late Oligocene (Chattian) to early Miocene (Aquitanian-Burdigalian) age. The biostratigraphic zonation is consistent with existing data from other sections of the Qom Formation and appears equivalent to biozones reported from the lower and upper parts of the Asmari Formation, which is deposited in the Zagros forland basin during the Oligocene-Miocene.

Key words: Biostratigraphy, Lithostratigraphy, Benthic Foraminifera, Qom Formation, Central Iran.

2.1 INTRODUCTION

The Qom Formation comprises Oligocene to Miocene marine marlstones and limestones with gypsum and silisiclastic rocks and is an important gas reservoir. Due to strong facies changes of the Qom Formation, no type section was introduced for it until now, but the Qom area has been introduced as its type area (Rahimzadeh 1994; Aghanabati 2004; Mohammadi 2011). Geological studies and analyses started firstly with the work of Loftus (1855). The Qom Formation was deposited disconformably on top of the gypsiferous and evaporitic red beds (Lower Red Formation) and is overlain disconformably by evaporitic red beds of Middle-Late Miocene age (Upper Red Formation). Rahaghi (1973, 1976, 1980) studied the biostratigraphy of larger benthic foraminifers and assigned an Oligocene to Miocene age for the Qom Formation. A revised biostratigraphy was presented by Naimi and Amirshahkarami (2011). This study presents new information on the biostratigraphy and lithostratigraphy of the Qom Formation at the Molkabad and Navab anticline sections of Central Iran. The age assignment of the Oligocene-Miocene marine beds of the studied sections is mainly based on the distribution of larger benthic foraminifera in the study areas. The recognized foraminiferal assemblages are compared to coeval assemblages from Europe and provide information on the paleoecology and paleogeography of the study area. Stratigraphic columns and benthic foraminiferal range charts are provided and are used for correlation of the two sections. The generated Oligocene-Miocene biostratigraphic framework for the studied sections in Central Iran will be useful for further regional geological investigations including applications in oil exploration.

2.2 GEOLOGICAL SETTING

Based on the sedimentary sequences, metamorphism, magmatism, intensity of deformations, and structural setting, the Iranian Plateau has been subdivided into eight continental fragments, including Zagros, Urumieh-Dokhtar, Sanandaj-Syrjan, Central Iran, Kopeh-Dagh, Alborz, Lut, and Makran (Heydari *et al.*, 2003; Fig 2.1). According to Mohammadi (2013) the deposition of the Qom Formation (Rupelian-Burdigalian in age) happened in three NW-SE trending basins: Sanandaj-Sirjan (fore-arc basin), Urumieh-Dokhtar magmatic arc (intra-arc basin) and Central Iran (back-arc basin)(Fig. 2.1). The transgression of the Tethyan Seaway on the Iranian Plate started from southeast and continued gradually northwestward (Fig. 2.2). The Qom basin extends along the Alborz Mountains from Semnan in the east to the Kuhrud Mountains NW of Tehran, and from there about 650 km to the south.

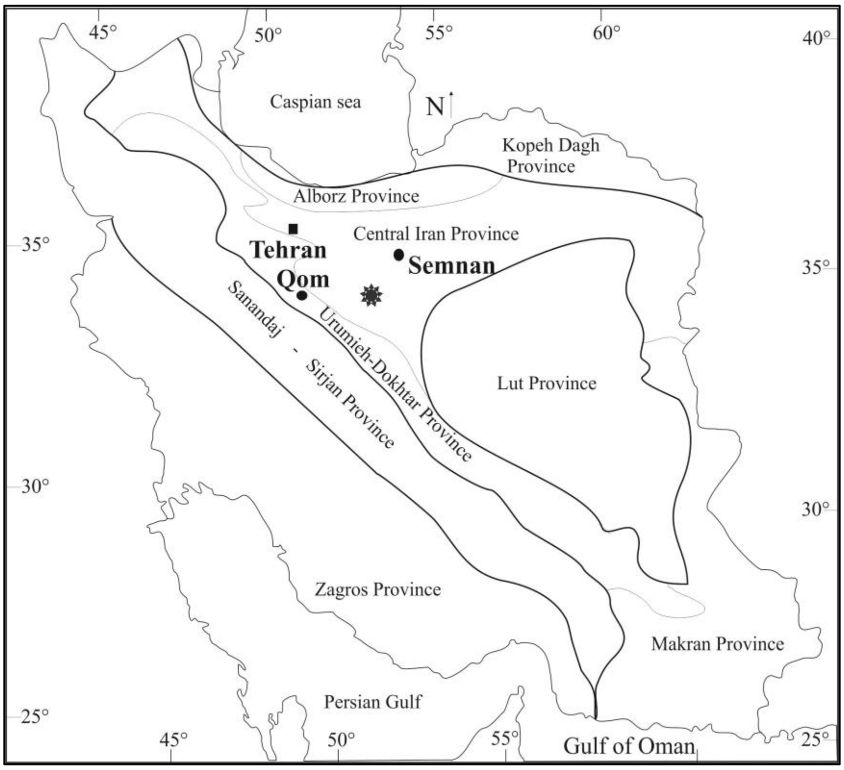

Figure 2.1: Subdivisions of the Iranian Plateau showing the eight geological provinces. Both studied sections are located in the Central Iran province (adapted from Heydari *et al.*, 2003).

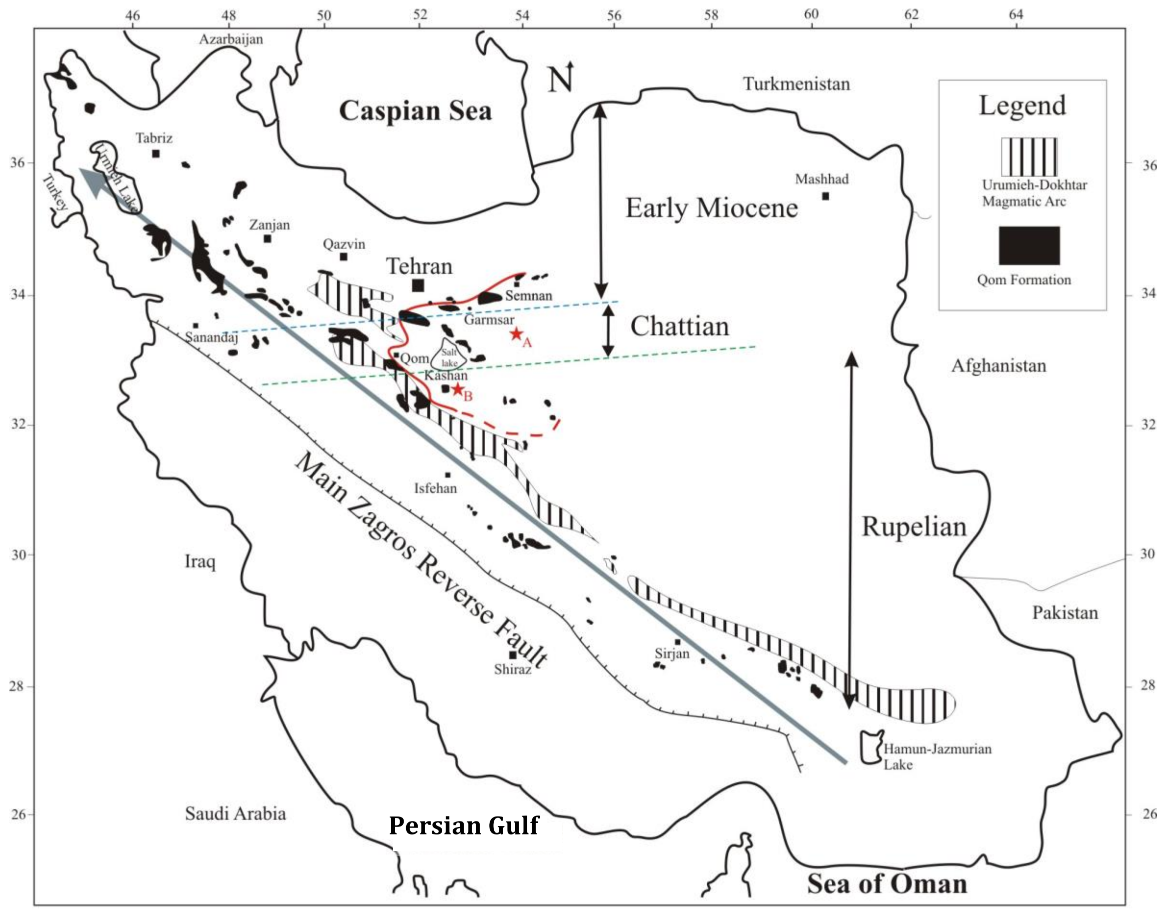

Figure 2.2: Timing and progression of the opening of the Tethyan seaway on the Iranian Plate documented by the deposition of the Qom Formation during the Rupelian, Chattian, and early Miocene. The transgression of the Tethyan Seaway started in the southeast and continued gradually northwestward as indicated by the grey arrow (modified from Mohammadi *et al.*, 2013).

2.3 Material and Methods

Two sections of the Qom Formation, which are located in the Qom back-arc basin were measured and sampled by the National Iranian Oil Company (NIOC) (Fig. 2.3a). The first of the studied sections is located in the Molkabad Mountains at 35°21’N and 52°43’E, southeast of Garmsar in central Iran (Fig. 2.3c), and the other section is located in the Navab anticline at 33°47’30”N and 51°37’30”E (Fig. 2.3b). The two sections of the Qom Formation are unconformably underlain by the Oligocene Lower Red Formation and unconformably overlain by the Miocene Upper Red Formation.

At total more than 146 Samples were collected. The samples were taken from both carbonate and marl layers. Thin sections were prepared from carbonate rocks, while marls were disaggregated and washed for foraminiferal analyzes.

Samples from boths sections were quantitatively analyzed with respect to the benthic foraminiferal fauna. On average 50g of dry marly sediment was treated with hydrogen peroxide for disaggregation and subsequently was washed through a 150 µm sieve. The residue was dried at 40˚C. The investigation of the benthic foraminiferal fauna was carried out on representative splits of the size fraction >150 µm. if possible, at least 300 specimens were counted for each sample. The picked samples were studied and documented by using a Scanning Electron Microscope (SEM) Zeiss LEO 1455 VP at the University of Hamburg.

All samples were studied in detail and particular attention has been paid to the foraminiferal association, since foraminifers are excellent paleoenvironmental indicators. Genus and species identification was performed according to studies of Biolzi (2005), Boudagher Fadel and Lokier (2005), Loeblich and Tappan (1998), and Lutze (1974).

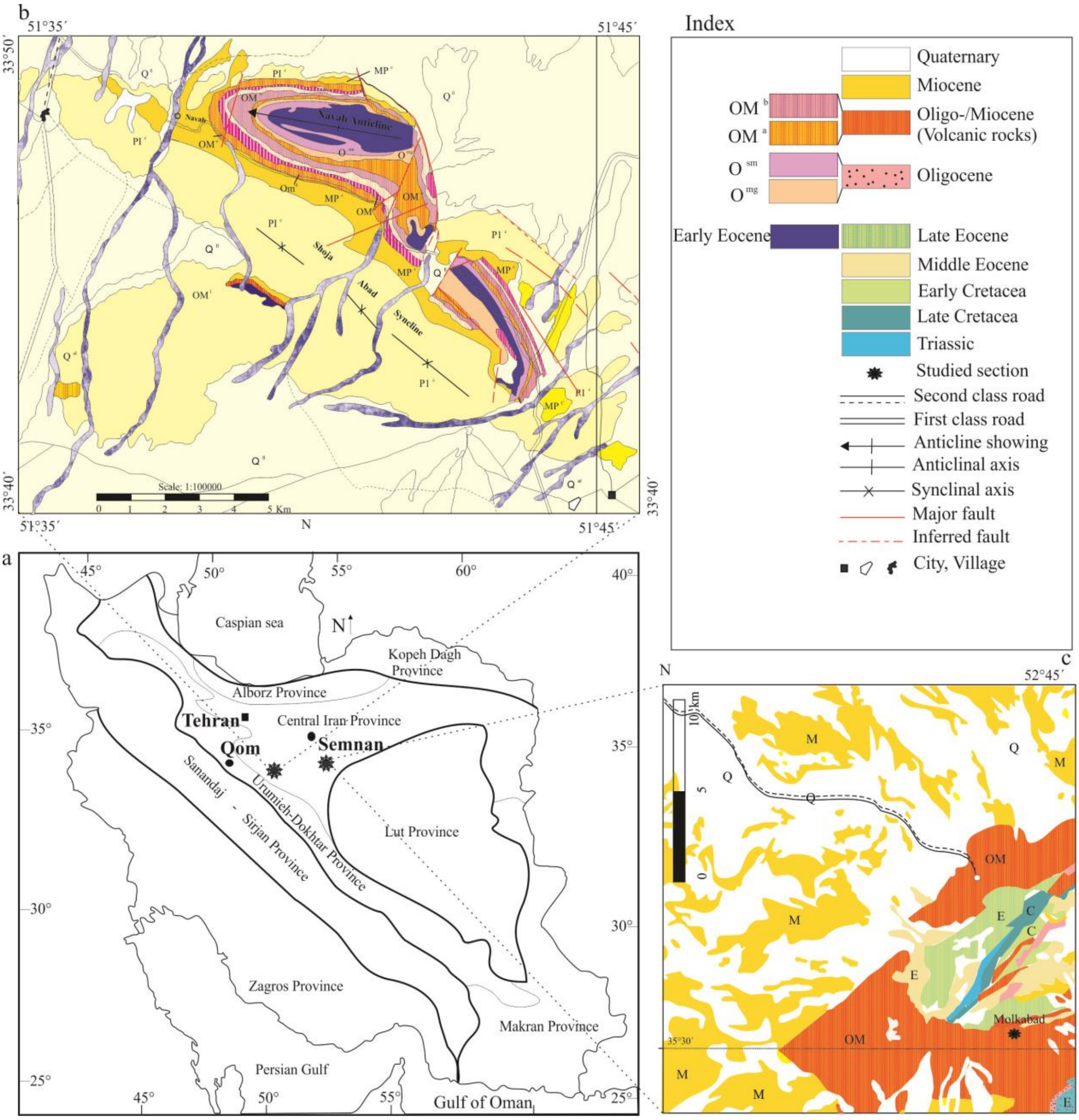

Figure 2.3: Map of the study areas with location of the Molkabad and Navab sections. (a), Locations of the Qom Basin, volcanic arc (dark grey) and Esfahan-Sirjan Basin are indicated according to Reuter *et al.* (2009). (b) Geological map of the study area in the vicinity of the Navab section (Map of Kashan city, Geologycal Survey of Iran 1:250000). (c) Geological map of the study area in the vicinity of the Molkabad section (Map of Kuh-e Gugerd, Geological Survey of Iran 1:250000).

2.4 RESULTS AND DISCUSSION

2.4.1 LITHOSTRATIGRAPHY OF THE MOLKABAD SECTION

The Molkabad section comprises a 760m thick succession of limestones and marls (Fig. 2.4). The section starts with a conglomerate, overlying disconformably the Eocene shallow marine carbonate beds. The base of the Qom Formation is characterized by a 127m thick succession of bedded and massive limestones with marly limestone intercalations, with abundant red algae and bryozoans, but rare benthic foraminifers. This unit is overlain by a 153m thick unit of bedded greenish to gray marls with gray limestone intercalations. Within this unit, samples number 552 to 575 and 576 to 594 represent the **c1** and **c2** members of the Qom formation, respectively. Above this unit a 94m thick succession of bedded and massive Bryozoan limestone represents the **c3** member of the Qom Formation documented by samples 594 to 604. This unit is poorly represented by paleontological data, due to a lack of samples. Finally, this section is overlain by a 384m thick succession of green to gray marls with intercalations of gypsum layers, representing the **c4** member of the Qom Formation. On top of this unit, yellow to gray marls of the **d** member are gradually changing into limestones of the **e** member of the Qom Formation.

2.4.2 LITHOSTRATIGRAPHY OF THE NAVAB SECTION

The Oligocene-Miocene sediments of the Navab section start with the Lower Red Formation, consisting of sandstones, red shales, gypsiferous marls and conglomerates as well as gradual transition to gypsiferous marls and gypsum with sandy marls. According to the lithologies six members (a-f) have been identified above the Lower Red Formation (Fig. 2.5). The **a** member is separated from the Lower Red Formation by an unconformity and consists of basal conglomerates, and fossil-rich (bryozoans, red algae etc.) massive and sandy limestones. The **b** member consists of limestones, sandstones and shales. The **c** member consists of the typical alternation of marls and limestones with abundant bryozoans and oysters overlain by well-bedded limestones, and greenish-gray to greenish-blue marls. The approximately 40 m thick **d** member mostly consists of gypsum: Because of folding its thickness differs considerably. The **e** member is represented by greenish marls with thick intercalations of reddish to white marly algal limestones. Besides of red algae this unit contains abundant bryozoans, gastropods and other organic remains (fossils). The **f** member is represented by a reef limestone with abundant coral fragments. This unit is intercalated with thin layers of foraminifer-rich algal limestone. The Upper Red Formation consists of marls, gypsum layers, sandstones, and conglomerates. The conglomerate clasts comprise limestones of the underlying Qom Formation and Eocene volcanic rocks.

2.4.3 BIOSTRATIGRAPHY OF THE MOLKABAD SECTION

The study of 113 samples taken from the studied section led to the identification of 20 genera and 17 species of benthic foraminifera, planktonic foraminifera, red algae and bryozoans (Fig. 2.6). Based on benthic foraminifera, which appeared in relatively high variety and abundance, the Molkabad section can be assigned to an age of late Oligocene to early Miocene.

***Austrotrillina howchini–Miogypsina–Miogypsinoides* assemblage Zone**

The 125m thick sediment succession comprises thick-bedded limestones with marl intercalations and a rich assemblage of benthic foraminifera, red algae and bryozoa (Table 3). This part of the succession contains a larger benthic foraminiferal assemblage of *Austrotrillina* sp., *Nephrolepidina* sp., *Miogypsina* sp., *Miogypsinoides* sp., *Schlumbergerina* sp., *Heterostegina* sp., and *Amphistegina* sp.. The assemblage of small benthic foraminifera includes *Elphidium* sp., *Elphidium (Porosononion) granosum, Elphidium advenum, Ammonia* sp., *Ammonia pauciloculata, Ammonia* group spp., *Heterolepa* sp., *Nonion asterizans, and Cancris auriculus* and various miliolids. This assemblage suggests an Early Miocene (Aquitanian) age (SBZ 24 zone after Cahuzac and Poignant, 1997).

***Borelis melo-Miogypsina* assemblage zone**

The approximately 633m thick upper part of the section consists of limestones, marls and evaporates. The larger benthic foraminiferal assemblage includes *Peneroplis farsensis, Peneroplis* cf. *thomasi, Nephrolepidina* sp., *Dendritina* sp., *Miogypsina* sp., *Meandropsina iranica, Archaias* cf. *kirkukensis, Borelis melo curdica, Schlumbergerina* sp., and *Sorites* sp.. The small benthic foraminiferal assemblage includes *Elphidium* sp., *Elphidium (Porosononion) granosum, Elphidium advenum, Elphidium hauerium, Ammonia* sp., *Ammonia pauciloculata, Ammonia* group spp., *Ammonia* cf. *tepida, Ammonia beccarii, Heterolepa mexicana, Heterolepa* sp., *Gavelinopsis lobatulus, Nonion asterizans, Cancris auriculus, Cibicides lobatulus*, and assorted miliolid taxa. In addition, planktonic foraminifera, ostracods and bivalves are abundant in this part of the section. This section also contains remains of red algae and bryozoa.

The distribution of larger benthic foraminifera refers to the *Borelis melo curdica* zone indicating the upper part of the Late Oligocene (Aquitanian) to Early Miocene (Burdigalian) This biozone can be considered as time-equivalent to the so-called *Neoalveolina (Borelis) melo curdica* zone #61 by Wynd (1965) and *Borelis melo* group, *Meandropsina iranica* assemblage zone # I of Adamas and Bourgeois (1967).

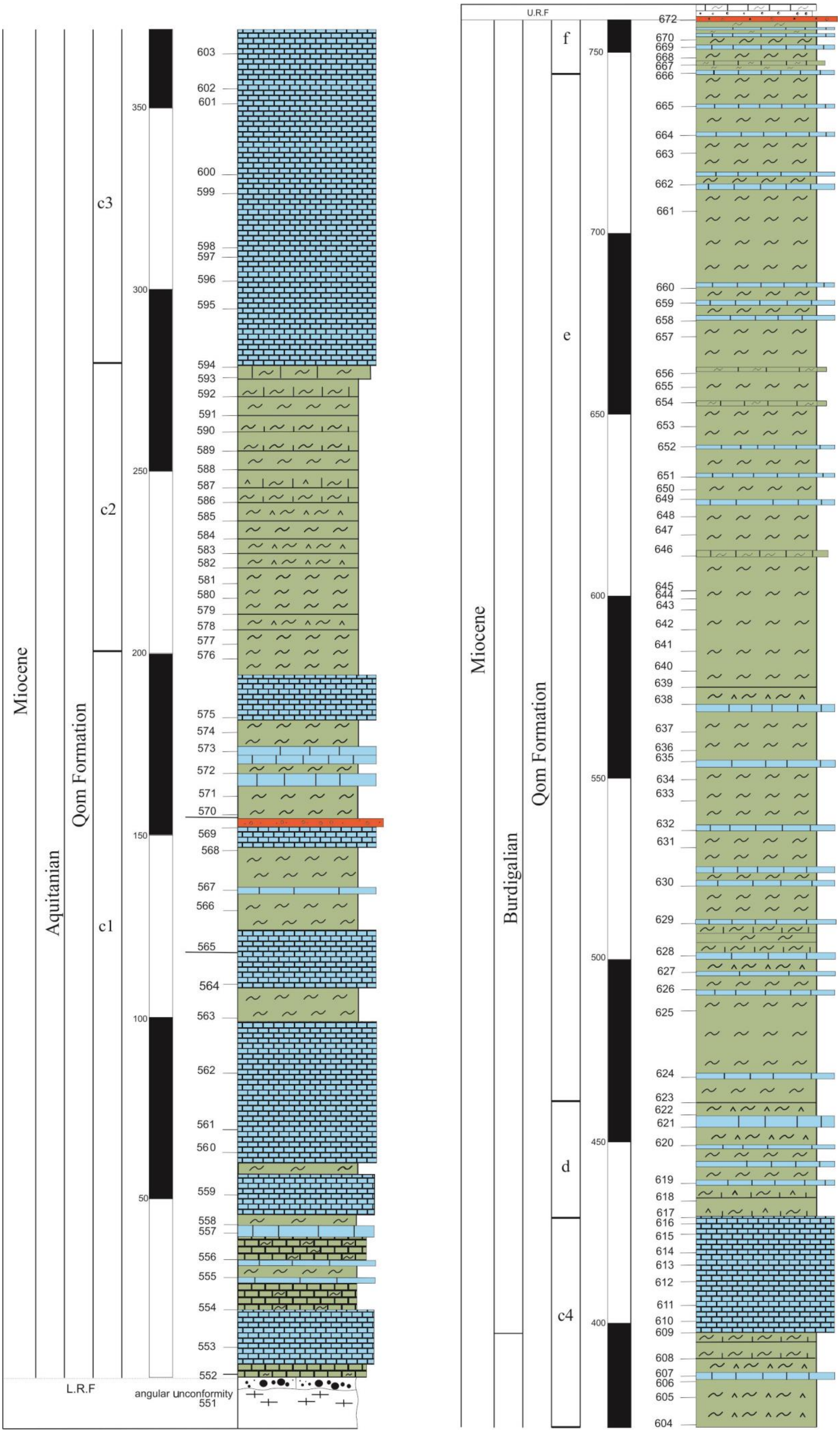

Figure 2.4: Lithology of the Molkabad section. From left to right chronostratigraphy, formation names, members, scale in meters, sampled beds, and lithology are given. For lithological legend see Fig. 2.5.
L.R.F= Lower Red Formation, U.R.F=Upper Red Formation.

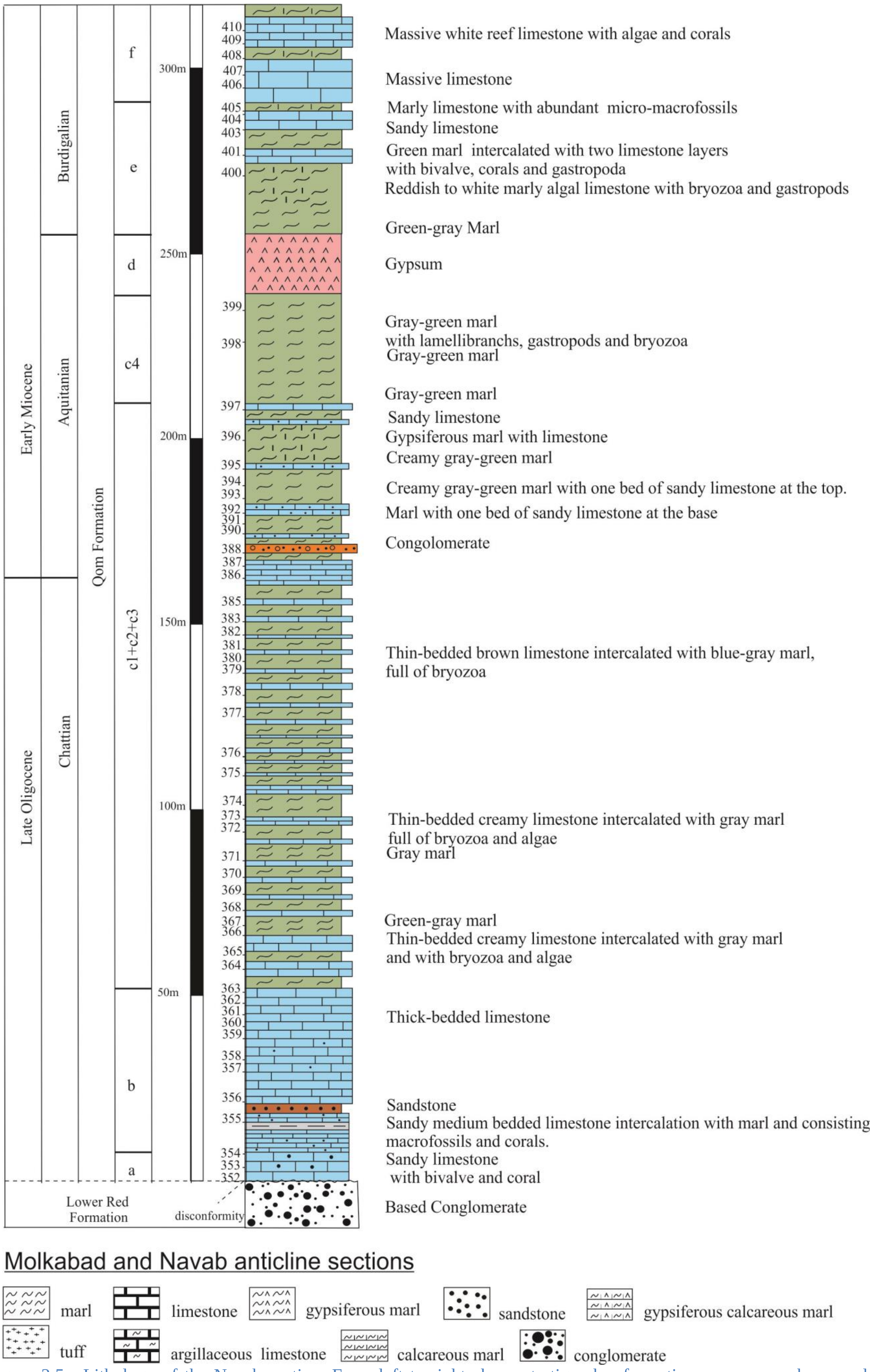

Figure 2.5: Lithology of the Navab section. From left to right chronostratigraphy, formation names, members, scale in meters, sampled beds, lithology and lithological description are given.

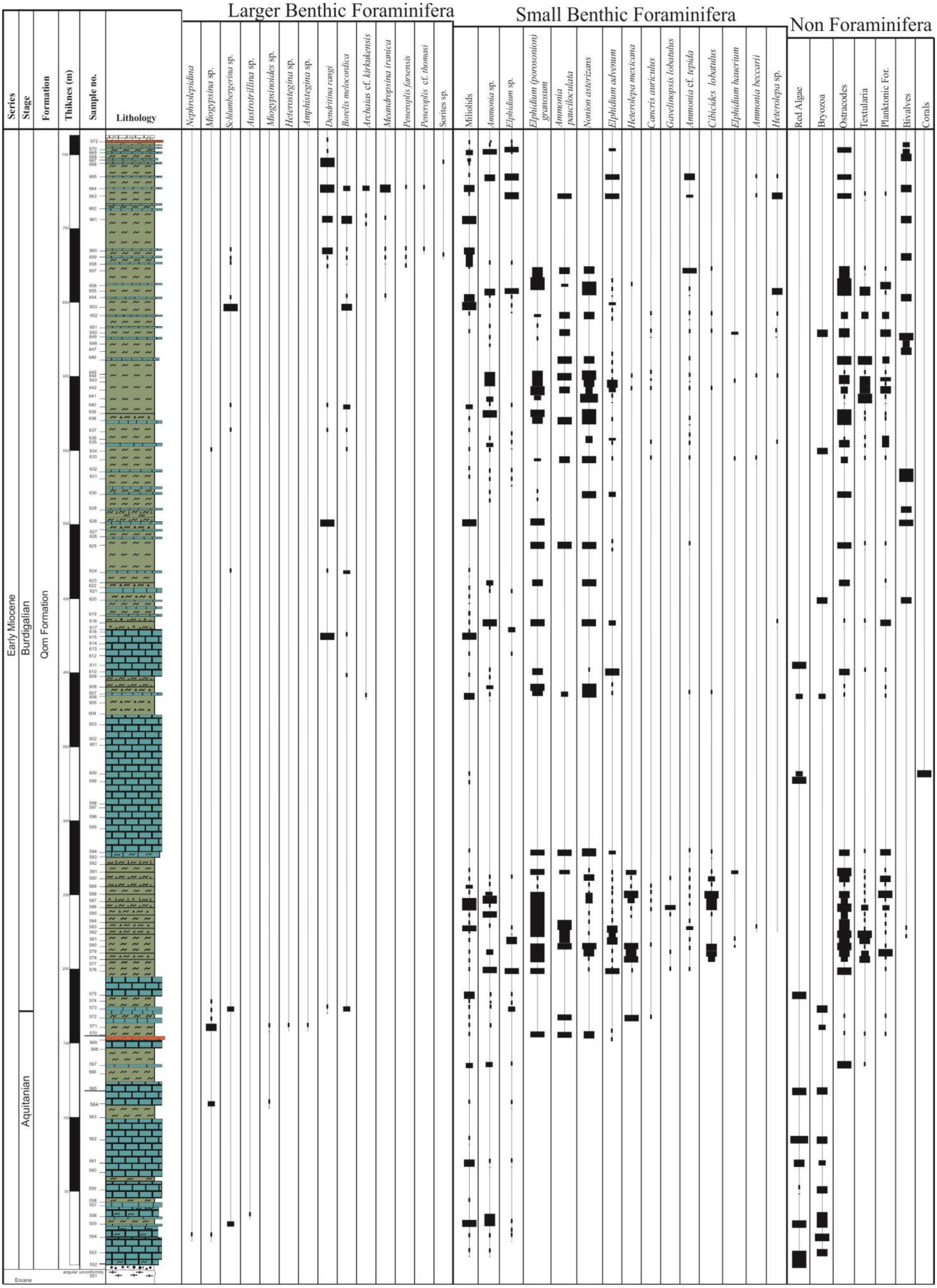

Figure 2.6: Biostratigraphy of the Molkabad section. From left to right chronostratigraphy, formation name, scale in meters, lithological succession, and the frequency of larger and small benthic foraminifera are given. For legend see Fig. 2.7.

2.4.4 BIOSTRATIGRAPHY OF THE NAVAB SECTION

The biostratigraphy of the Navab section is primarily based on the presence of short-ranging, stratigraphic index species. Their first occurrences (FO) and /or the last occurrences (LO) as well as the co-occurrence of two or more taxa have been used for finer biostratigraphic subdivision. The benthic foraminiferal biozones have been established based on Cahuzac and Poignant (1997).

A total of 28 genera and 13 species of benthic foraminifera have been identified in sediments from the Navab section. The age determination was mainly based on the distribution of larger foraminifera rather than that of planktonic foraminiferal index taxa. The results indicate a Chattian-Aquitanian-Burdigalian age for the studied section. Accordingly, the biozones SBZ 23, SBZ 24 and SBZ 25 of Cahuzac and Poignant (1997) have been identified.

Interval between sample numbers 352 and 385

The 150 m thick succession comprises massive limestones, sandy limestones, and marl and contains larger benthic foraminifera indicative of the late Oligocene.

The identified benthic foraminifera (Fig. 2.7) are as follows:

Rotalia viennotti, Dendritina sp., *Asterigerina* sp., *Rotalia* sp., *Sphaerogypsina globolus, Operculina* sp., *Nephrolepidina* sp., *Valvulina* sp., *Operculina complanata, Eulepidina dilalata, Amphistegina* sp., *Lepidocyclina* sp., *Spiroclypeus blankenhorni, Spiroclypeus tidoenganensis, Nephrolepidina tournoueri, Nephrolepidina* cf. *marginata, Miogypsina* sp., *Miogypsinoides* sp., *Asterigerina rotula, Schlumbergerina* sp., *Textularia* sp., *Planorbulina* sp.

Additional smaller benthic foraminifera include *Elphidium* sp.14, *Ammonia beccari, and Elphidium* sp., Furthermore, this section contains remains of calcareous algae, brozoans such as *Tubucellaria* sp., lamellibranchia such as *Ostrea* sp., corals, gastropods, ostracods, and echinoderms.

In the study area the abundant appearance of *Eulepidina dilalata* indicates a Chattian age. Similar foraminiferal assemblages, typical for the late Oligocene, have been mentioned in biostratigraphic studies for the entire Tethyan province (Cahuzac and Poignant, 1997).

Interval between sample numbers 386 and 399

This interval starts with thin-bedded brown limestones intercalated with blue-gray marls followed by a 53m thick succession of marly sandy limestones and evaporates. The interval is represented by 13 samples. The larger benthic foraminifera indicate an early Miocene age, belonging to SBZ 24 (Cahuzac and Poignant, 1997) (Fig. 2.7).

The benthic foraminiferal assemblage includes the larger benthic foraminifer *Archaias* sp. and the small benthic foraminifers *Pyrgo* sp., *Triloculina* sp., and abundant *Elphidium* sp..

Furthermore, sediments of this interval contain remains of red algae, echinoids and brachiopods.

An early Miocene age (SBZ 24) is documented by the LO of *Eulepidina dilalata* and FO of *Archaias* sp. consistent with the zonation of Adams and Bourgeois (1967), but inconsistent with the zonation of Cahuzac and Poignant (1997).

Interval between sample numbers 400 and 410

This interval starts with evaporates, overlain by an 115m thick succession of massive reefal limestones and marls. Based on the occurrence of benthic foraminifers the sediments cannot be assigned to a biozone, however the stratigraphic position of this unit suggests a Burdigalian age.

2.4.5 STRATIGRAPHICAL INTERPRETATION

The different lithological units of the Qom Formation laterally change over relatively short distances (Fig. 2.8). Therefore, the correlation of different units determined in outcrops or sediment cores needs a proper biostratigraphic framework based on (larger) benthic foraminifera, which are the main representatives of the foraminiferal association in the shallow marine Qom Formation. The Oligocene-Miocene deposits of the Molkabad and Navab anticline sections represent typical inner-neritic depositional environments supported by the predominance of marls and algal and bryozoan limestones. The interpretation of a shallow-marine depositional setting is corroborated by the presence of small benthic foraminifera, such as the genera *Ammonia* and *Elphidium*.

For the zonal assignment of the Qom Formation in the Molkabad section, the important biostratigraphic markers in the assemblage mentioned above are *Austrotrillina* sp., *Miogypsina* sp., *Miogypsinoides* sp., and *Borelic melo curdica*. Their ranges are equivalent to SBZ 24 to SBZ 25 (Cahuzac and Poignant, 1997) indicating an Aquitanian to Burdigalian age.

The biozonation for the Navab anticline section is based on a combination of larger benthic foraminifera (such as *Archaias* and *Eulepidina*, Cahuzac and Poignant, 1997) and further aided by the occurrence of planktonic foraminifers suggesting a Chattian-Aquitanian-Burdigalian age.

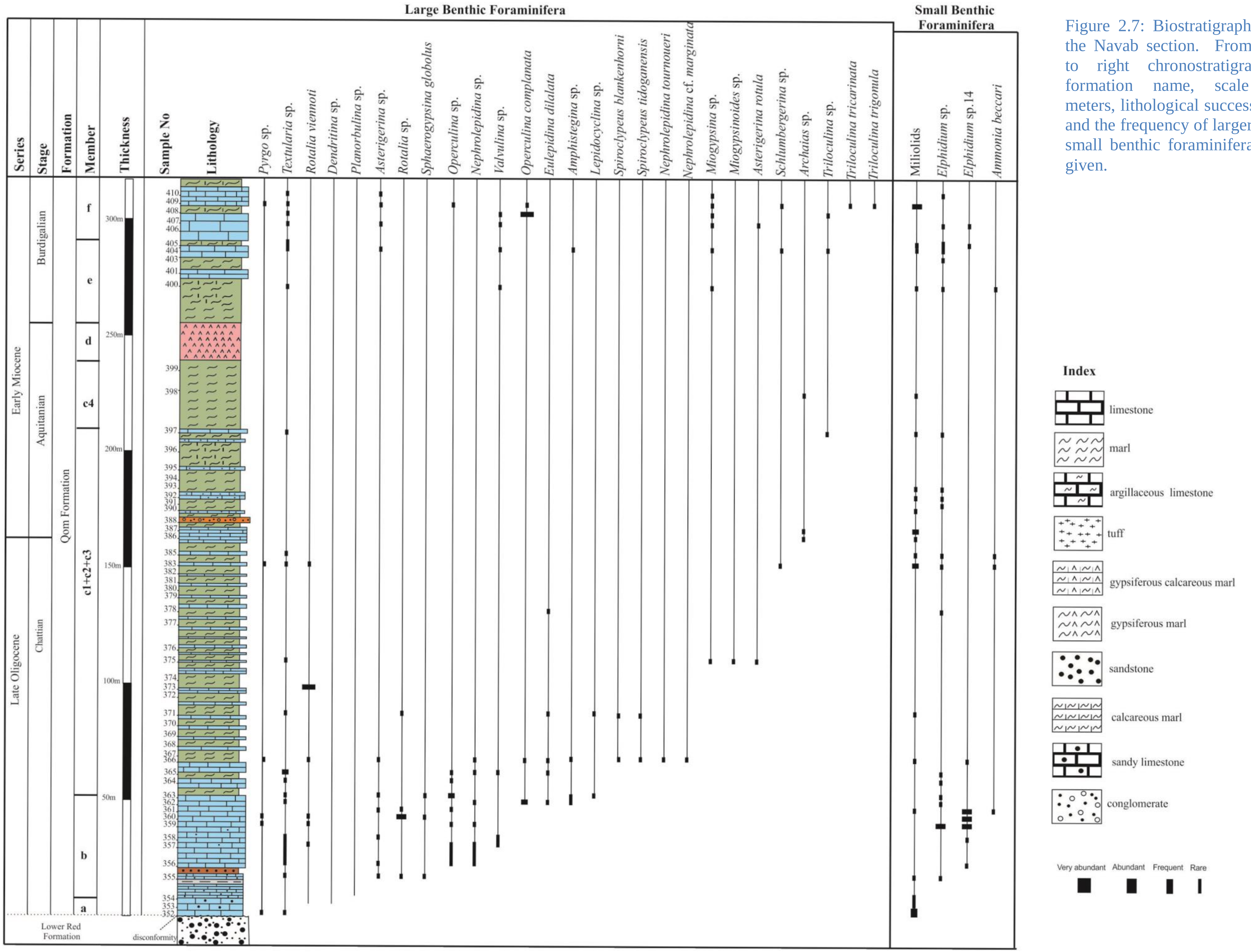

Figure 2.7: Biostratigraphy of the Navab section. From left to right chronostratigraphy, formation name, scale in meters, lithological succession, and the frequency of larger and small benthic foraminifera are given.

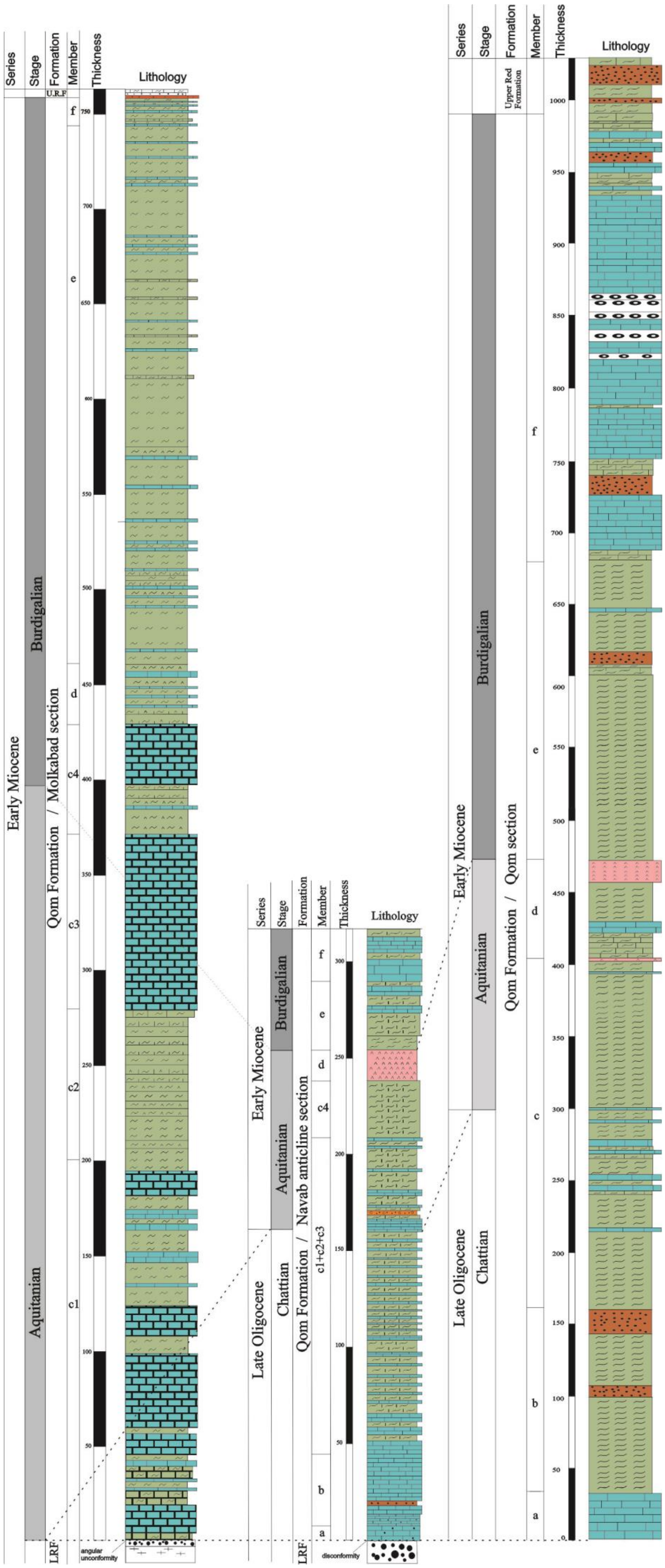

Figure 2.8: Chronostratigraphic scheme and correlation for the Qom Formation at sections of Molkabad and Navab anticline (this study), in comparison to the section of Qom (Reuter *et al.*, 2009). The Molkabad section comprises two foraminiferal biozones in the Aquitanian and Burdigalian stages, the Navab anticline section three foraminiferal biozones in the Chattian, Aquitanian, and Burdigalian stages. In the Qom section three foraminiferal biozones have been identified in the Chattian, Aquitanian, and Burdigalian stages (Reuter *et al.*, 2009).

2.5 CONCLUSIONS

- The Qom Formation was deposited with extensive mixed carbonate –siliclastic sediments in the northeastern part of the Tethys Ocean.
- Two sediment successions of limestones, argillaceous limestones, gypsum beds and marls of the Qom Formation have been studied in the frame of this study, comprising the 318m thick Navab anticline section and the 760m thick Molkabad section. Sediments from both sections contain plenty of fossil remains, mainly from foraminifera, red and green algae and bryozoans, among which larger foraminifera are particularly abundant.
- The studied benthic foraminiferal faunas reveal a total of 36 genera and 26 species for the Molkabad section and 28 genera and 13 species for the Navab section. Detailed investigation of the larger benthic foraminifera provides regional biostratigraphic frameworks for the Oligocene-Miocene shallow-marine successions of the Qom Formation.
- Among all identified foraminifera, certain taxa proved particularly useful in biostratigraphic age assessment. Useful indicator taxa include *Ammonia beccarii, Dendritina rangi*, *Miogypsina* sp., *Nephrolepidina tournoueri, Operculina complanata*, *Rotalia viennoti, Spiroclypeus blankenhorni, Triloculina tricarinata, Eulepidina dilalata*, *Archaias* cf. *kirkukensis,* and *Borelis melo curdica.*
- For the Molkabad section, foraminiferal index species assigned an Early Miocene (Aquitanian-Burdigalian) age and for the Navab anticline section a Late Oligocene (Chattian) to Early Miocene (Aquitanian/Burdigalian) age. This biostratigraphic assessment is in accordance with SBZ 23 to 25 of Cahuzac and Poignant (1997). As a result, Molkabad sediments can be correlated with the **c** to **f** members of the Qom Formation at the type locality. Accordingly, Navab anticline sediments can be correlated with the **a** to **f** members of the Qom Formation.
- The recognized larger benthic foraminiferal faunas at the studied sections from Central Iran allowed a super-regional comparison with coeval assemblages from the Middle East and Europe.

3 CHAPTER: DEPOSITIONAL ENVIRONMENTS OF THE OLIGOCENE-MIOCENE QOM FORMATION BASED ON FACIES ANALYSIS OF SEDIMENT SUCCESSIONS FROM THE CENTRAL QOM BASIN, IRAN

ABSTRACT

The Qom Formation developed in Central Iran during the final marine transgression of the Oligocene-Miocene. The Qom Formation can be divided into nine members classified from oldest to youngest: a, b, c1 to c4, d, e, and f. member e is 300m thick and constitutes the main gas and oil reservoirs. In the Central Iran Basin, the Qom Formation is deposited between the Oligocene Lower Red Formation and the middle Miocene Upper Red Formation. The Qom Formation was studied at the Molkabad and Navab sections in order to determine its microfacies and depositional environment. In both sections, carbonate deposition occurred on a shallow marine ramp. The textural, floral and faunal analyses at Molkabad section revealed eight microfacies, representing tidal flats, semi-restricted lagoons, lagoons, and patch reefs of the inner and middle ramp environments. The textural, floral and faunal analyses reveal ten microfacies for the Navab section representing semi-restricted lagoons, lagoons, patch reefs and open marine environment of inner, middle and outer ramp environments.

Keywords: Qom Formation, Central Iran, Oligocene-Miocene, Benthic foraminifera, Tethyan Seaway.

3.1 INTRODUCTION

The Qom Formation has been deposited during the Oligocene and Miocene and represents the terminal phase of the Tethyan Seaway, which represented the gateway between the North Atlantic and Indian oceans. So far, the high facies variability of the Qom Formation impeded the establishment of a type section, but the Qom area has been presented as its type area (Rahimzadeh 1994; Aghanabati 2004; Mohammadi *et al.*, 2011). Microfacies analysis and paleoenviromental interpretation of the Qom Formation shows that the associated sediments were deposited under a wide range of depositional conditions. In general, the facies types of the Qom Formation represent alluvial-deltaic, carbonate platform-evaporated, slope and basin (deep-sea) depositional conditions (Rahimzadeh 1994). The high facies changes and small-scale variability of the Qom Formation within intra-mountain basins hampers the establishment of a representative depositional model for the entire area of Central Iran. In this context, the Qom Formation was associated with an open shelf depositional system in the areas southeast of Kashan (Momenzadeh, 2003), west of Ardestan (Vaziri-Moghaddam and Torabi, 2004), and southeast of Qom (Sedighi, 2008). In contrast a homoclinal ramp depositional system was proposed for other areas, including the Qom area (Okhravi and Amini, 1998), east of Teheran (Naeije, 2000), Charkha mountains (Natanz region, Seyrafian *et al.*, 2006) and Navab anticline (southeast of Kashan, Sedighi, 2008). Faiz-Nia and Mosafi (1998) introduced an epicontinental sea for the deposition of the Qom Formation. Based on sequence stratigraphic analyses of two sections from the Esfahan-Sirjan and Qom basins, Reuter *et al.*, (2009) concluded that the Qom Formation was deposited on extended, mixed carbonate-siliciclastic, homoclinal ramps.

In the existing facies studies of the Qom Formation the appearance of larger benthic foraminifera provided important environmental information. Larger foraminifera have repeatedly developed in the Phanerozoic from small-sized ancestors (Lee *et al.*, 1979). Due to episodes of rapid diversification and abrupt extinction, larger foraminifera are biostratigraphically important zonal fossils (Hallock, 1985). Their appearance is often related to periods of global warming, raised sea levels, relative drought, reduced oceanic circulation, and expansion of tropical and subtropical habitats (Hallock and Glenn, 1986). Besides their biostratigraphic importance, larger foraminifera are useful paleoenvironmental indicators because their distribution depends on specific conditions of light, temperature, water depth, substrate, nutrient supply, hydrodynamic energy, and symbiosis.

In the frame of this study, the microfacies of sediments from the Qom Formation at the Navab anticline and Molkabad sections have been studied in detail. Based on this information, paleoenvironmental conditions were reconstructed and a regional depositional model for the Qom Formation was established.

3.2 STUDY AREAS

As part of the Iranian plate, the Qom Basin is situated on the southeastern margin of the Paratethys. Sediment archives of the Qom Basin contain important information on the regional paleogeography of the late Oligocene to early Miocene, particularly on the gateways between the Paratethys, the Mediterranean Tethys and the Indo-Pacific realm (Stöcklin and Setudehina, 1991; Seyrafian and Torabi, 2005; Reuter *et al.*, 2009, Khaksar and Maghfouri Moghaddam, 2007; Daneshian and Ramezani Dana, 2007; Mohammadi *et al.*, 2011; Behforouzi and Safari, 2011; Yazdi *et al.*, 2012). In the frame of the present study, two sediment successions of the Qom Formation are investigated, one section is located in the Molkabad Mountains southeast Garmsar in central Iran at coordinates 35°21´N, 52°43´E (Fig. 3.1) and the other section is located in the Navab anticline at coordinates 33°47’30”N, 51°37’30”E (Fig. 3.1). The two sections of the Qom Formation are unconformably under and overlain by the Oligocene Lower Red Formation and Miocene Upper Red Formation, respectively.

3.3 MATERIAL AND METHODS

At the Molkabad section with 760m thickness and the Navab anticline section (318m thickness) of the Qom Formation were measured and sampled (Figs. 3.2, 3.3). In total, 146 samples were collected based on field evidence and litho-facies changes. Samples were taken from carbonate and marly layers. Thin sections were made for carbonate rocks. Marl samples have been treated with hydrogen peroxide for disaggregation and subsequently washed through a 150-µm sieve. The dried residue was sieved at 150 µm, and the size fraction >150 µm was analyzed. All samples were studied in detail under the microscope and have been investicated for the foraminiferal assemblages, since foraminifera are excellent paleoenvironmental and biostratigraphic indicators. Genera and species were identified according to different studies (e.g. Loeblich and Tappan, 1987 and Lutze 1974). Petrographic analyses together with image analysis of rock components in a total of 135 thin sections were used to determine the depositional facies and diagenetic processes of marine carbonates of the Qom Formation. Facies analysis is based on standard models and microfacies descriptions (e.g. Dunham 1962; Flügel, 1982 and 2004).

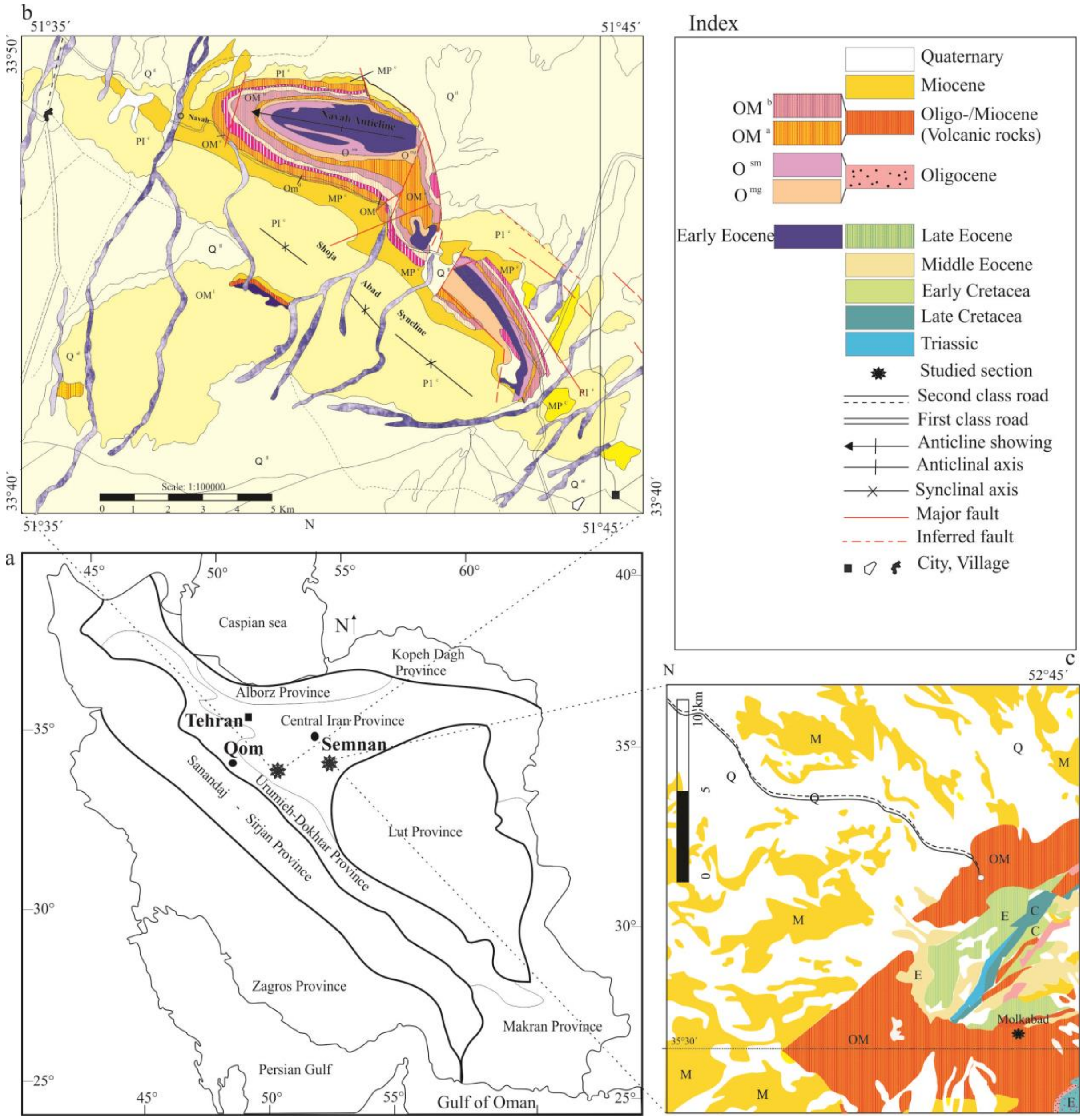

Figure 3.1: Map of the study areas with location of the Molkabad and Navab sections. (a), Locations of the Qom Basin, volcanic arc (dark grey) and Esfahan-Sirjan Basin are indicated according to Reuter *et al.*, (2009). (b) Geological map of the study area in the vicinity of the Navab section (Map of Kashan city, Geologycal Survey of Iran 1:250000). (c) Geological map of the study area in the vicinity of the Molkabad section (Map of Kuh-e Gugerd, Geological Survey of Iran 1:250000).

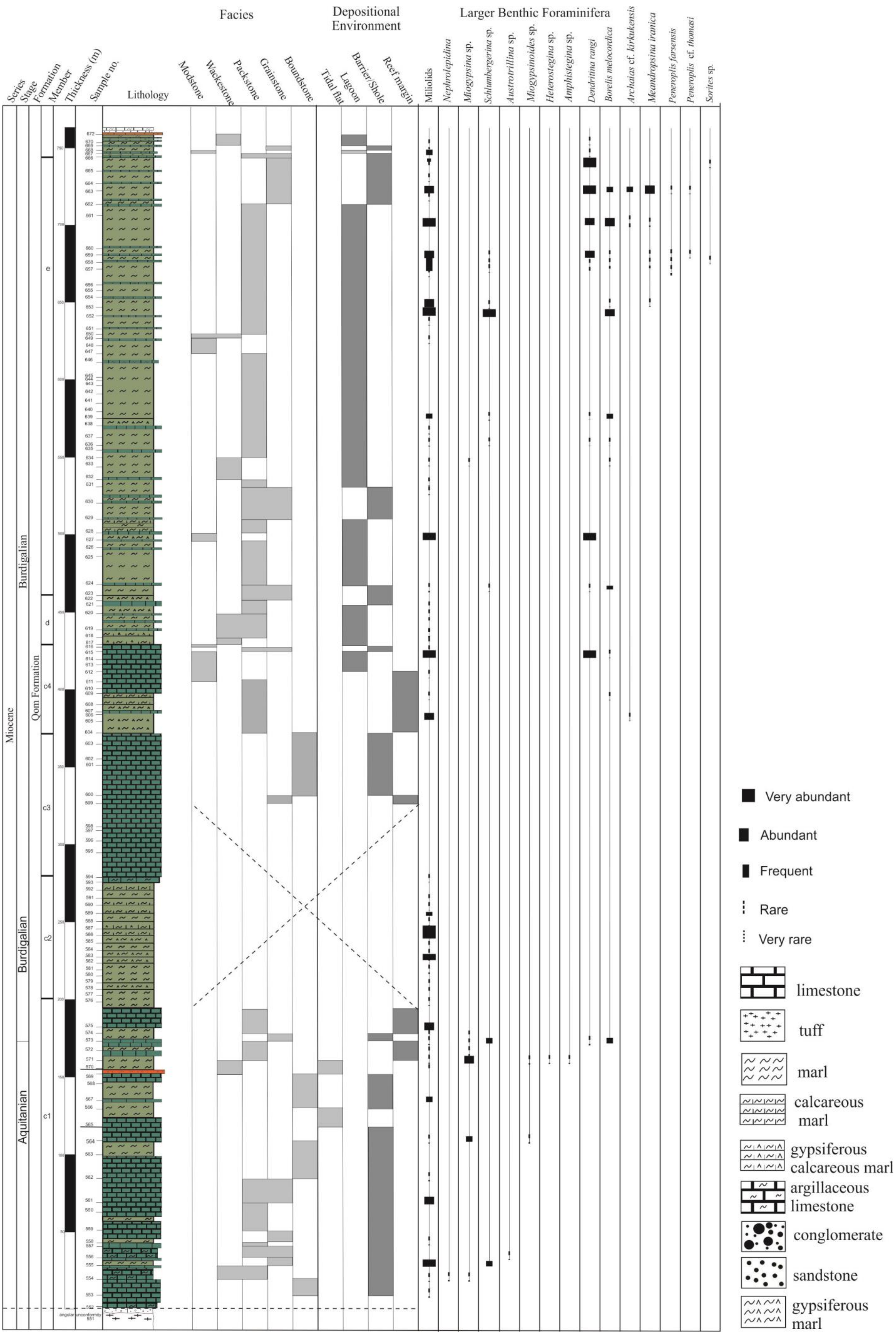

Figure 3.2: Qom Formation at Molkabad section, Qom Basin. Given are chronostratigraphy, formation and member names, lithology, occurrence of benthic foraminifera, sediment facies and inferred depositional environment.

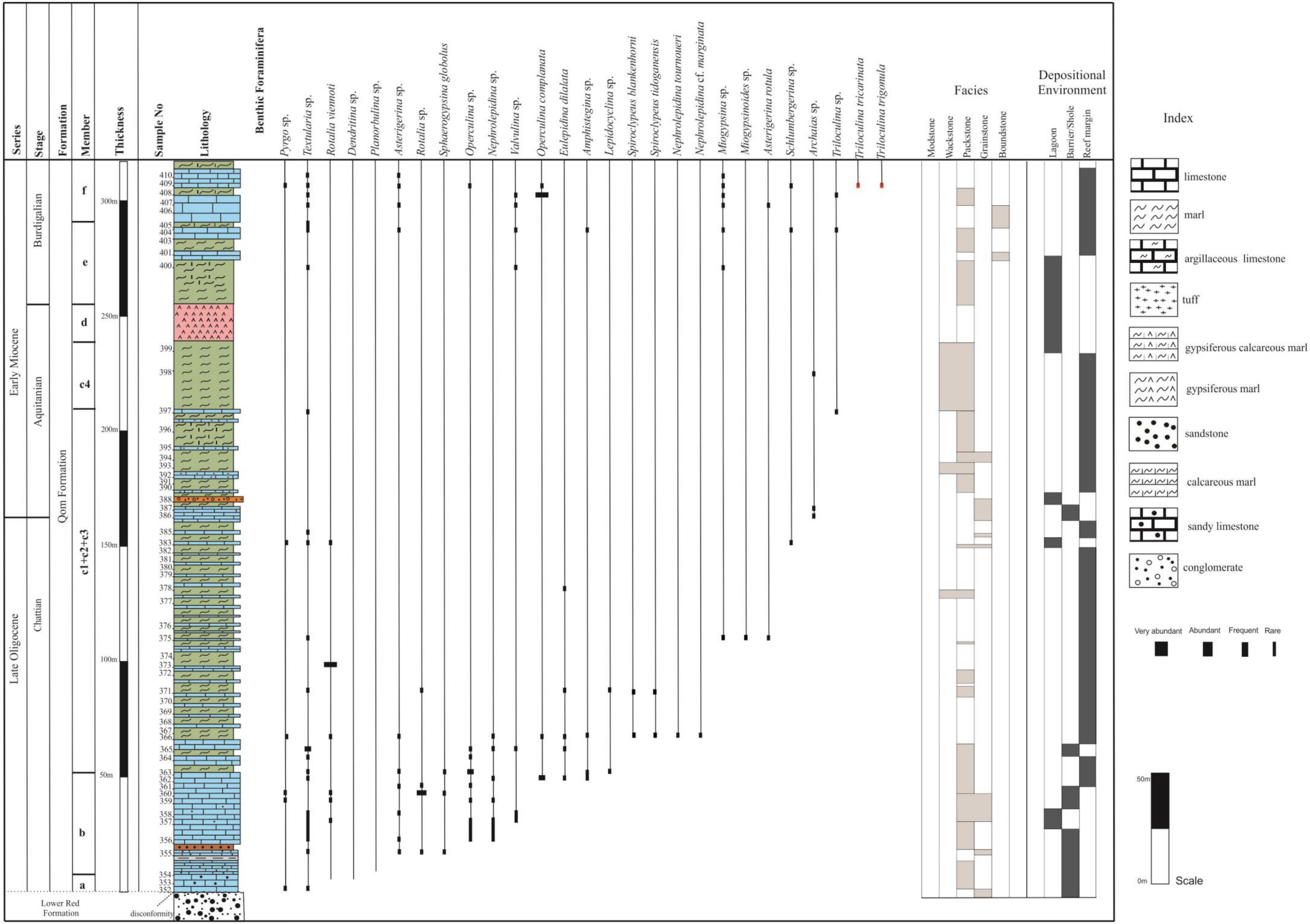

Figure 3.3: Qom Formation at Navab anticline section, Qom Basin. Given are chronostratigraphy, formation and member names, lithology, occurrence of benthic foraminifera, sediment facies and inferred depositional environment.

3.4 RESULTS AND DISCUSSION

3.4.1 MOLKABAD SECTION

3.4.1.1 MICROFACIES TYPES

Based on the fabric features of the sediments and the dominant biogenic components, eight microfacies (MF) types were identified for the Qom Formation at the Molkabad section (Figs. 3.2, 3.4). The microfacies types can be associated with tidal flat, semi-restricted lagoon, lagoon and patch reef environments.

MF A: Gypsum

This facies is characterized by light color and medium to large crystals. The gypsum facies has been observed in the c1 member at the lower part of the Molkabad section. These sediments have an Aquitanian age (Figs. 3.2, 3.4).

The Oligocene–Miocene Qom Formation includes marine limestones and marlstones with siliciclastic rocks and gypsum. In the Qom section, gypsum is indicative of a very shallow environment.

MF B: Sandy mudstone

This facies is characterized by fine-grained micrite with very fine quartz grains and is poorly fossiliferous. Sediments microfacies have a Burdigalian age and have been observed within the c4 member (Figs. 3.2, 3.4).

Microfacies B is characterized by very fine quartz sand grains scattered in a muddy matrix. According to Flügel (2004), micofacies B represents a very shallow and low-energy environment in a restricted lagoon of an inner shelf setting close to the shore. Mohammadi *et al.*, (2011) recorded the same facies from the Qom Formation in the Kashan area and interpreted it as deposits from the shoreward shallow parts of the lagoon.

MF C: Imperforate foraminifera bioclastic packstone

This microfacies mainly consists of biogenic components, comprising imperforate larger foraminifera such as *Dendritina* and *Borelis*, other miliolids, echinoid debris, bivalves and ostracods. Peloids represent some parts of this microfacies. Hyaline foraminifera such as the genera *Rotalia, Ammonia, Elphidium, Reussella*, and *Discorbis* are scattered in this microfacies. Microfacies C has a grain-supported texture, a micrite matrix and represents wackestones to packstones (Fig. 3.4). Sediments of this microfacies are located at the upper part of the e member at the Molkabad section. This microfacies has a Burdigalian age.

The occurrence of porcelaneous larger benthic foraminifera like *Dentritina* and *Borelis*, and other miliolid taxa suggest deposition in the upper photic zone and a rather low-energy setting likely representing a shallow lagoon environment (Leutengger 1984; Romero *et al.*, 2002). Accordingly, the frequent presence of thick-shelled foraminifera (e.g., miliolids) has been associated with a low-energy environment with sufficient food and high light intensity (Sinclair *et al.*, 1998). Microfacies C is comparable with facies RMF 20 recorded by Flügel (2004) who related it to the inner ramp. Similar facies types have been associated with restricted lagoon environments in the Zagros Basin (Vaziri-Moghadam *et al.*, 2006). Restricted shallow-water environments with low diversity of skeletal fauna, occurence of imperforate larger foraminifera (*Dendritina*) and other miliolids, peloids, and no evidence of water loss have been reported in a number of studies (Reiss and Hottinger 1984; Buxton and Pedly 1989; Romero *et al.,* 2002; Barattolo *et al.,* 2007).

MF D: Imperforate foraminifera *Dendritina rangi* wackestone

This microfacies is characterized by a wackestone texture with micrite matrix (Fig. 3.4). Larger imperforate foraminifera (*Dendritina rangi*) are a main component. In addition, this microfacies contains peloids and quartz grains. Sediments of this microfacies are located within the f member of the Molkabad section, and have a Burdigalian age.

Porcelaneous benthic foraminifera like *Dendritina* and other miliolids have been associated with a low-energy environment in the upper photic zone, representing a shallow lagoon depositional setting (Romero *et al.*, 2002; Leutengger 1984). Similarly, the presence of thick- and dark-shelled benthic foraminifera (like miliolids) has been associated with a shallow-water and nutrient-rich environment (Sinclair *et al.*, 1998). *Dendritina* prefers to live in less than 30 m water depth (Bassi *et al.*, 2007). Microfacies D is equivalent to facies RMF20 of Flügel (2004) and facies number 2 of Buxton and Pedly (1989) representing the inner ramp.

MF E: Miliolid ooid grainstone

Microfacies E is dominated by ooids embedded in sparitic cement. It has been identified in sediments of an Aquitanian age and is located in the lower part of the c1 member. The ooids can be assigned to the tangential type and have fair and tolerable sorting and roundness (Fig. 3.4). The majority of the ooids are characterized by core liquidation. In some sections, the ooids are micritic and have lost their initial fabric. The other skeletal and non-skeletal components of this facies are mainly imperforate foraminifera, which occur in variable numbers. Abundant occurrences of imperforate foraminifera in some samples result in packstone-grainstone bioclastic facies containing peloids and ooids.

The existence of ooids indicates that this microfacies has been formed in a high-energy depositional environment in an offshore shoal (Bernaus *et al.*, 2003). Similarly, this facies was assigned to a high-energy barrier area (Geel, 2000) and is equivalent to RMF-29 of Flügel (2004) and contributed to facies belt number 3 of Buxton and Pedley (1989). Similar facies types have been reported from Oligocene-Miocene sediments in southeastern Italy and Malta (Pedley, 1998), and from various locations in the Zagros Basin (Yazdani 2014, and Zabihi *et al.*, 2013).

MF F: Coral boundstone

The microfacies F is characterized by colonial corals (*Porites* sp.) and has been identified in sediments of Burdigalian age. It is located at the c3 members of Molkabad section (Fig. 3.4).

Scattered branching corals are typical for areas with reduced water energy located in the lowest part of the euphotic zone (Schuster and Wielandt, 1999). However, the common coral debris may have originated from adjacent patch reefs or could have been produced in-situ from isolated colonies that have grown in sea grass environments (Brasier, 1975). According to the standard microfacies introduced by Wilson (1975) and expanded by Flügel (2004), microfacies F is related to reef deposition. The discontinuous occurrence of coral boundstone interbedded with lagoonal sediments suggests a lagoonal patch reef depositional environment. Commonly, coral reef communities thrive under oligotrophic conditions and various studies have shown that coral reefs suffer from increased nutrient concentrations (Hallock and Schlager, 1986; Flügel, 2004). Therefore, microfacies F indicates oligotrophic conditions. The same facies has been reported for the Qom section by Amirshahkarami *et al.*, (2014) and Mohammadi *et al.*, (2011).

MF G: Corallinaceaen bryozoan bioclastic packstone to wackstone

Microfacies G is characterized by the dominance of coralline red algae (*Lithothamnium*) and echinoid debris (Fig. 3.4). This microfacies also contains bryozoans and subordinate components include the larger foraminiferal genera *Miogypsinoides* and *Lepidocyclina*. At Molkabad section, this microfacies occurs in sediments of an Aquitanian age. This facies is equivalent to RMF 8 of Flügel (2004) and can be assigned to a middle ramp depositional setting at a water depth below the fair weather base, but above the storm wave base.

The association of corralinacean red algae and presence of larger perforate benthic foraminifera places the middle ramp environment in an oligophotic (Brandano and Corda, 2002; Cordan and Brandano, 2003) to mesophotic zone (Hottinger, 1997; Pomar, 2001). The same facies has been reported from Malta (Corda and Brandano 2003), and the Zagros Basin (Vaziri-Moghaddam *et al*., 2006; Dill *et al.*, 2010).

MF H: Bryozoan corallinacea boundstone

The framework of microfacies H comprises corallinacea and bryozoans (Fig 3.4). A minor component is *Kuphus* (marine bivalve). This facies is associated with sediments of an Aquitanian age at the c1 member.

The association of corallinacea and bryozoans suggests sediment export from a moderately deep environment on the middle ramp. Coralline red algae can abundantly thrive in oligotrophic waters of low light intensity (Halfar and Mutti 2005). Bryozoans are independent from light and can thus live in deeper waters with low energy (Pomar 2001a, b, Beavington-Penny and Racey, 2004). Coralline red algae can be well developed under raised nutrient levels (Bassi 2005; Halfar and Mutti 2005) and reduction of light penetration (Halfar and Mutti 2005). Based on the nutrient limitation model of Wood (1993) a facies dominated by coralline red algae may be characteristic for mesotrophic conditions. Similar facies have been reported from other sections of the Qom formation (Reuter *et al.*, 2007).

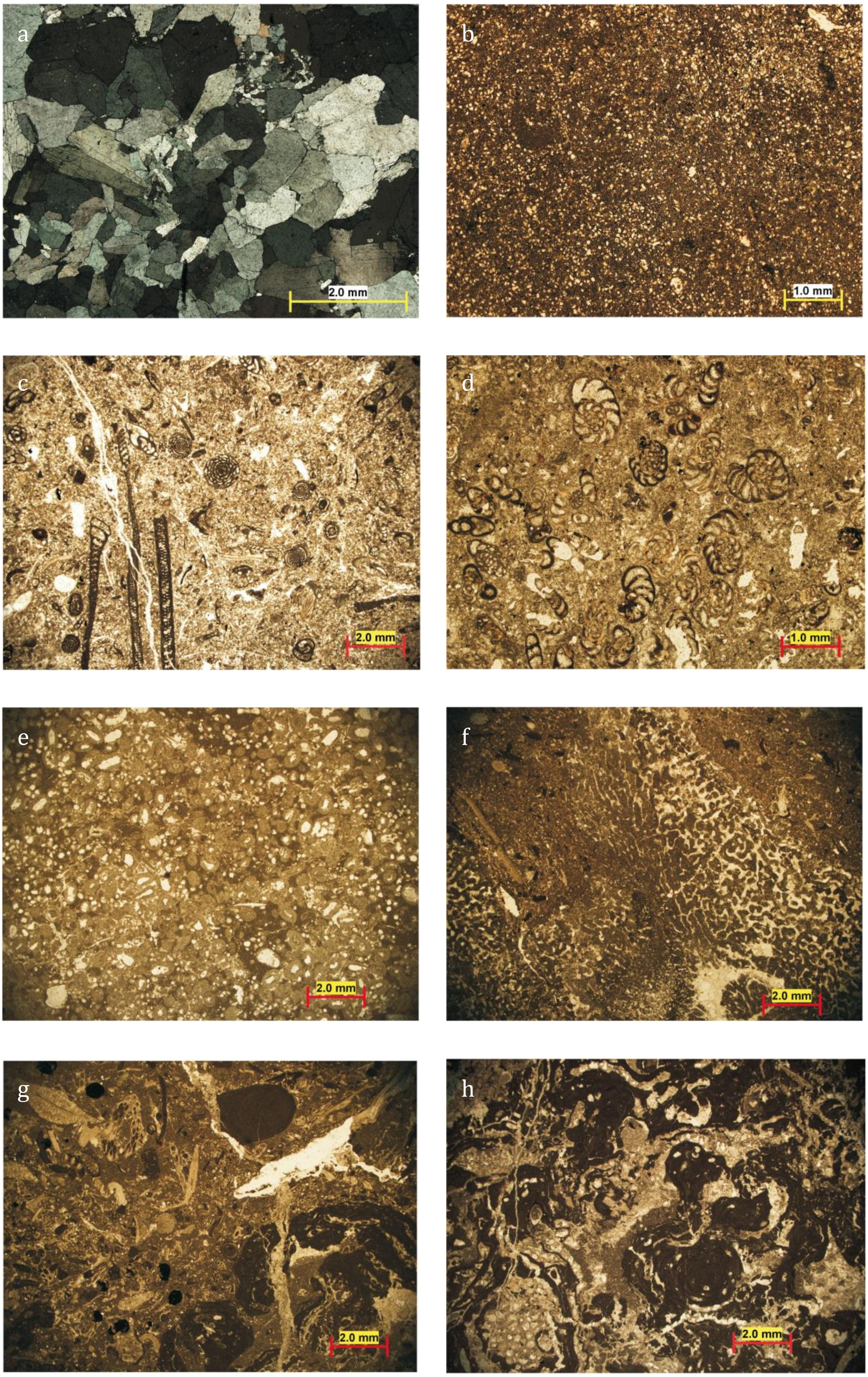

Figure 3.4: Images of microfacies types at Molkabad section. a) MF A: Gypsum (No. 565), b) MF B: Sandy mudstone (No. 614), c) MF C: Imperforate foraminifera bioclastic packstone (No. 661), d) MF D: Imperforate foraminifera *Dendritina rangi* wackestone (No. 667), e) MF E: Miliolid ooid grainstone (No. 559), f) MF F, Coral boundstone, (No. 600), g) MF G, Corallinacean bryozoan bioclastic packstone to wackestone (No. 554), h) MF H, Corallinacea bryozoan boundstone (No. 563).

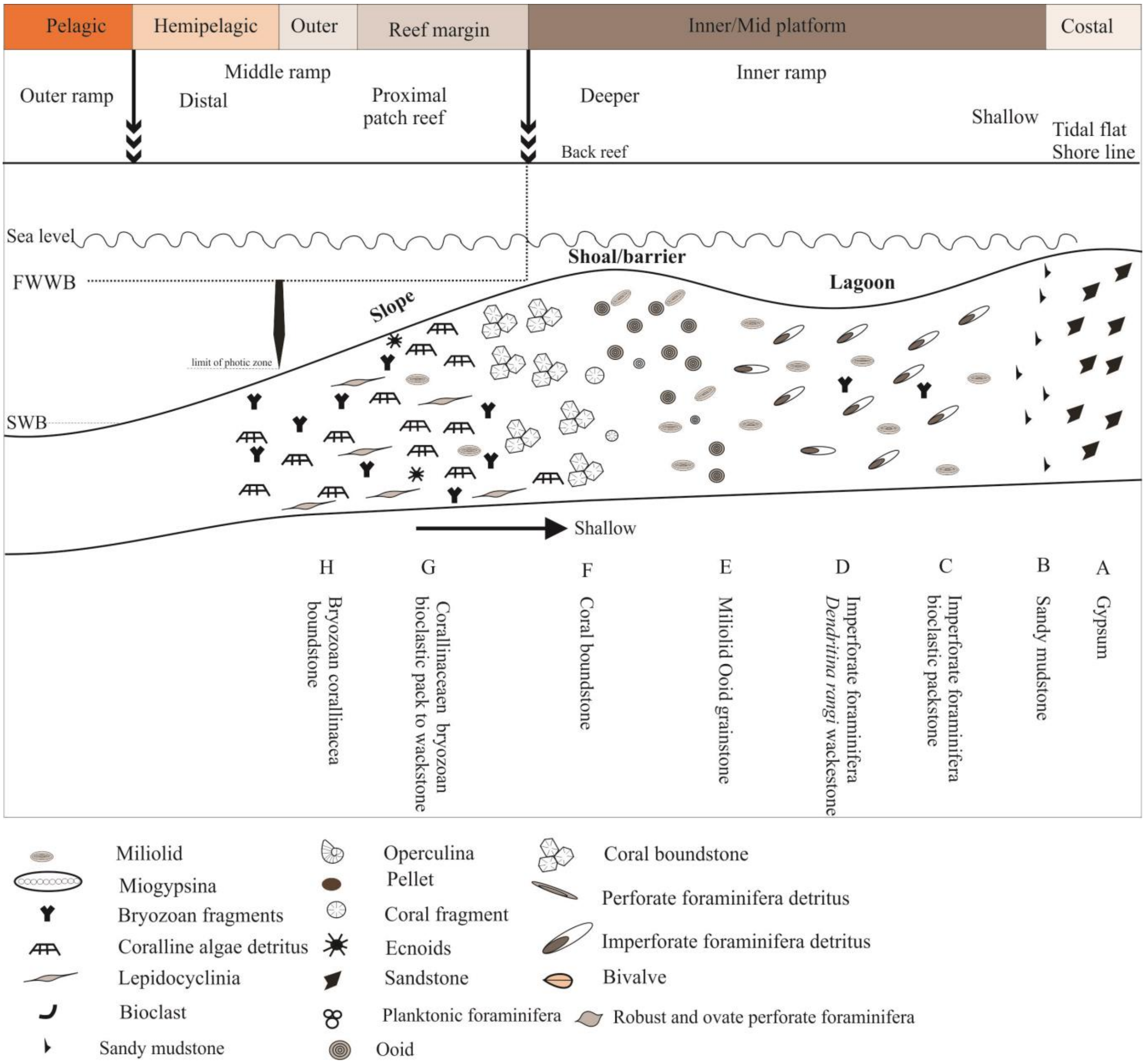

Figure 3.5: Qom Formation depositional model for the Molkabad section, adapted from Amirshahkarami and Karavan (2014). In accordance to the identified facies types at Molkabad section, four major depositional environments could be recognized along the carbonate ramp, including all parts of the inner and middle ramp. SWB: Storm wave base; FWWB: Fair weather wave base.

3.4.1.2 RECONSTRUCTION OF DEPOSITIONAL ENVIRONMENTS AT MOLKABAD SECTION

In accordance to the vertical distribution of facies types, sedimentary texture and fossil associations, the Qom Formation was deposited on a carbonate ramp. Based on Burchette and Wright (1992) ramp depositional environments can be divided based on the fair weather wave base (FWWB) and the storm wave base (SWB).

The facies distribution in the studied section allows for the distinction of four major depositional systems along the carbonate ramp. The proposed depositional model corresponds to the Eocene-Miocene ramp model of Corda and Brandano (2003) and Brandano *et al.*, (2010) (Fig. 3.5). (1) The shallow part of the inner ramp (proximal) is documented by microfacies types MF A, MF B, MF C, and MF D. Deposition likely occurred above the FWWB. This environment is associated with the occurrence of porcelaneous benthic foraminifera like *Borelis*, *Meandropsina*, *Peneroplis*, *Triloculina*, and *Austrotrillina.* (2) The deeper part of the inner ramp (distal) and transition to the shallower part (proximal) of the middle ramp are documented by microfacies types MF E and MF F. The sediments were deposited under a constant wave-agitated environment across the FWWB. The deeper parts of the inner ramp and shallower parts of the middle ramp are inhabited by larger hyaline benthic foraminifera like *Miogypsina*, *Miogypsinoides*, *Neorotalia*, and *Amphistegina.* (3) The shallow parts of the middle ramp (proximal) is documented by microfacies type MF G. Sediments of this facies were deposited under the influence of the FWWB and are characterized by corals and corallinacean red algae. (4) The deeper parts (distal) of the middle ramp are documented by facies type MF H. Sediments of this facies were deposited below the FWWB and near the SWB.

3.4.2 NAVAB SECTION

3.4.2.1 MICROFACIES TYPES

Based on the sediments fabric features and the dominant biogenic components, ten microfacies (MF) types were identified in sediments of the Qom Formation at the Navab anticline section (Figs. 3.3, 3.6, 3.7).

MF A: Bioclastic corallinaceaen packstone

Microfacies A occurs in the Miocene part of the section and is characterized by relatively fine-grained packstones (Figs. 3.3, 3.6). Corallinacean red algae are the main element of this microfacies. In this facies both perforate and imperforate benthic foraminifera appear together.

Miliolids exists in most sections. Imperforate benthic foraminifera include the genera *Austrotrillina*, *Quinqueloculina*, *Triloculina*, *Dendritina*, and *Miogypsina.*

The presence of perforate foraminifera, red algae, and imperforate foraminifera suggests deposition in the transition zone between lagoonal and open marine environments and absence of an effective barrier (Romero *et al.*, 2002). Similar facies types have been reported from Miocene successions in Italy (Corda & Brandano, 2003), from late Oligocene successions in Austria (Lower Inn Valley, Nebelsick *et al.*, 2001), from early Oligocene successions in Southern Italy (Pomar *et al.*, 2014, Salento peninsula), and from Oligocene-Miocene inner ramp successions of the Zagros Basin (Vaziri-Moghaddam *et al.*, 2006; Amirshahkarami, 2013).

MF B: Echinoid sandy bioclastic corallinacean packstone to wackestone

Microfacies B is characterized by a packstone–wackestone texture with unsorted sandy particles. This microfacies is dominated by coralline algae, making up more than 60% of all components, and occurs in sediments of Burdigalian age (Figs. 3.3, 3.6). This microfacies contains small amounts of bryozoans, brachiopods, echinoids, miliolids, small benthic foraminifera, and very few planktonic foraminifera.

This microfacies was likely deposited in a restricted marine environment, confirmed by small and low diversity of rotaliids and echinoids. The presence of a low-diverse benthic foraminiferal fauna and the dominance of mud-rich textures with miliolids are suggestive of deposition on a restricted platform with low hydraulic energy (Geel, 2000). The presence of stenohaline organisms such as echinoderms and the high abundance of bioclasts prove normal marine salinity conditions.

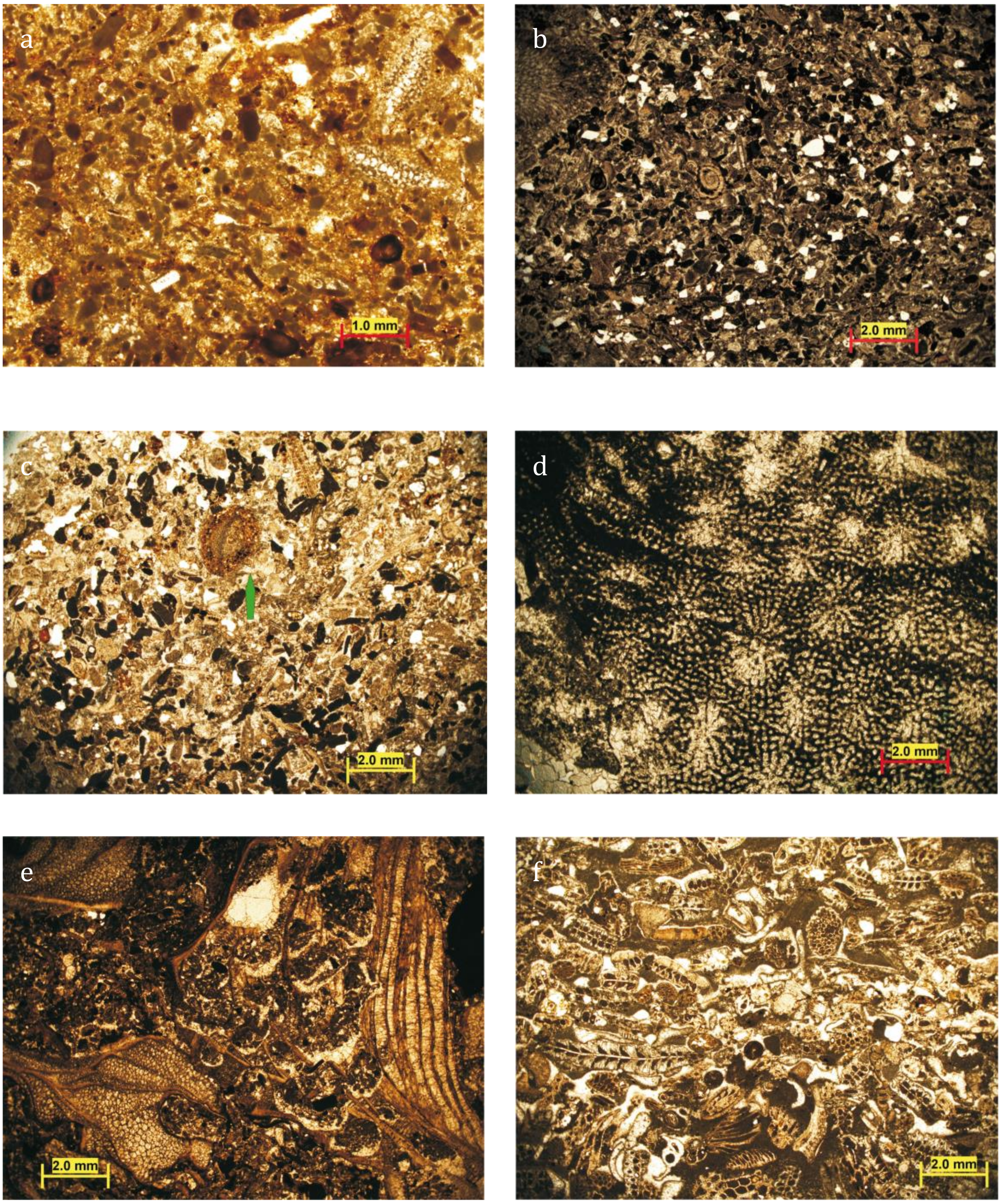

Figure 3.6: Images of microfacies types a to g at the Navab section. a) MF A: Bioclastic corallinaceaen packstone, (No. 400), b) MF B: Echinoid sandy bioclastic corallinacea packstone to wackestone (No. 383), c) MF C: Corallinacean bioclastic grainstone (No. 356), d) MF D: Coral boundstone (No.401), e) MF E: Oyster rudstone (No. 380), f) MF F: Bioclastic bryozoan packstone (No. 353), g) MF G: *Operculina* corallinacean packstone (No.408).

MF C: Corallinaceaen bioclastic grainstone

The main element of this facies is red algae. Associated components include larger benthic foraminifera of the family Nummulitidae, lepidocyclinids (*Nephrolepidina*), *Valvulina* sp., *Textularia* sp., *Asterigerina* sp., brachiopods, and bryozoan debris (Figs. 3.3, 3.6).

Coralline algae are able to live under oligotrophic conditions and are abundant in waters with low light penetration (Halfar and Mutti 2005). This microfacies was likely deposited on a barrier of the carbonate ramp.

MF D: Coral boundstone

Microfacies D is characterized by colonial corals and is associated with a Burdigalian age (Figs. 3.3, 3.6).

Colonial corals are in-situ organism, which exist in reef environment (Wilson, 1975; Flügel, 2004). Mehdi Yazdi *et al.* (2012) reported colonial corals of the Qom Formation from the Dizlu area. In the study area, there are some rich coral faunas present in patches. The existence of in-situ organisms such as colonial corals suggests a reef environment (Wilson, 1975; Flügel, 2004). Commonly, coral reef communities are accustomed to oligotrophic conditions (Hallock and Schlager, 1986; Flügel, 2004). The growth and colonization of Cenozoic corals in marine environments dependent on multiple ecological factors, including salinity, sedimentation rate, temperature, light penetration, lithofacies features of the substrate, water energy and turbidity (Dodd and Stanton 1990; Veron 1995; Riegl and Piller 2000; Vennin *et al.*, 2004; Tsaparas and Marcopoulou-Diacantoni 2005; Bosellini and Perrin 2008).

MF E: Oyster rudstone

Microfacies MF E is dominated by robust bivalve shells accounting for approximately 75% of all components (Figs. 3.3, 3.6). Other large bioclasts comprise fragments of corals, bryozoans and red algae. This microfacies corresponds to RMF 15 of Flügel (2004) and is common on open inner ramp environments.

Bivalves are prevalent components in freshwater, brackish and marine environments, which contribute to the bioclast content of limestone. High numbers of bivalve shells contribute to the formation of bioclasts in wackestones, packstones, floatstones and rudstones. Bivalve limestones form in a number of different marine depositional settings, from the beach across the shelf and the shelf margin to the slope (Flügel 2004).

MF F: Bioclastic bryozoan packstone

Microfacies MF F is characterized by a packstone texture in a micritic matrix. The components are dominated by bryozoan fragments (up to 80% of all components). Associated bioclasts comprise corallinacean algae (10%) and few perforate foraminifera (*Rotalia viennoti*) and imperforate foraminifera (miliolids). This microfacies occurs in sediments of Chattian age (Figs. 3.3, 3.6).

Microfacies MF F has likely been deposited in an open marine environment. The bioclastic bryozoan corallinacean packstone indicates the absence of an effective barrier to the open marine environment (Wilson, 1975; Flügel, 2004). Bryozoans do not need light to live because they are heterotrophs (Brandano and Corda 2002). A similar microfacies has also been reported from the Qom section (Amirshahkarami and Karavan, 2014).

MF G: *Operculina* corallinacean packstone

Microfacies MF G is characterized by a grain-supported packstone texture. The major components of this microfacies include coralline algae (60%) and well-preserved perforate foraminifera such as large and robust Nummulitidae (*Operculina*). Occasional components are *Miogypsina*, miliolids, *Textularia* and *Valvulina* (Figs. 3.3, 3.6).

Coralline algae live under oligotrophic conditions and are abundant in water depths at low light intensities (Halfar and Mutti 2005). Oligotrophic conditions in middle shelf settings are characterized by numerous corallinacea and larger benthic foraminifera (such as *Operculina*) (Brandano and Corda 2002; Amirshahkarami *et al.*, 2007). Similarly, shallow water ecosystems under the influence of open marine conditions are inhabited by perforate foraminifera with symbiotic algae (e.g. Lepidocyclinidae, larger and flat Nummulitidae) (Geel 2000). Based on the ecological requirements of the main biogenic constituents, MF G was likely deposited in the upper part of the slope under oligophotic to mesophotic conditions.

MF H: Bioclastic Lepidocyclinidae packstone

Microfacies H has a grain–supported texture in a micritic matrix (packstone). The major allochems are perforated larger benthic foraminifera such as *Amphistegina, Operculina*, *Eulepidina* and *Nephrolepidina.* Other skeletal grains include *Textularia* and bryozoans. This microfacies occurs in sediments of a Chattian age. (Figs. 3.3, 3.7)

The dominance of large and flat tests of nummulitids and lepidocyclinids (*Eulepidina*) is representative of this microfacies. According to Hallock (1985) and Hallock and Glenn (1986) large-sized lepidocyclinids and discoidal flat tests (such as those of *Eulepidina*) are typical for a low-energy oligophotic environment on the outer ramp. Equally, large and flat Lepidocyclinidae, Nummulitidae and bryozoans are commonly found components in more open-marine conditions (Hottinger, 1983, Hottinger, 1997, Leutenegger, 1984, Reiss and Hottinger, 1984, Hohenegger, 1996, Hohenegger *et al.*, 1999; Romero *et al.*, 2002). Similar microfacies and faunal associations have been reported from a number of sections and time intervals, including the Bijegan and Tanbour sections of the Qom Formation (Anjomshoa and Amirshahkarami, 2014; Karavan *et al.*, 2015), the Rupelian–Chattian lower beds of the Asmari Formation in the Zagros Basin, southwest of Iran (Vaziri-Moghaddam *et al.*, 2010; Amirshahkarami, 2013 a), the Oligocene-Miocene deposits in the southwest of Zagros Basin (Roozpeykar and Moghaddam, 2016), and the Abadeh section (Reuter *et al.*, 2007) of the Asmari Formation .

MF I: Planktonic bioclastic wackestone to packstone

A wackestone–packstone texture with a low diversity of imperforate foraminifera, such as miliolids, and other small benthic foraminifera characterize Microfacies I. This microfacies has been identified in sediments of Burdigalian age (Figs. 3.3, 3.7)

Planktonic foraminifera are characteristic for open marine environments. Accordingly, abundant planktonic foraminiferal tests in sediments indicate deposition at deeper and more pelagic conditions (Mateu-Vicens *et al.*, 2008a). According to Geel (2000), the lack of larger benthic foraminifera is indicative of deposition at water depths of more than 200 m (aphotic zone). The same facies of Oligocene sequences is recorded by Reuter *et al.* 2013, and at the base of the Asmari Formation from different parts of the Zagros area (Amirshahkarami *et al.*, 2007; Sadeghi *et al.*, 2009, Vaziri-Moghaddam *et al.*, 2010).

MF J: Sandy planktonic peloidal packstone

Microfacies J is characterized by a packstone texture. Both skeletal and non-skeletal components are the main elements of this microfacies. Skeletal components contain planktonic foraminifera, whereas peloids represent the dominant non-skeletal elements, with more than 80% relative abundance. This microfacies has been identified in sediments of Burdigalian age (Figs. 3.3, 3.7).

As already discussed above (MF I), the frequent presence of planktonic foraminifera indicates deposition of this microfacies in a deep and calm environment under the influence of normal-saline waters (Wilson, 1975; Buxton and Pedley, 1989; Flügel, 2004).

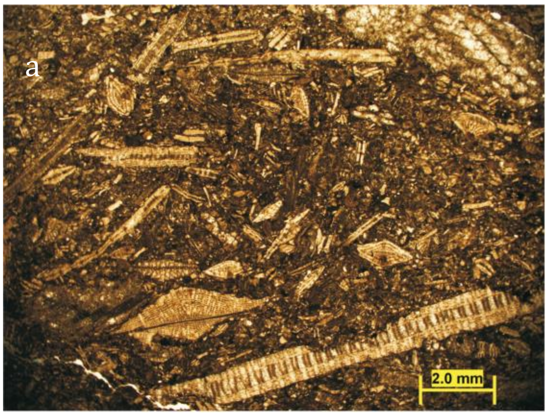

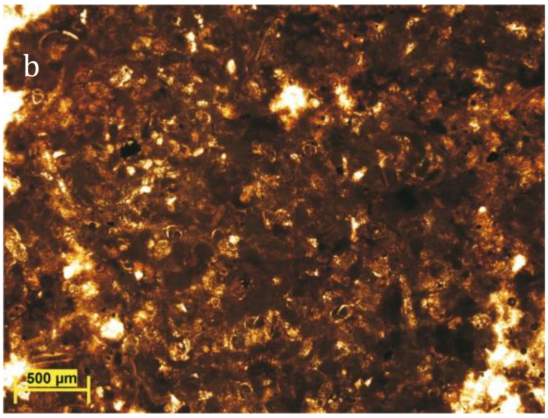

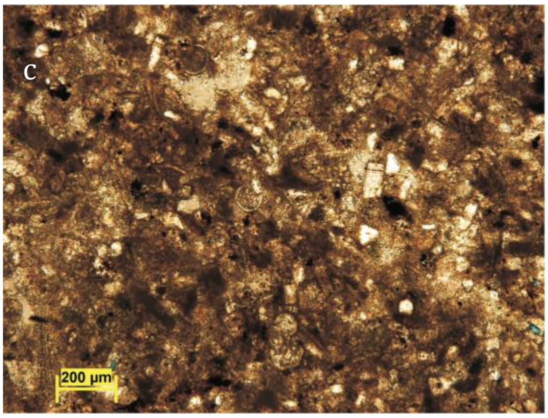

Figure 3.7: Images of microfacies types at Navab anticline section .a) MF H: Bioclastic Lepidocyclinidae packstone (No. 362), b) MF I: Planktonic bioclastic wackestone to packstone (No. 393), c) MF J: Sandy planktonic peloidal packstone (No 396).

3.4.2.2 RECONSTRUCTION OF THE DEPOSITIONAL ENVIRONMENT AT THE NAVAB ANTICLINE SECTION

Microfacies analysis of sediments from the Navab section of the Qom Formation is indicative of open marine, patch reef, lagoon, and semi-restricted lagoon environments. The paleoenvironmental reconstruction suggests deposition of the Navab section on a homoclinal carbonate ramp (Fig. 3.8). On the basis of the classical facies model of Burchette and Wright (1992), a carbonate ramp is divided into inner ramp, middle ramp and outer ramp. Accordingly, the Navab section corresponds to an inner–middle ramp environment. Lagoonal environments are representative of the inner ramp, and shallow-water open marine and similarly patch reef environments are characteristic of the middle ramp. The outer ramp environment has not been recognized in the studied section. The most commonly found microfacies types of the inner ramp are wackestone, packestone, and grainstone with imperforate foraminifera (microfacies A, B and C). In a lagoon environment, imperforate foraminifera (e.g. miliolids in microfacies A and B) are abundant (Hallock and Glenn, 1986;

Geel, 2000). Microfacies C was deposited in a semi-restricted lagoon environment and was recognized by the co-existence of imperforate and perforate foraminifera. The middle ramp includes proximal and distal parts. The proximal part of the middle ramp is differentiated by patch reefs and reef-derived bioclasts such as colonial corals (microfacies D and E). The distal part of the middle ramp contains perforate foraminifera such as Lepidocyclinidae and *Nummulites* (microfacies G, and H). At the Navab section sedimentary environments are equivalent to an inner–middle ramp. Middle ramp environments are more widespread than inner ramp environments in the Aquitanian–Burdigalian part of the succession.

3.5 CONCLUSIONS

The depositional environments of the Oligocene-Miocene sediments of the Qom Formation were interpreted based on facies analysis and the identified foraminiferal associations. The sediment textures and microfacies of sediments from the Molkabad and Navab anticline sections suggest deposition on a homoclinal carbonate ramp. Inner ramp environments are more widespread than middle ramp environments in the Aquitanian-Burdigalian parts of the Molkabad section, and the Chattian–Aquitanian parts of the Navab section. A total of eighteen facies types were identified, representing tidal flat, semi-restricted lagoon, lagoon, patch reef and open marine environments of the inner, middle and outer ramp. The environmental interpretations show that the inner and middle parts of a homoclinal ramp were most prominent during the deposition of the Qom Formation in Central Iran.

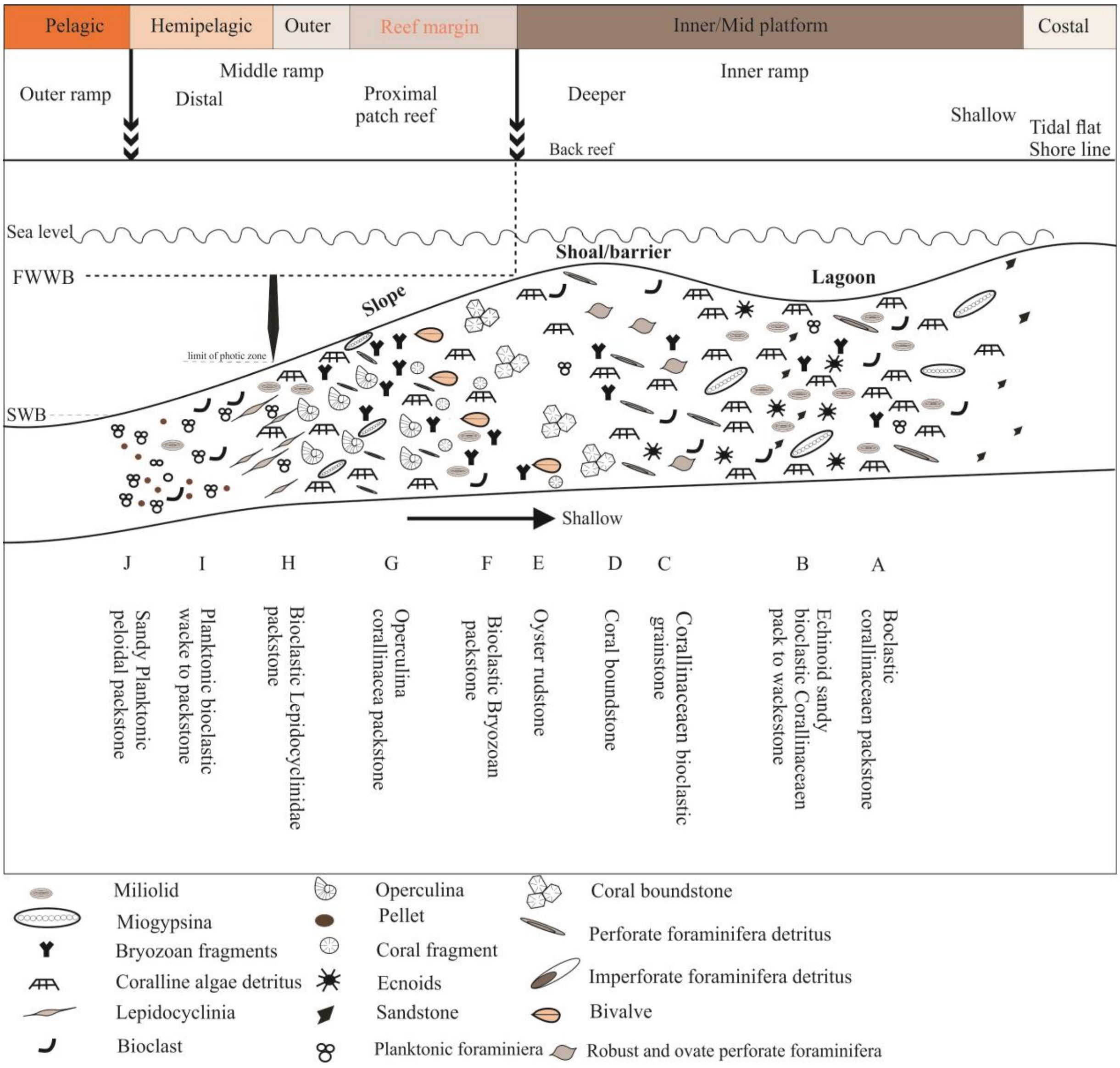

Figure 3.8: Depositional model for the Navab Section, adapted from Amirshahkarami and Karavan, 2014. The Palaeoenvironmental reconstruction suggests a homoclinal carbonate ramp. Based on classical facies models of Burchette and Wright (1992) the depositional system at Navab anticline can be separated into an inner ramp and middle ramp environment. FWWB: Fair weather wave base; SWB: Storm wave base.

4 CHAPTER: PALEOENVIRONMENTAL RECONSTRUCTION OF THE OLIGOCENE-MIOCENE DEPOSITS OF THE TETHYAN SEAWAY, QOM FORMATION, CENTRAL IRAN

ABSTRACT

The Qom Formation was deposited in the central Iranian back-arc basin during the Oligocene-Miocene and documents the closure of the Tethyan Seaway. Based on sedimentological data, various depositional models have been presented for the Oligocene-Miocene successions of central Iran, Sanandaj-Sirjan and Urumieh Dokhtar magmatic arc provinces in Iran. In this study, foraminiferal faunas were studied based on a total of 45 samples from the Molkabad section, located northwest of Molkabad Mountains. Changes in the composition of the benthic foraminiferal fauna were used to reconstruct the paleoenvironmental evolution during deposition of the Qom Formation. The Molkabad section mainly consists of limestones, calcareous marls, marls, and gypsum-bearing marls with a total thickness of 760 meters. The Qom Formation at Molkabad sections overlies Eocene rocks with an unconformity. The studied sediments contain a variety of red algae, bryozoans and benthic and planktonic foraminifers. The distribution of index larger benthic foraminifers in Molkabad section suggests a late Oligocene (Chattian) to early Miocene (Aquitanian-Burdigalian) age, comprising the *Miolepidociyclina-Miogypsinoides* and *Borelis melo curdica-Meandropsina iranica-schlumbergerina* assemblage zones.The small benthic faunas of the Molkabad section represent typical inner-neritic depositional environments supported by the predominance of marls and algal and bryozoan limestones in this section. The preliminary bathymetric reconstruction suggests deposition of the succession in water depths commonly shallower than 50m. The estimated values of water depth range between 36 and 94 m but the strong predominance of the genera *Ammonia* and *Elphidium* points to an even lower water depth in some intervals.

4.1 INTRODUCTION

The closure of the Tethyan Seaway is best documented in the Oligocene/Miocene Qom Formation that represents the last marine transgression in Central Iran. During the so called Terminal Tethyan Event, the Tethyan Seaway was closed due to the collision of the African/Arabian and Iranian/Eurasian plates. The Qom Formation has been deposited on extensive mixed carbonate-siliciclastic ramps in the central Esfahan-Sirjan and Qom basins that are separated by an island arc complex (Reuter *et al.*, 2009)(Fig. 4.1). It mainly contains marine marls, limestones, gypsum and silisiclastics. Facies analyses from the Molkabad section indicate sedimentation of the Qom basin along a carbonate platform ramp.

The Qom Formation is one of the most important gas and oil reservoirs of Central Iran, analogous to the Asmari Formation of Southwest Iran (Vaziri-Moghaddam *et al.*, 2006). Organic geochemical analysis indicated that the hydrocarbons migrated from deeper source rocks, likely of Jurassic age (Sabouhi *et al.* 2010). Marine sediments of the Qom formation contain rich foraminiferal faunas that have not yet been studied in detail. In addition, little is known on the interplay between climate and regional tectonic changes on the paleo environments and marine ecosystems of the Iranian gateways. Particularly, accurate regional sea-level reconstructions and a proper correlation to the up-to date global sea-level records are still missing. This study will contribute to this subject, exploiting the paleo environmental potential of the foraminiferal fauna. Hence, I define important foraminiferal assemblages and reconstruct the paleo environmental setting of the Qom Formation in the Molkabad outcrop. Ecological information from modern faunas of the Persian Gulf will be used as Recent equivalents and are applied to the assessment of paleo water depth and paleo salinity.

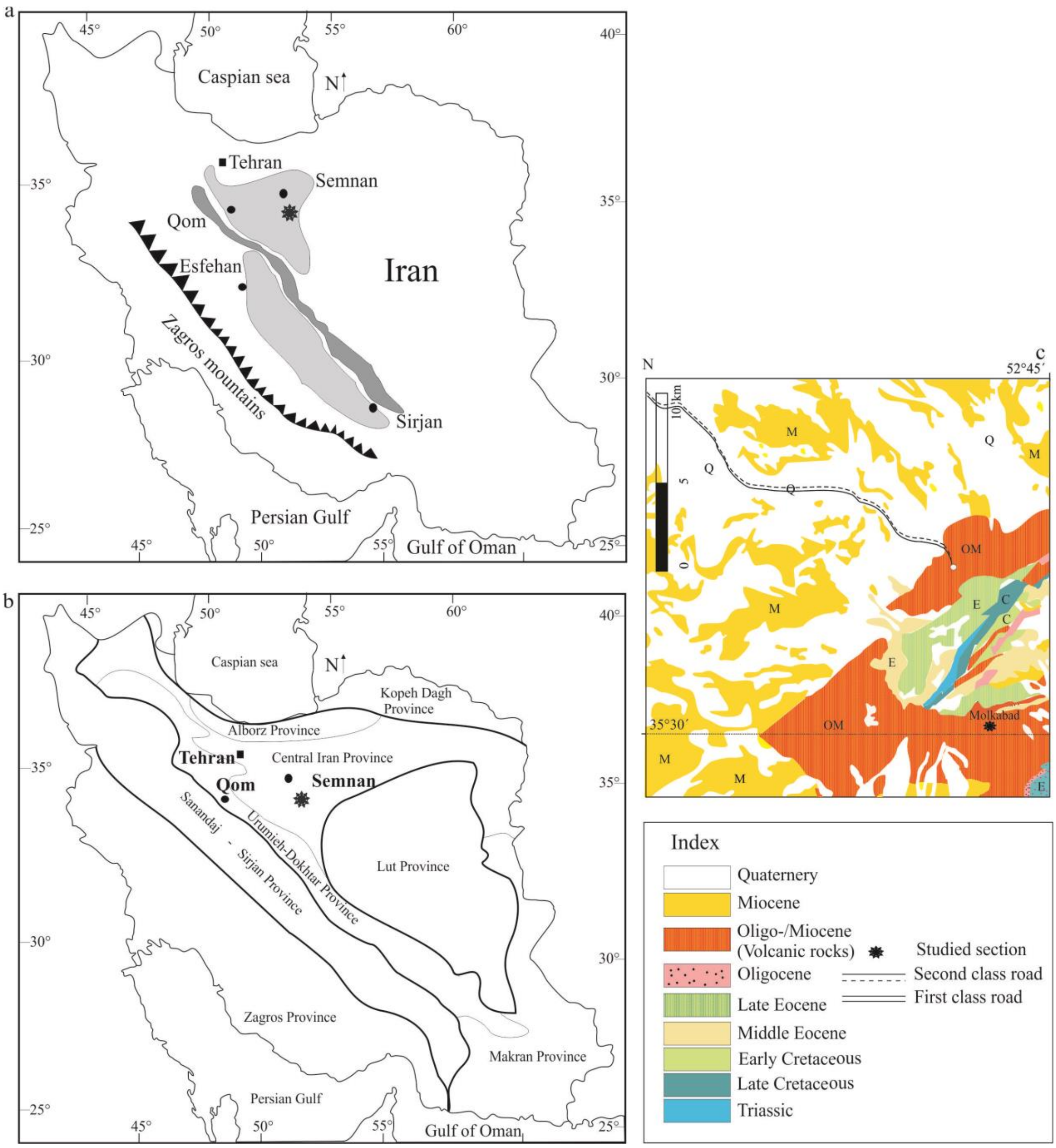

Figure 4.1: Location map of the study area in the Molkabad Mountains. (a) Position of the studied profile, the position of the Esfehan-Sirjan and the Qom basins in light gray and the volcanic arc in dark gray (modified from Schuster and Wieland, 1999; Reuter *et al.*, 2009), (b) the studied locations in central Iran and the position of continental fragments of the Iranian Plateau. (Modified from Geological Survey of Iran). Zagros, Sanandaj-Syrjan, Urumieh-Dokhtar, Central Iran, Alborz, Kopeh-Dagh, Lut, and Makran (modified after Heydari et al, 2003; Aghanabati, 2004) and (c) Geological map of the study area in the vicinity of the Molkabad section.

4.2 GEOLOGICAL SETTING

The Molkabad section is located in the Molkabad Mountains southeast Garmsar in central Iran at coordinates 35°21´ N, 52°43´ E (Fig. 4.1). The Qom Basin at the Molkabad Mountains represents an Early Miocene carbonate platform (Fig. 4.1). The Qom Basin, and the Iranian Plate, represent the southeastern margin of the Paratethys, and contains sedimentary archives for the documentation of the paleogeographic history, particulary the separation of the Mediterranean Sea and Indo-Pacific region during the Late Oligocene to early Miocene (Stöcklin and Setudenia, 1991; Rögl, 1998; Seyrafian and Toraby, 2005; Reuter *et al.*, 2009, Khaksar and Maghfouri Mogaddam, 2007; Daneshian and Ramezani Dana, 2007; Mohammadi *et al.*, 2011; Behforouzi and Safari, 2011; Yazdi *et al.*, 2012).

4.3 MATERIAL AND METHOD

The Molkabad section of the Qom Formation is located in the Molkabad area, southeast of Garmsar 35°21´ N, 52°43´ E. The Molkabad section comprises a 760 m thick succession of limestones and marls. The succession can be divided into four different lithological units, comprising the Lithothamnium Limestone, Lower Marl Unit, Bryozoa Limestone and Upper Marl Unit. (Fig. 4.2).

In this study a total of 45 marl samples have been studied for quantitative benthic foraminiferal faunal analysis from the Molkabad section (Fig 4.2). On average 50 g of dry sediment was treated with hydrogen peroxide for disaggregation and subsequently was washed through a 125µm sieve. The residue was dried at 40C°. The investigation of the benthic foraminiferal fauna was carried out on representative splits of the size fraction >125µm. At least 300 specimens were counted for each sample. The picked samples were studied and documented by using a Scanning Electron Microscope. Species determination was mainly based on AGIP (1982) and Lutze (1974).

The foraminiferal data were statistically evaluated for paleoenvironment interpretation by using the software PAST of Hammer *et al.* (2001) and Microsoft Excel:

1) Number of species (S) and total number of individuals (n)

2) Diversities were determined following the Shannon-Wiener information equation (Buzas and Gibson, 1969). The Shannon diversity index (Magurran 1988) was calculated as:

$$H(s) = -\sum p_i \ln p_i$$

3) Relative abundance (%) of benthic foraminifera

4) Percentage dominance, i.e. the highest percentage occurrence of a species in a sample

5) The relative abundance (%) of agglutinated taxa

6) The relative abundance (%) of porcellaneous taxa

7) Faunal assemblages were extracted using a Q-mode Principal Component Analyses (PCA). PC loadings >0.4 were regarded as statistically significant (Malmgren and Haq, 1982). PC scores >3 were assigned to dominant taxa and PC scores between 0.5 and 3 to important associated taxa of an assemblage.

The function Water depth (m) = e (3.58718+ (0.03534* %PF)) of Van der Zwaan *et al.* (1990) was used to assess the paleo water depth, based on the relative proportion of planktonic foraminifera (PF).

8) Paleo awter depth was estimated using P/B ratio, where P is the total number of planktonic foraminifera and B is a total number of benthic foraminifera (Sen-Gupta and Machain-Castillo, 1993; Drinia *et al.*, 2007; Holcová, & Zágoršek, 2008). The relative abundance of the planktonic foraminifera is associated with distance from shore (Van der Zwaan *et al.*, 1990; Wilson, 2003, Murray and Alve, 1999, Murray, 2006; Mandic and Harzhauser, 2003); the inner shelf environment (inner neritic) was defined with proportions of planktonic foraminifera of < 20%, the middle shelf (middle neritic) with 20-50%, and 50-70% for the outer shelf (outer neritic) environment (Murray, 1991, 2006; Pippèrr, 2011).

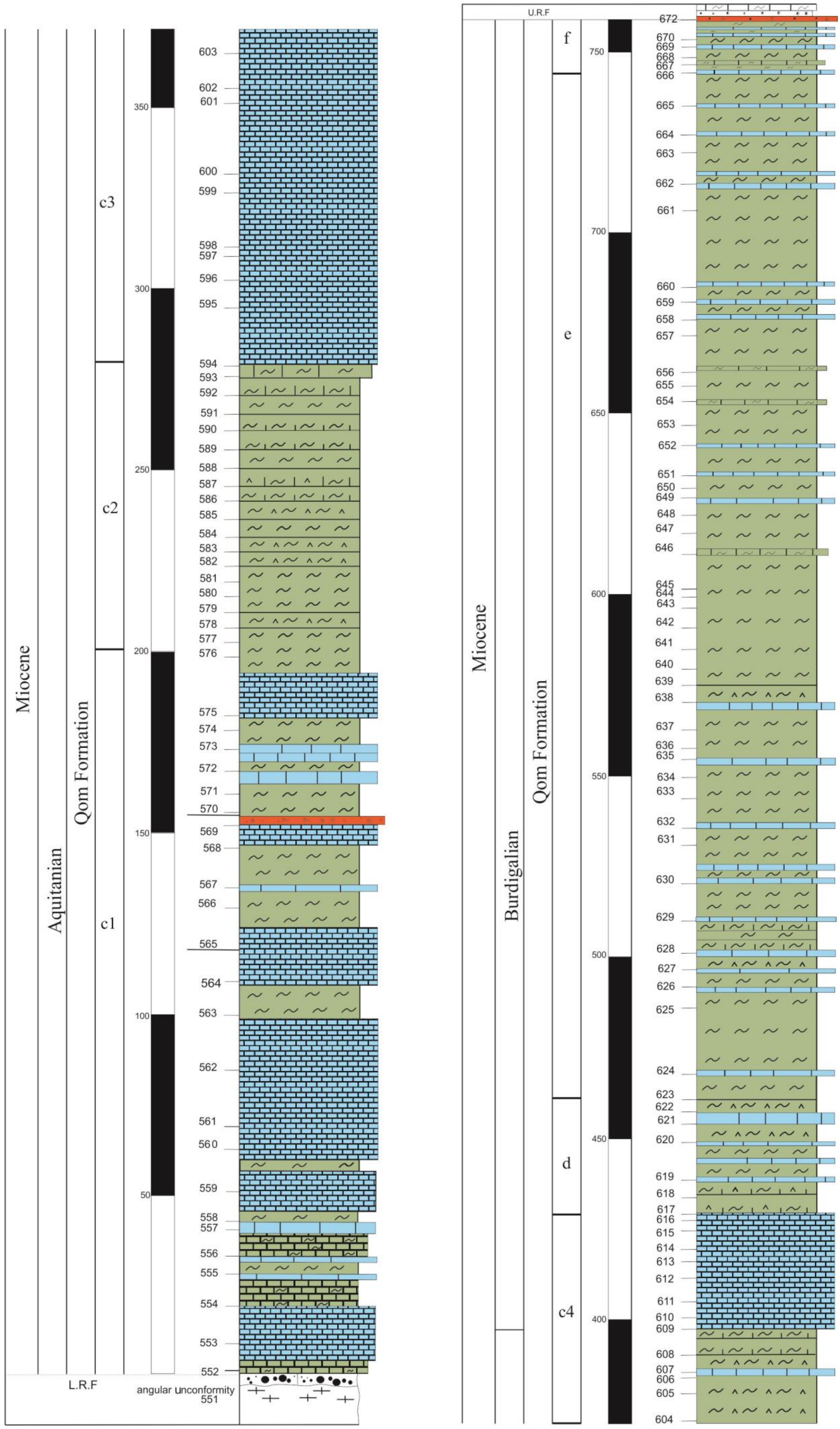

Figure 4.2: Schematic lithology and stratigraphy of the lower Miocene Qom Formation at the Molkabad Section. From left to right: chronostratigraphy, formation names, members, scale in meters, sampled beds, and lithological succession.

4.4 RESULTS

4.4.1 LITHOSTRATIGRAPHY OF MOLKABAD SECTION

The Molkabad stratigraphic section starts with a conglomerate, unconformably overlying the Eocene shallow marine carbonate beds and underlying strata of the Qom Formation (Fig. 4.2). The base of the Qom Formation is represented by a 127m thick succession of bedded and massive limestones with marly limestone intercalations, abundant in red algae and bryozoans. Small benthic foraminifera are rare. This unit is overlain by a 153m thick-bedded succession of greenish to gray marl with gray limestone intercalations. Sample numbers 552 to 575 represent the **c1** member and sample numbers 576 to 594 represent the **c2** member of the Qom formation. 94m of thick-bedded and massive bryozoan limestones overlie the thick marly succession and represent the **c3** member of the Qom Formation, including samples 594 to sample 604. Finally, the section is overlain by 384m thick green to gray marls, which are alternating partly with gypsiferous layers representing the **c4** member and with yellow to gray marls representing the **d** member. The upper part of the section is represented by thin-bedded limestones of the **e** member. At the top of the section thin-bedded limestones belong to the **f** member.

4.4.2 NUMERICAL FAUNAL PARAMETERS

In total, 45 marl samples were collected for benthic foraminiferal faunal analysis from the Molkabad section. The foraminiferal fauna of the marly sediments of the studied section is strongly dominated by benthic foraminifera. Planktonic foraminiferal tests only comprise between 0 and 24.35% of the total fauna (Fig 4.3). The diversity of the benthic foraminiferal fauna is comparatively low and fluctuates between H (S)=0.66 and 2.26. Maximum diversities are restricted to several intervals with enhanced numbers of planktonic foraminifera in the upper part of the Lower Marl Group (150m to 175m) and the central part of the Upper Marl Group (500m to 650m). These intervals also comprise highest proportions of arenaceous tests, mainly comprising various *Textularia* species. Miliolids mainly appear in the lower part of the studied section (225m to 275m) where they comprise up to 32.7% of the total benthic foraminiferal fauna. The majority of benthic foraminiferal tests are hyaline, including taxa typical for inner-neritic environments, such as *Ammonia* spp., *Elphidium* spp., *Nonion asterizans* etc.

4.4.3 BENTHIC FORAMINIFERAL ASSEMBLAGES

The Q-mode of Principal Component Analysis was used to reduce the data into a total of four main assemblages accounting for 76.15% of total variance of data set (Fig. 4.4, Tab. 4.1). SEM pictures of selected dominant and associated species of these faunas are figured on plates 8,9 .

The *Nonion asterizans* fauna (PC1) explains 42.10% of the total variance of the data set and contains *Elphidium granosum*, *Ammonia pauciloculata*, *Ammonia* spp., *Textularia* spp., and *Elphidum advenum* as associated taxa. This fauna mainly dominates samples from the central and upper part of the Molkabad succession. The *Elphidum granosum* fauna (PC2) with 14.10% of the total variance includes *Ammonia* spp., *Heterolepa mexicana*, and assorted miliolids, *Textularia* spp., and *Cibicides lobatulus* as associated taxa. This fauna is restricted to the lower part of the section. The *Ammonia / Elphidium* spp. fauna (PC3) with 10.9 % of the total variance includes *Elphidium advenum* and miliolids as associated taxa. This fauna is restricted to the repeated short intervals of the section. The *Ammonia pauciloculata* fauna (PC4) with 9.05% of the total variance comprises *Elphidium* sp., *Elphidum advenum*, *Textularia* spp. and *Ammonia* cf. *tepida* as associated taxa. This fauna is restricted to the uppermost part of the Upper Marl Group between 690 and 780 m, as well as a short appearance at about 250m in the Lower Marl Group.

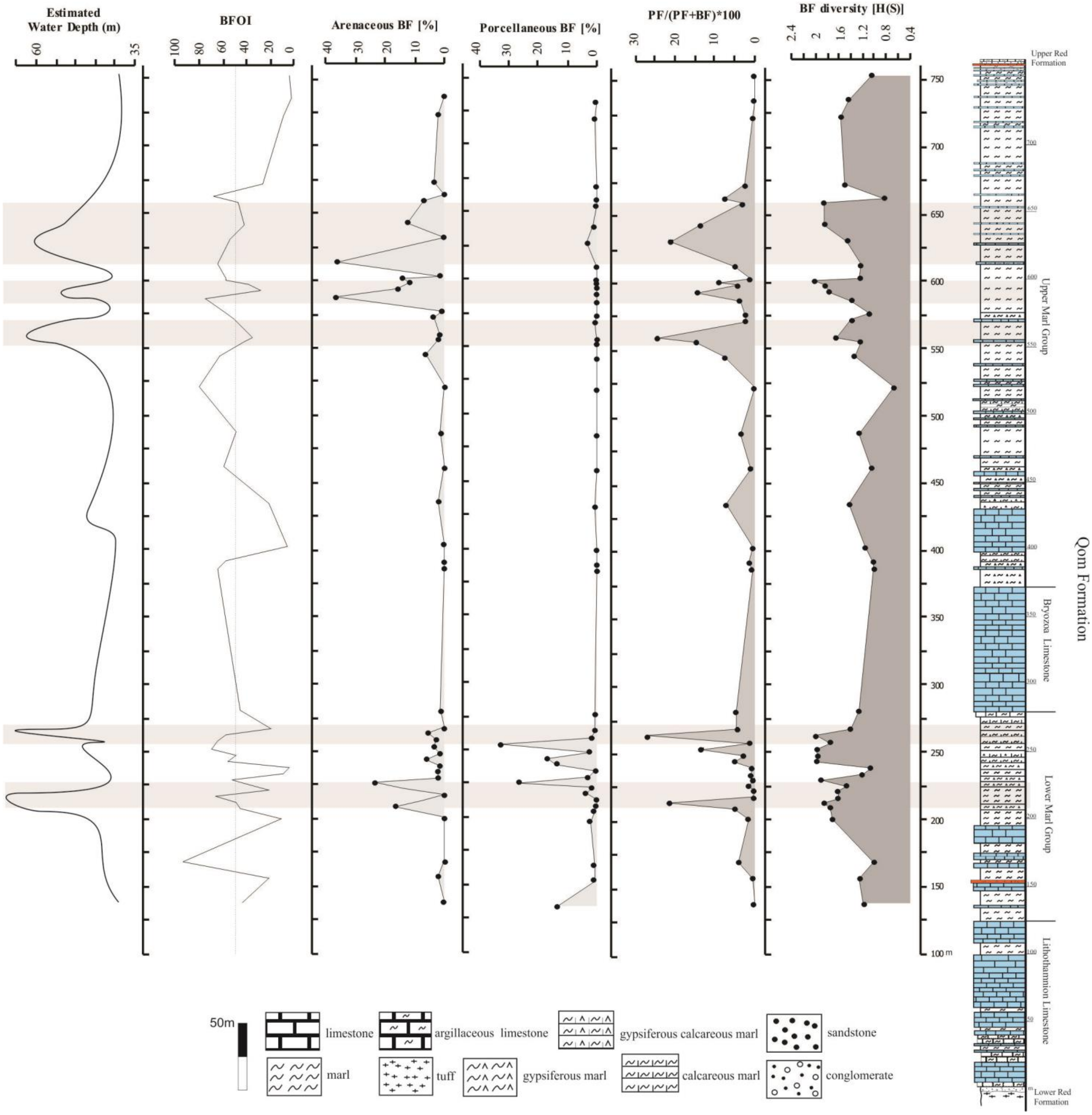

Figure 4.3: Generalized lithology, benthic foraminiferal diversity H(S), relative abundance of planktonic and benthic foraminifera, relative proportion of arenaceous (agglutinating) and porcellaneous (miliolid) taxa, and the smoothed curve of the reconstructed water depth is shown. Grey bars indicate intervals deposited below 50 m water depth. Highest benthic foraminiferal diversities are restricted to deepest intervals. The legend also applies for Figures 4.4.

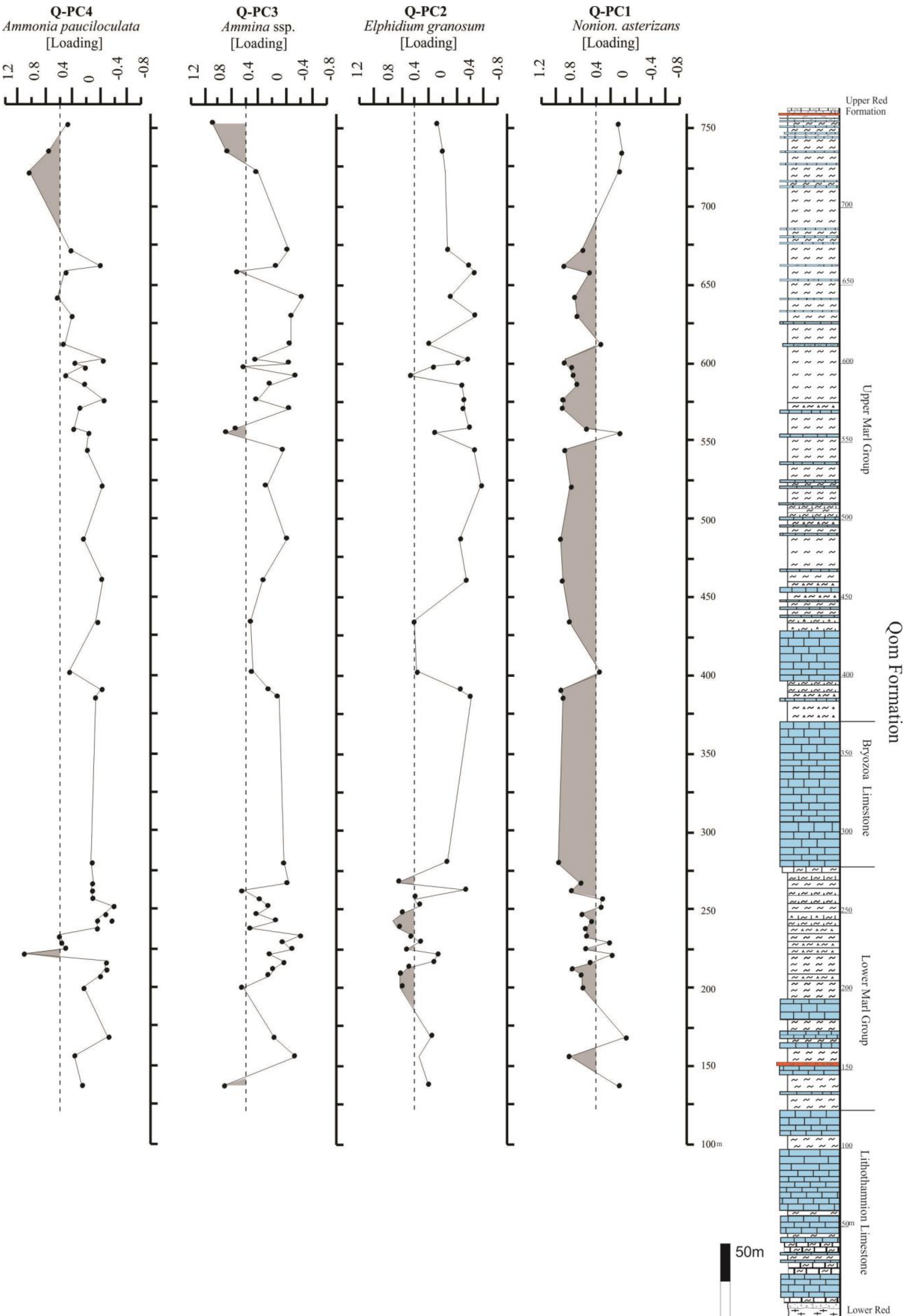

Figure 4.4: Q-mode benthic foraminiferal assemblages (four-component model) of the Molkabad section and generalized lithology. Statistically significant PC loadings >0.4 are indicated by gray shading.

Table 4.1: Species composition of the Q-mode benthic foraminiferal assemblages of the Molkabad section. Principle component number, dominant and associated benthic foraminiferal species with PC scores and explained variance are given.

No.	Dominant Taxa	Score	Associated Taxa	Score	Variance (%)
PC1	*Nonion asterizans*	16	*Elphidium granosum*	13.3	42.1
			Ammonia pauciloculata	4.1	
			Ammina spp.	3.3	
			Textularia spp.	2.7	
			Elphidium advenum	1.4	
PC2	*Elphidium granosum*	9	*Miliolids*	2.3	14.7
			Ammonia spp.	2.1	
			Heterolepa mexicana	2	
			Textularia spp.	1.2	
			Cibicides lobatulus	1.2	
PC3	*Ammonia* spp.	8.3	*Elphidium* sp.	5	10.94
			Elphidium advenum	2.8	
			Miliolids	1	
PC4	*Ammonia pauciloculata*	6.2	*Elphidium* sp.	6.2	9.05
			Elphidium advenum	3.9	
			Textularia spp.	2.6	
			Ammonia cf. *tepida*	1.7	

4.5 DISCUSSION

The distribution of small benthic foraminifera from the Molkabad section provides a variety of valuable paleoenvironmental information during the Miocene. This study will focus on the reconstruction of water depth, salinity and temperature discussing the available environmental information below. The comparison of the fossil faunas with equivalents from modern marine environments (Persian Gulf) will support the paleoenvironmetal recounstruction.

4.5.1 ENVIRONMENTAL SETTING

The Persian Gulf basin with an approximate area of 239,000 km^2 and a volume of 8780km^3 is located south of Iran. It is bounded to the North by flat land (the delta of Iranian and Iraqi rivers), to the Northeast by the Zagros mountains, and to the Southwest by the desert of Saudi Arabia. It is around 1000 km long and 200-300 km wide and has an average depth of 35m, and a maximum of around 100m in the easternmost part. The shoreline of the basin on the Iranian side is defined by mountains forming narrow coastal plains, whereas on the Arabian side, the gulf is constrained by low deserts and rocky topography.

The Persian Gulf has formed on a continental shelf (Fig. 4.6) and is linked to the Indian Ocean via a 60 km wide natural canal, the Straits of Hormuz. This basin is located in a tropical/subtropical biogeographic region causing a rise in the temperature and salinity of the water compared with the average recorded values of the open ocean for the same latitude. In addition, the arid climate of the region means that the evaporation exceeds the precipitation in the gulf by ca. 1000 mm per year. As a result, the water exchange with the Indian Ocean is remarkably low.

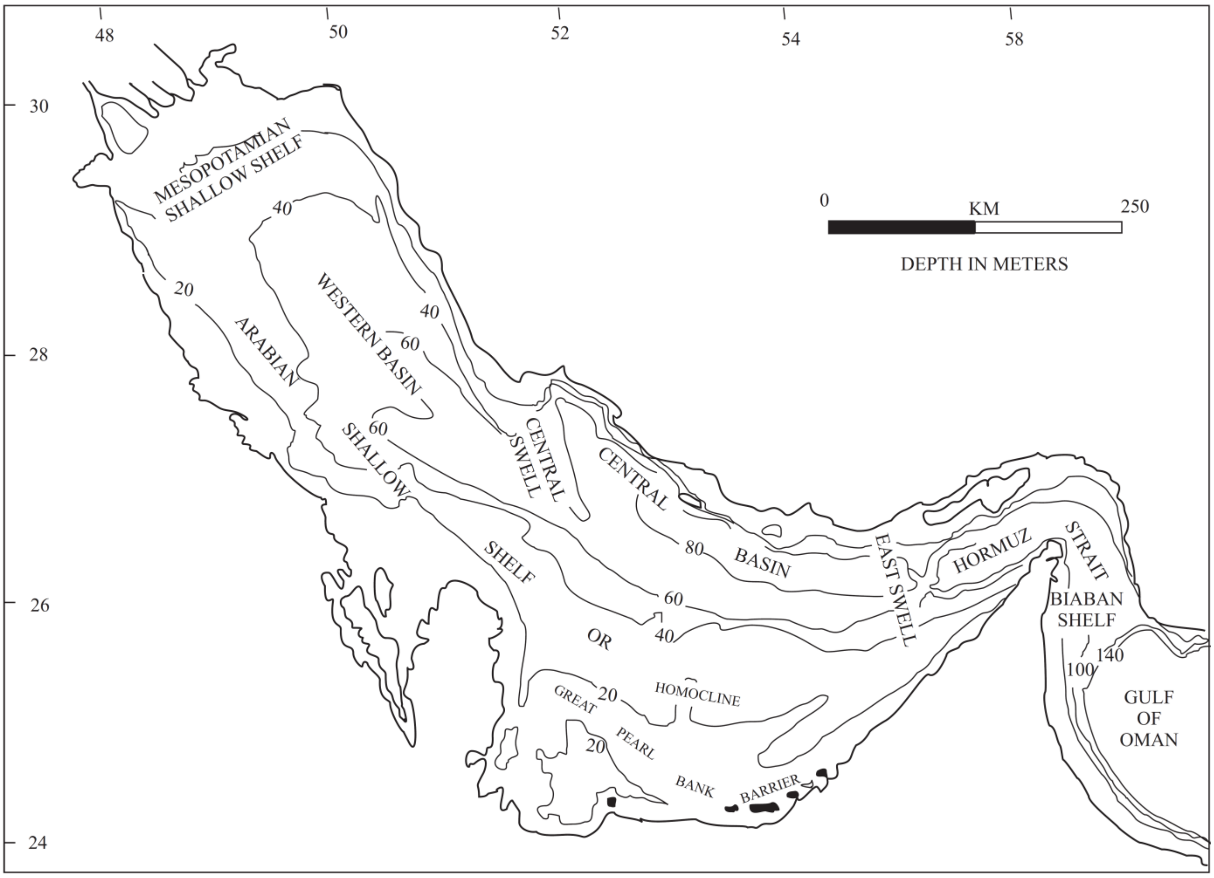

Figure 4.5: Bathymetry and topographic names of the Persian Gulf (modified after Seibold and Volbrecht (1969).

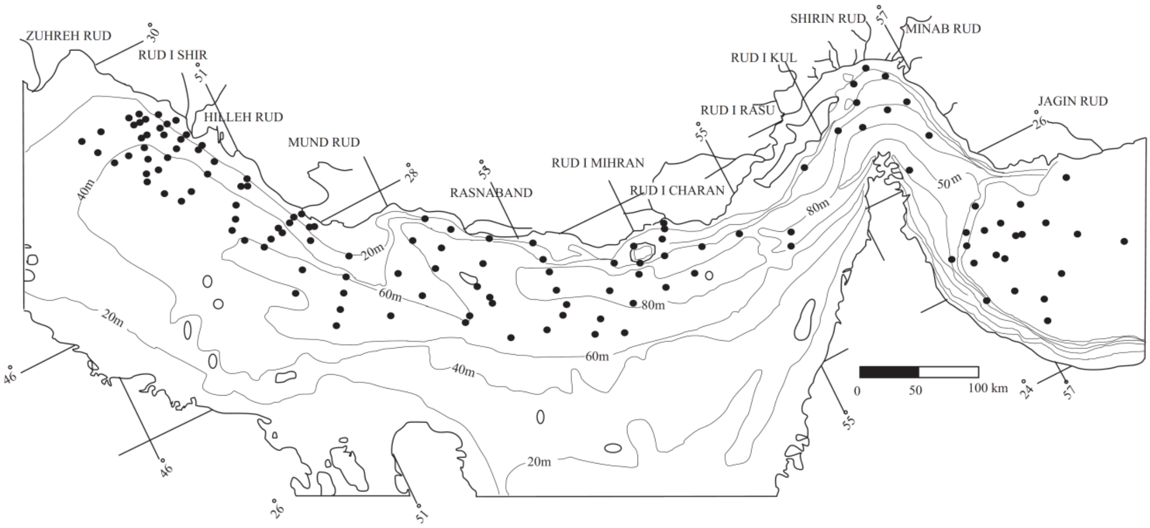

Figure 4.6: Persian Gulf station, sampled during “Meteor” cruise 1965. (modified after Lutze 1974).

4.5.1.1 DISTRIBUTION OF RECENT DEAD BENTHIC FORAMINIFERAL ASSEMBLAGES IN THE PERSIAN GULF (IRANIAN SIDE)

The dead foraminiferal fauna of the Persian Gulf (Iranian side, Lutze 1965) is strongly dominated by benthic foraminifera. Planktonic foraminiferal tests comprise between 0 and 3.3% of the total dead fauna (Fig 4.7). The diversity of the benthic foraminifera fauna of the study area is high and fluctuates between H (S) = 1.3 and 2.7. Benthic foraminiferal exist in the whole part of the study area with few enhanced numbers of planktonic foraminifera in the deeper part (80-100m) and the shallower part (3-20m) of the Iranian side of the Persian Gulf. The benthic foraminiferal fauna is dominated by rotaliids (61.73%) followed by miliolids with 17% and textulariids with 12.63% of the total benthic foraminifera. Miliolids appear in the intire study area.

On the base of a Q-mode Principal Component Analysis (PCA), applied on the dead foraminiferal data set (Lutze, 1965), five main assemblages were established, accounting for 84,39% of the total variance of the data set (Fig.4.8, Tab.4.2). Significant loadings of the *Bolivina persiensis* fauna (PC1) occur at the deep part of the study area (54m-100m) and explain 19.22 % of the total variance of the data set. (PC1) contains miliolids and *Bulimina marginata biserialis* as associated taxa. This fauna dominates samples of the deeper part of the study area. The *Ammonia* spp. fauna (PC2) exhibits statistically significant factor loadings in the 3-25m depth of the study area. (PC2) explains 19.19% of the total variance and it is mainly associated with *Protelphidium* aff. *schmitti*, *Ammobaculites persicus* and miliolids. This fauna is restricted to the shallower part of the Persian Gulf. The *Bulimina marginata biserialis* fauna (PC3) explains 31.38% of the total variance of the data set. (PC3) occurs in a middle water depth of the study area and associated with *Nonion asterizans*. The *Textularia* fauna (PC4) occurs in the entire area and is associated with *Ammonia* sp., *Protelphidium* aff. *schmitti*, and *Ammobaculites persicus* The *Protelphidium* aff. *schmitti* fauna (PC5) exhibits a limited distribution and is associated with miliolids. The *Nonion asterizans* fauna (PC5) is associated with Miliolinae and occurs mostly in shallow depths of the Persian Gulf (Fig. 4.8, Tab. 4.2).

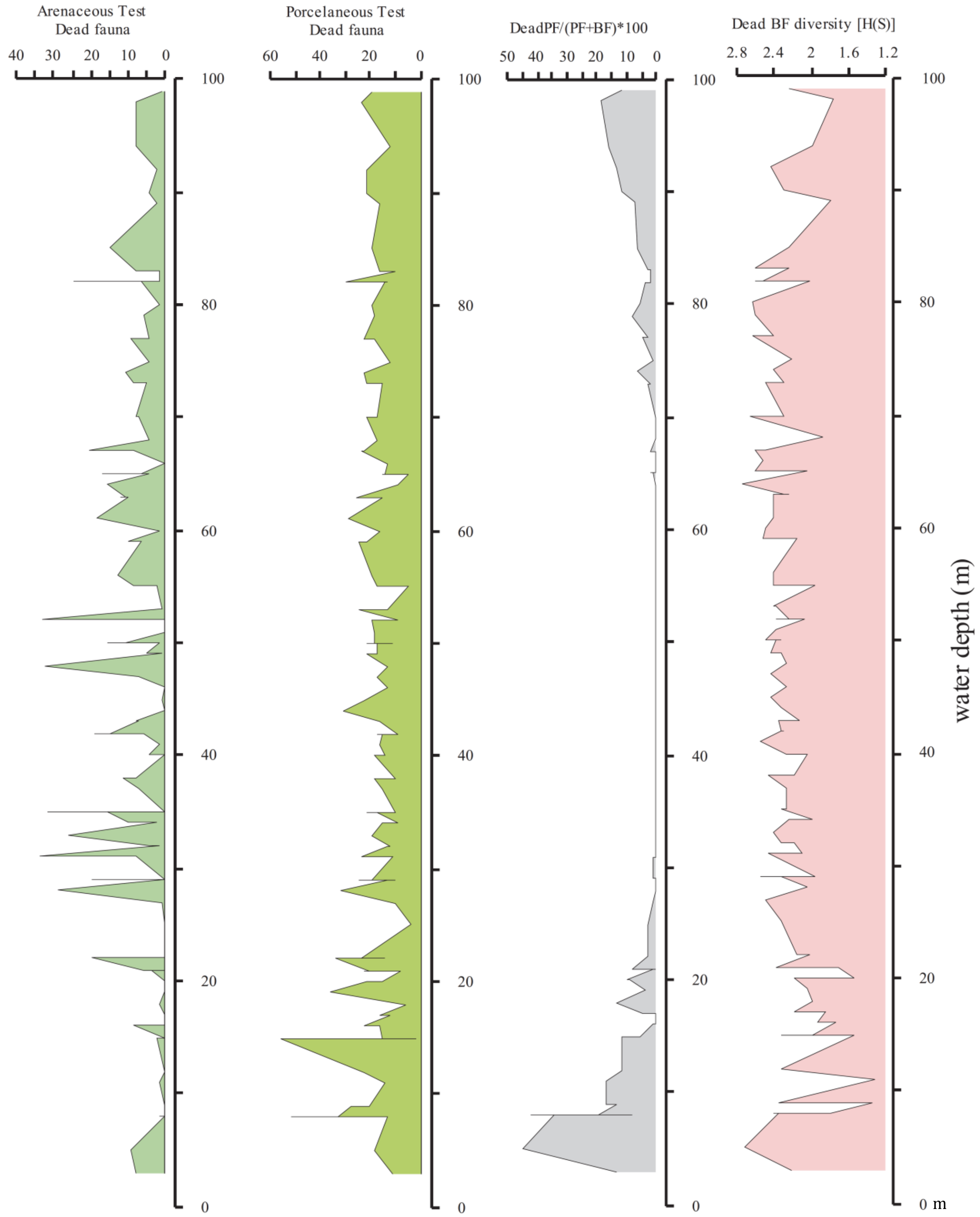

Figure 4.7: Benthic foraminiferal diversity H (S), relative abundance of planktonic foraminifera (BP), and relative proportion of arenaceous (agglutinating) and porcellaneous (miliolid) taxa shown against water depth (m). Raw data are from Lutze (1974).

Table 4.2: Composition of the Q-mode benthic foraminiferal assemblages from the investigated dead Recent benthic foraminifera in the Persian Gulf (raw data from Lutze, 1974). Principal Component Number, dominant taxa and important associated taxa with Varimax Principle Component Score, and explained variance in percent of total variance are given.

No.	Dominant Taxa	Score	Associated Taxa	Score	Variance (%)
PC1	*Bolivina persiensis* n. sp.	6.84	miliolids *Bulimina marginata biserialis*	1.71 1	18.99
PC2	*Ammonia* sp.	5.43	*Protelphidium* aff. *schmitti* *Ammobaculites persicus* miliolids	3.33 2.25 1.65	15.61
PC3	*Bulimina marginata biserialis*	6.76	*Nonion asterizans*	1.6	29.50
PC4	*Textularia* spp.	5	miliolids	4.57	13.66
PC5	*Nonion asterizans*	4.54	miliolids	3.6	10.18

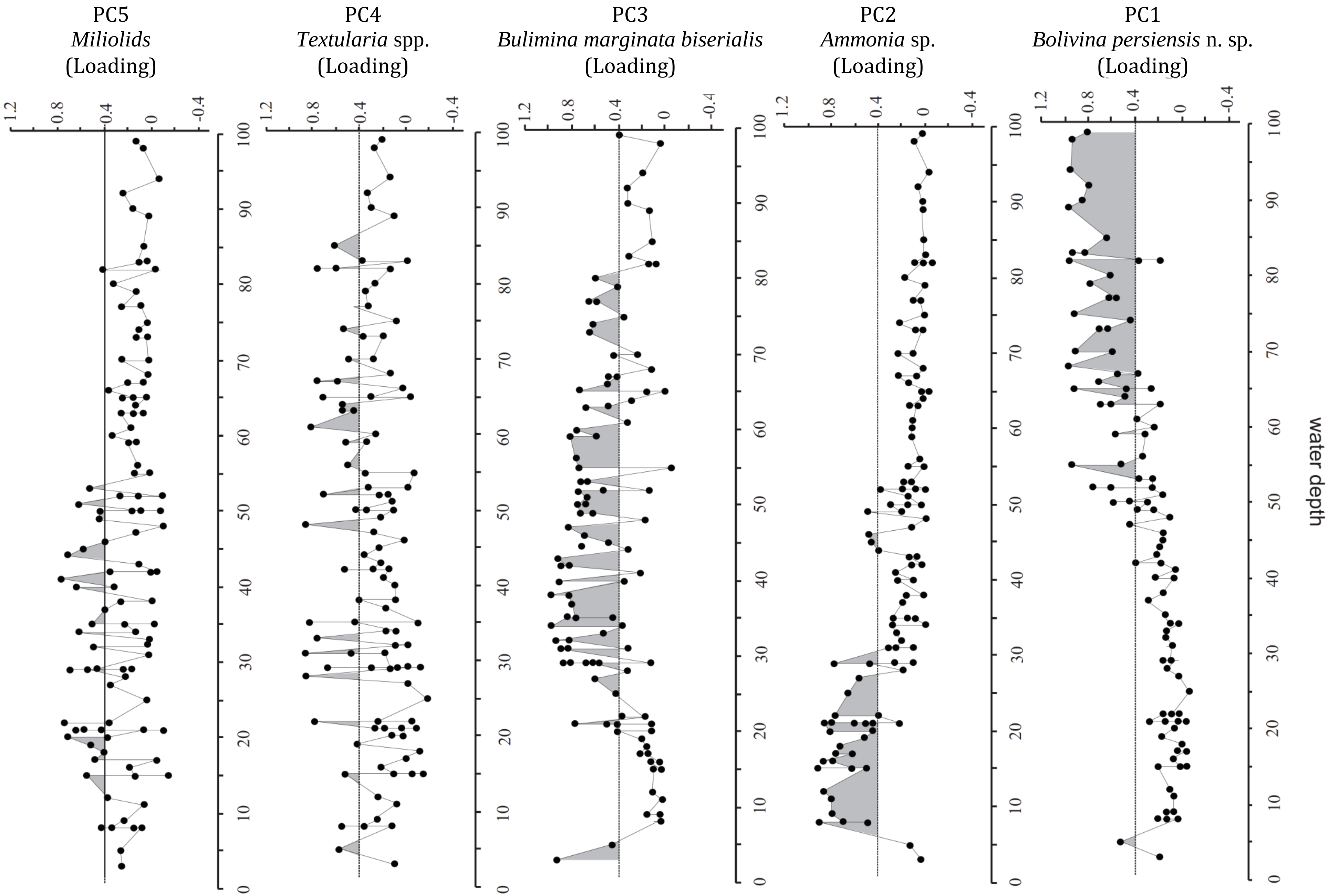

Figure 4.8: Q-mode benthic foraminiferal assemblages of the Persian Gulf plotted against water depth (raw data from Lutze 1974)

4.5.2 PALEOENVIRONMENTAL RECOUNSTRUCTION FOR THE MOLKABAD SECTION

The paleo waterdepth can be estimated by the relative proportion of planktonic foraminifera but also by the distribution of different benthic foraminiferal species and faunas. The relative abundance of planktonic foraminifera in samples of the Molkabad section is generally low (P/B<24.35%), suggesting a shallow marine (inner neritic) environment (Pippérr and Reichenbacher, 2010). This interpretation is supported by high percentages of *Nonion asterizans*, *Elphidium* spp., and *Ammonia* sp. in combination with high abundances of bryozoans and bivalve fragments. This foraminiferal assemblage clearly supports deposition in a shallow, inner neritic environment (Drinia *et al.*, 2007, Holcova and Zagorsek, 2008; Pippérr, 2011). Assemblages rich in miliolids and elphidiids are characteristic of warm inner neritic environments (0-30m water depth) (Boltovskoy & Wright, 1976; Culver *et al.*, 1996; Sen Gupta, 1999). The depth distribution of Recent benthic foraminifera of the Persian Gulf in comparison with Oligocene to Miocene foraminiferal faunas of the Qom Formation, suggests a deposition of the succession commonly shallower than 50m. The estimated water depth ranges between 36 and 94m due to strong predominance of genera *Ammonia* and *Elphidium*. The lack of *Bolivina persiensis* and *Bulimina marginata biserialis* species points to lower water depth in some intervals (Murray 1991). In the Molkabad outcrop, *Nonion* spp. and *Elphidium* spp. are more abundant and typical shallow marine taxa. The preliminary bathymetric reconstruction suggests deposition of the succession commonly shallower than 50 m water depths for the Oligocene-Miocene of the Qom Formation. Based on foraminiferal assemblages of the studied section the paleosalinity and paleo water temperature can be reconstructed. Diversity of benthic foraminiferal faunas and species composition from shallow water environments are strongly dependent on temperature and salinity of the water mass (Culver *et al.*, 1996; Sen Gupta, 1999). *Ammonia beccarii* is a common euryhaline taxon in marginal marine and inner-neritic environments (e.g. Sen Gupta 1999; Murray 2006). Faunas with a low-diversity and dominance of large miliolids are typical for subtropical and tropical lagoons, which are warm an often hypersaline environments (Murray, 1991). The widespread occurance of euryhaline genera like *Ammonia*, *Nonion*, and *Elphidium* along the profile proof that normal seawater salinity dominates. Normal marine environments are indicated for the study section by low diversities, small test-sizes, and high abundance of foraminifera.

4.6 CONCLUSIONS

The composition and abundance of benthic and planktonic foraminifera of the Aquitanian-Burdigalian (Miocene) succession of the Molkabad section from the Qom Basin (Central Iran) were examined in order to reconstruct environmental parameters such as paleo bathymetry (paleo waterdepth), temperature and salinity.

1) The estimated values of water depth range between 36 and 94 m due to strong predominance of genera *Ammonia* and *Elphidium*. Lack of *Bolivina* and *Bulimina* species point to even lower water depths in some intervals (Murray, 1991, Lutze, 1965).
2) High proportions of miliolid foraminifera (up to 32.7% of the total fauna) in the inner neritic deposits reveal a transitional environment between warm-temperate and tropical conditions (16-23° C following Betzler *et al.*, 1997).
3) The comparison of Qom Formation with Persian Golf is: The diversity of the benthic foraminiferal fauna in the Persian Gulf is higher than at the Molkabad section, but at both studied area, benthic foraminiferal numbers are high across whole basin or section only with few planktonic foraminifera.
4) The majority of the benthic foraminiferal tests in both study areas are hyaline. The fauna of the Molkabad section represents a typical inner-neritic depositional environment supported by the predominance of marls, algal and bryozoan limestones in this section.
5) The distribution depth of Recent benthic foraminifera of the Persian Gulf in comparison with Oligocene-Miocene foraminiferal faunas of Qom the Formation suggests a deposition of the succession commonly shallower than 50 m water depth.

APPENDIX

A.1 Tables

Table: Counted Benthic, Planktonic foraminifera and ostracods (percentagse).

	Sample No.:	567	570	572	576	578	579	580	581	582	583	584
	Depth (m)	137	156	168	200	208	212	216	221	225	229	233
1	***Elphidium granosum***	0	42.51	1.7	30.36	29.19	25.55	15.73	0	22.88	9.92	28.06
2	***Elphidium advenum***	0	2.09	0	10.53	1.08	2.36	3.27	18.92	4.84	7.17	2.38
3	***Elphidium hauerium***	0	0	0	0	0	0	0	0.7	0	0	0
4	***Elphidium* sp.**	5.18	0	0	9.48	0	0	0	17.52	0	0.98	0
5	***Ammonia pauciloculata***	0	27.82	0	0	0	0	7.93	21.26	10.41	14.53	32.48
6	***Ammonia* cf. *tepida***	0	0	0	1.04	0	0	0.072	1.86	0	3.33	0.51
7	***Ammonia beccarii***	0	0	0	0	0	0	0.94	0	0	0.88	0
8	***Ammina spp.***	10.97	0	3.06	18.59	12.57	5.6	0	0	0	0.98	0
9	***Heterolepa mexicana***	0	0	46.59	0.37	16.14	11.83	36.92	0	0	0	0
10	***Heterolepa* sp.**	0	0	0	0	0	0	0	0	0	0	0
11	***Gavelinopsis lobatulus***	0	0	0	1.42	0	0.24	0	0	0	0	0
12	***Nonion* sp.**	0.6	0	0.68	2.37	0	0	0	0	0	0	0
13	***Nonion asterizans***	0	16.53	0	2.27	4.03	8.84	15.87	0	1.08	0	0.85
14	***Cancris auriculus***	0	0	0.34	0	0	0	0.94	0	0	0	0
15	***Cibicides lobatulus***	0	0	0	0	2.95	5.97	3.64	0	0	0	0
16	***Cibicides* sp.**	0	0	23.12	0.18	0	0	0	0.23	0	0	0
17	***Reussella* sp.**	0	0	0	0	3.1	1.99	0.8	0	1.57	0	0
18	***Quinqueloculina* sp.**	0	0	0.34	0	0	0	0.072	0	0	20.33	0
19	***Heterolepa praecincta?***	0	0	0	0	0	0	0	0	0	0	0
20	***Miliolids***	11.28	0.78	0.68	1.89	0.77	0.12	0	3.27	1.57	17.97	2.38
21	***Textularia***	0.3	2.36	0	0	15.37	5.85	0.072	12.14	23.12	1.66	2.04
22	***Ostracods***	56.09	7.61	4.08	10.34	7.45	7.22	11.21	11.91	31.84	9.72	10.88
23	***Planktonic Foraminifera***	0	0.26	3.74	1.23	4.5	19.9	0.072	0	0.96	0.29	0.51
24	**Unknown**	15.5	0	15.6	9.85	2.79	5.84	2.4	12.1	1.6	12.2	19.9

	Sample No.:	585	586	587	588	589	590	591	594	607	608	610
	Depth (m)	238	243	247	252	257	262	267	280	386	391	402
1	***Elphidium granosum***	45.05	24.86	22.53	11.86	12.93	4.08	46.69	33.15	21.53	27.75	18.96
2	***Elphidium advenum***	0.67	2.78	1.84	1.19	4.31	0.81	2.46	2.76	2.63	4.7	38.79
3	***Elphidium hauerium***	0	0	0	0	0	0	6.22	0	0	0	0
4	***Elphidium* sp.**	0	0	0	0	0	6.53	0	0	0	0	0
5	***Ammonia paunciloculata***	0	0	0	0	0	0	8.69	12.35	9.09	0	0
6	***Ammonia* cf. *tepida***	0	0	0.49	0.29	0.86	0.27	0.25	0.3	0.23	0	0
7	***Ammonia beccarii***	0	0	0	0	0	0	0	0	0	0	0
8	***Ammina* spp.**	33.83	1.71	12.31	6.081	6.03	7.9	0	0	0	5.84	8.33
9	***Heterolepa mexicana***	0.16	1.07	5.78	14.95	2.58	1.089	9.98	0	0	0	0
10	***Heterolepa* sp.**	0	0	0	0	0	0	0	0	0	0	0
11	***Gavelinopsis lobatulus***	0.67	9.43	0	1.89	0	0.81	0	0	0	0	0
12	***Nonion* sp.**	0	2.78	0	0	0	0	0	0	0	0	0
13	***Nonion asterizans***	0.16	0	5.54	5.48	4.31	15.8	3.11	37.6	58.85	50.16	1.14
14	***Cancris auriculus***	0	2.14	1.6	2.093	0.86	0	0	0	0	0	0
15	***Cibicides lobatulus***	0.5	8.36	9.23	25.82	4.31	4.63	1.16	0.61	0.23	0	0
16	***Cibicides* sp.**	0	0	0	0	0	0	0	0	0	0	0.28
17	***Reussella* sp.**	2.51	0.42	0.61	2.49	0	1.089	0.38	0	0	0	0
18	***Quinqueloculina* sp.**	0	0	0	0	0	0	0	0	0	0	0
19	***Heterolepa praecincta?***	0	0	0	0	0	0	0	0	0	0	0
20	***Miliolids***	0.33	11.14	14.16	1.79	31	1.36	0.64	0.23	0	0	0
21	***Textularia***	1.5	4.93	1.23	2.79	2.58	4.087	0.25	1.53	0	0	0.28
22	***Ostracods***	6.53	11.68	9.35	6.08	25	23.43	13.22	5.29	2.63	3.89	21.26
23	***Planktonic Forminifera***	0.5	4.18	2.33	12.46	0.86	20.7	3.76	4.45	0.47	1.13	0.28
24	**Unknown**	7.52	14.5	12.9	4.67	4.31	7.35	3.11	1.69	4.29	6.49	10.6

	Sample No.:	618	623	625	630	633	635	636	638	639	641	642
	Depth (m)	434	461	487	521	544	555	558	571	576	586	592
1	***Elphidium granosum***	34.45	15.64	20.22	6.04	12.18	0	0	14.46	15.75	8.02	27.82
2	***Elphidium advenum***	6.61	2.23	2.91	0	1.01	0.3	19.27	0.9	0	4.98	7.11
3	***Elphidium hauerium***	0	0	0	0	0.25	0	0	0	0	0	0
4	***Elphidium* sp.**	0	0	0	0	0	4.62	6.02	0	0	0	0
5	***Ammonia paunciloculata***	0	0	17.77	0	13.95	0	0	18.26	0	0	17.15
6	***Ammonia* cf. *tepida***	0	0	0.37	0	1.77	0.61	7.22	1.98	0	0	0.83
7	***Ammonia beccarii***	0	0	0	0	0.25	0	0	0	0	0	0
8	***Ammina* spp.**	22.68	8.93	0	5.11	0	26.54	12.04	0	15.75	8.02	0
9	***Heterolepa mexicana***	0	0	0	0	0	0	0	0	0	0	1.25
10	***Heterolepa* sp.**	0.31	0	0	0	0	0.92	0	0	0	0	0
11	***Gavelinopsis lobatulus***	0	0	0	0	0	0	0	0	0	0	0
12	***Nonion* sp.**	0	0	0	0	0	21.29	0	0	0.83	0	0
13	***Nonion asterizans***	14.07	39.38	37.06	44.65	45.93	0	21.68	32	39.64	35.57	6.48
14	***Cancris auriculus***	0	0	0	0	0.76	0.92	0	0	0	0	0.83
15	***Cibicides lobatulus***	0	0	0	0	0	0	0	0	0	0	0.2
16	***Cibicides* sp.**	0	0	0	0	0.25	0	1.2	0	0	0	0
17	***Reussella* sp.**	1.26	0	0	0.23	0	0	0.6	0.18	0	1.95	2.09
18	***Quinqueloculina* sp.**	0	0	0	0	0	0	0	0	0	0	0
19	***Heterolepa praecincta?***	0	0	0	0	0	0	0	0	0	0	0
20	***Miliolids***	0.42	0	0	0	0	0	0	0.54	0	0	0
21	***Textularia***	1.68	0	1.59	0	6.34	1.54	1.2	3.79	0.67	35.57	13.38
22	***Ostracods***	3.15	26.53	17.12	42.09	10.65	20.98	6.02	26.4	25.73	2.38	7.11
23	***Planktonic Foraminifera***	6.72	0.55	2.63	0	6.59	12.34	22.89	1.44	1.59	3.47	13.17
24	**Unknown**	8.61	6.7	0.28	1.86	0	15.4	1.8	0	0	0	2.48

	Sample No.:	643	644	645	646	650	652	655	656	657	663	665	670
	Depth (m)	597	600	602	612	630	642	658	662	672	722	735	753
1	***Elphidium granosum***	13.7	11	17.2	8.85	2.82	10.4	0	18.9	16	0	0	0
2	***Elphidium advenum***	11.7	4.48	2.02	0.41	0	0.77	8.15	0.21	0	12.1	16.2	5.44
3	***Elphidium hauerium***	1.22	0	0	3.43	0	0	0	0	0	0	0	0
4	***Elphidium* spp.**	0	0	0	0	0	0	22.8	0	0	28.2	21.5	31.6
5	***Ammonia paunciloculata***	0	10.1	0	8.58	22.9	25.6	0	3.6	16	16.6	0	0
6	***Ammonia* cf. *tepida***	0	2.15	0	0.27	1.56	3.62	2.5	0	29	5.21	17.9	0
7	***Ammonia beccarii***	0	0.33	0	0	0	0	0	0	0	0.42	0.15	0
8	***Ammina* spp.**	17	0	20.9	0	0	0	7.89	0	0	0	10.6	35
9	***Heterolepa mexicana***	0	0.16	0	0	0	0	0	0.21	0	0	0	0
10	***Heterolepa* sp.**	0	0.99	0	0	3.76	2.07	5	0	0	3.94	1.05	0
11	***Gavelinopsis lobatulus***	0	0	0	0	0	0	0	0	0	0	0	0
12	***Nonion* sp.**	0	0	0	0	0	0	0	0	0	0.21	0	1.81
13	***Nonion asterizans***	14.3	21.3	54.1	2.81	27.6	16.3	22.9	46.2	17.5	0	0	0
14	***Cancris auriculus***	0	0.33	1.01	0	2.82	1.55	0	0	0	0	0	0
15	***Cibicides lobatulus***	0	0	0	0	0.31	0	0	0	0.41	0	0	0
16	***Cibicides* sp.**	0	1.49	0	0	0.31	1.29	2.89	0	0	0	0	0
17	***Reussella* sp.**	2.45	3.32	1.35	0	0	1.03	1.97	0	0	0.1	0	0
18	***Quinqueloculina* sp.**	0	0	0	0	0	0	0	0	0	0	0	0
19	***Heterolepa praecincta?***	0	5.48	0	0	0	0	0	0	0	0	0	0
20	***Miliolids***	0	0	0	0	2.5	0.77	0	0	0.2	0.53	0.15	0
21	***Textularia***	11.1	12.1	1.35	35.4	0	10.1	6.71	0	3.49	2.02	0	0
22	***Ostracods***	20.7	16.9	0.33	37.2	17.9	8.03	16.8	25	15.6	30.4	21.9	20.6
23	***Planktonic Foraminifera***	3.27	7.3	1.01	3.02	17.2	12.4	2.36	5.57	1.84	0.21	0	0
24	**Unknown**	4.49	2.49	0.66	0	0.31	5.95	0	0.2	0	0	10.6	5.43

Table: Retaltive abundance of selected dead benthic foraminifera from the Persian Gulf (from Lutze 1974)

Water depth m	**Textularia**	**Miliolids**	***Cancris* sp.**	***Ammonia* sp.**	***Elphidum* sp.**	***Protelphidium* sp.**	***Heterolepa praecincta***	***Nonion* sp.**	**% Proportion of planktonic foraminifera**
3	7.6	11.4	5.5	2.4	2.1	1	0	17.6	0.3
5	9.3	18.6	1.5	3.7	0.7	0.5	4.8	4.1	12.9
8	0	13.4	0	22.4	7.3	21.6	0	6.2	0
8	1.4	12.8	0	21.4	2.4	21.3	0	6.6	0
8	0	51.4	0	11.7	2.3	8.9	0	1.4	0
8	0	32.5	0	18.1	1.9	6.3	0	3.1	0
9	0	28.1	0	51.8	2.4	2.8	0	6.4	0
9	0	20.9	0	12.2	5.2	21.5	0	7	0
11	1.5	14	0	63.4	7.7	3.1	0	2.7	0
12	0	22.2	0	20.5	3	14.8	0	10.9	0
15	2.3	56	0	23.5	3.8	2.3	0	14	0
15	0.5	5.5	0	23	1	29.5	0	3	0
15	0.5	1.7	0	23.9	0	24.4	0	6.3	0
15	0	15.8	0	8.6	3	12.8	0	4.1	0
16	8.9	16.4	0	45.2	5.3	5.1	0	11	0
16	0	22.8	0	36.6	1.7	11.7	0	1.1	2.2
17	0	12.1	0	5.3	1.5	44.2	0	10.6	0
17	0	16	0	20.8	3.4	16.9	0	25.1	0
18	1.3	6.4	0	34	3	2.6	0	26	0
19	0	36.2	0	8.5	2.3	4	0	7.9	0
20	0.5	21.5	0	6.5	0	5	0	25.5	0
20	0	14.8	0	38.6	0.5	0.5	0	20.5	2.8
21	3.8	8	0	49.4	5	12.3	0	10.8	0.8
21	1	11.5	0	10.5	0	6	0	31	0
21	0.5	8.2	0	16.4	0	40.9	0	6.8	0
21	0	18.6	0	11.1	0	13.9	0	22.2	0
21	0	22.9	0	14.3	0	1.4	0	17.1	0.9
21	5.8	20.1	3.6	5.8	2.7	1.3	0	15.6	2.1
22	19.9	34.5	0.5	13.3	4.7	1.4	0	8.1	0
22	0.9	13.8	0	11.2	0	2.3	0	33.5	0
22	0	23.9	0	12.9	0	17.4	0	9.5	0
25	0.4	4	0	9.8	3.9	24.6	0	15.2	0
27	1	9.7	0.5	14.1	3.9	4.4	0	16	0
28	28.6	32.4	1.9	4.3	3.3	3.3	0	5.2	0
29	0.4	13.2	0	9.3	1.1	8.2	0	19.6	0.4
29	19.8	24.6	0	1.3	3.5	0.4	0	5.2	0
29	9.3	17.3	0	5.6	2.4	6.5	0	9.3	0
29	2.6	9.8	0	6.9	3.2	0.1	0	7.6	0

Water depth m	*Textularia*	Miliolids	*Cancris* sp.	*Ammonia* sp.	*Elphidum* sp.	*Protelphidium* sp.	*Heterolepa praecincta*	*Nonion* sp.	% Proportion of planktonic foraminifera
29	0	11.1	0.8	7.7	0.8	0.8	0	33.5	0
29	0.5	19.9	0.5	32	2.9	0	0	17.5	5.1
31	8.1	11.2	0	5.3	3.2	12.3	0	9.2	0
31	15.9	16	0	2.1	4.2	1.1	0	4.8	0
31	33.7	24.1	0	8.1	5.1	2.7	0	1.8	0
32	1.4	13.7	0	7.7	0.5	0	0	19.9	0
32	4.5	12.5	0.3	5.9	1.3	9	0	6.2	0
33	26.4	19.8	1	7.6	6.3	3.1	0	3.8	0
34	2.3	15.1	0	8.2	3.6	0	0	16.4	5.8
34	10	9	0	1.6	2.5	1.1	0	16.1	0
35	15.4	17.1	3.3	2.9	3.3	0.8	0	12.1	0.4
35	31.4	21.7	1.2	5.1	1.9	1.9	0	1.6	0
35	0	9.9	0.4	9.5	0.8	0	0	20.2	0
37	7.5	15	2.5	7.5	3.5	0	0	20	0
38	11.1	18.2	4.5	3.3	3.7	2.9	0	10.7	0
38	7.8	9.6	1.3	2.5	3.4	4.1	0	7.5	0
40	0	18.9	1	8.1	0.3	0	0	12.1	1.3
40	4.4	14.3	4	5.5	3.6	0	0	18.4	0
41	1.6	16	2.1	7.2	0	0	0	14	14.3
42	5.8	15.6	2.5	4	4.3	0.4	0	17.7	0.4
42	18.9	17.4	2.4	5.2	1.8	1.4	0	3.3	0
42	14.6	8.8	7.9	5.5	2.8	0	0	6.3	0
43	7.3	16.3	2.8	6.9	1.4	2	0	6.3	0
43	8	15.9	2.2	5.7	3.2	0	0	8.7	0
44	0	30.4	3.1	10.6	3.1	0	0	14.3	0.9
45	0.6	22.6	1	11.3	1.3	4.5	0	10.3	0.5
46	0.5	13.3	0	18.2	0.5	1.4	0	11.5	0
47	7.2	17	3.8	6	3.4	0.4	0	5.7	0
48	32.3	12.7	5.8	0.9	3.5	0	0	0	20.9
49	0.8	21.3	0.8	15.8	2.5	0.4	0	11.7	0.5
49	5.1	17.6	4.4	6.6	5.5	0.4	0	16.8	2.5
50	1.4	17.2	3.7	11.2	4.2	0.5	0	13.9	0.4
50	13	17.9	7.6	2.3	3	0.4	0	3.4	0.5

Water depth m	*Textularia*	Miliolids	*Cancris* sp.	*Ammonia* sp.	*Elphidum* sp.	*Protelphidium* sp.	*Heterolepa praecinta*	*Nonion* sp.	% Proportion of planktonic foraminifera
50	10.9	21.4	5.3	6.8	1.1	0	0	4.5	0
50	15.3	10.8	6	4.7	3	0	0	3.4	0
50	10.5	18.1	8.7	2.5	3.3	0.4	0	4	0.4
51	0.5	18.2	2.7	5	0.9	0	0	15.5	3.8
52	0	19.2	0.9	19.3	0	0	0	6.4	10.5
52	6	16.6	3	8.7	4.5	0	0	4.5	0.4
52	8.2	12.3	3.3	4.9	3.6	0.4	0	9.8	0
52	32.7	9.2	8.4	1.3	4.9	0.5	0	5.7	12.8
53	1.6	24.4	4.3	4.9	4.9	0	0	10.9	2.4
53	0.7	13.5	4.2	4.5	2.1	0	0	22.5	2.7
55	2.2	4.9	7.4	4.4	3.9	0	0	5.7	8.6
55	8.7	17.4	5.8	7	2.5	0	0	5.8	0.6
56	12.7	19.3	6.3	2.8	2.8	0	0	2.8	0
59	6.4	24.8	6.8	4.9	0.5	0	0	4.5	0.4
59	10	21.5	5	4	4.5	0	0	2	0.8
60	1.3	16.6	3.9	3.9	0.4	0	0	7	4
61	18.6	28.5	4.9	1.5	4.9	0	0.5	1	0.5
63	10.1	15.3	4.7	2.7	1.2	0	0	9	4.5
63	11.8	22.3	4.3	5.9	4.3	0	0	0.4	0.7
63	10.7	25.6	4.5	3.3	6.6	0	0	1.6	0.8
64	15.8	9.4	5.8	2.6	3.7	0	0	7.4	32.5
65	4.6	4.7	3.7	5	0	0	0	7.8	14.8
65	17	15.5	6	2	1	0	0	4.5	23.5
65	6.5	14.5	1.9	0.9	6.5	0	0	6.1	7
66	0	13.5	1	5.8	0	0	0	12	2.6
67	8.3	23.8	4.2	7.2	3.1	0.4	0.4	1.1	3
67	20.2	22.3	5.6	3	2	0	0	1	0.3
68	4.5	17.4	0.6	1.8	0.3	0	0	0.9	3.5
70	7.1	21.3	3.5	7.9	3.1	0	0	3.1	1.4
70	7.6	16.9	1.7	5.9	0.8	0	0	0	2.5
73	5.1	14.8	3	3	0.9	0.9	0.4	2.6	2.9
73	8.5	21.9	2.4	3.2	3.2	0	0	3.2	3.2
74	10.9	22.4	2.6	9.3	2.6	0	0	0	3
75	4.1	12.6	1.6	2.4	1.2	0	0	3.7	2.3

Water depth m	***Textularia***	**Miliolids**	***Cancris* sp.**	***Ammonia* sp.**	***Elphidum sp.***	***Protelphidium sp.***	***Heterolepa praecinta***	***Nonion* sp.**	**% Proportion of planktonic foraminifera**
77	9	18	1.5	2.5	5	0	0.5	1	20.5
77	4.1	23	0.5	4.1	0	0	0	4.1	20
79	5.5	18	4.5	1	0	0	0	1.5	6.3
80	1.7	19.5	2.3	5.2	0.6	1.1	0	6.3	8.3
82	6.4	14	0.4	3.2	0.8	0	0	0	7.1
82	25	13.6	1.8	0.7	2.9	0	9.9	0.4	14.7
82	1.9	29.7	5.2	0	0	0	4.7	1.4	18
83	1.6	10.4	1	2.1	0.5	0	0	5.2	9.2
83	7.9	16.2	1	1	3.2	0	0	2.9	3.3
85	14.8	19.4	1.7	0.8	0.4	0	4.2	0	10.6
89	2.5	16.5	1	2.5	0	0	0	1	2.1
90	4.2	21.5	2.1	0.5	0	0	0	1	10.2
92	2.6	21.9	3.6	1.6	0	0	0	2.1	15.2
94	7.9	12.6	0.4	0.8	2.1	0	0	0.4	8.6
98	7.6	23.3	0	3.6	0.4	0	0	0.4	7.6
99	0.6	19.2	1.2	1.8	0	0	0	0	12.7

Table: Loadings of the Q-mode Principle Component Analysis (PCA), applied on the foraminiferal fauna from the Persian Gulf (raw data from Lutze, 1974).

Water depth (m)	PC1	PC2	PC3	PC4	PC5
3	0.184	0.901	-0.165	0.317	-0.086
5	0.823	0.208	0.019	0.436	-0.005
8	0.123	0.034	0.581	-0.211	0.756
8	0.108	0.071	0.573	-0.130	0.794
8	0.925	0.170	0.170	0.021	0.293
8	0.807	0.205	0.464	-0.011	0.301
9	0.332	0.162	0.917	-0.050	0.134
9	0.459	0.151	0.209	-0.157	0.826
11	0.052	0.012	0.992	-0.063	0.076
12	0.451	0.357	0.547	-0.119	0.596
15	0.830	0.394	0.348	0.055	0.163
15	-0.141	-0.140	0.471	-0.175	0.828
15	-0.279	-0.029	0.566	-0.173	0.740
15	0.575	0.164	0.255	-0.126	0.744
16	0.084	0.190	0.961	0.104	0.141
16	0.376	0.028	0.848	-0.079	0.363
17	-0.034	0.014	-0.153	-0.174	0.959
17	0.026	0.700	0.410	-0.158	0.562
18	-0.210	0.608	0.756	-0.073	0.082
19	0.882	0.371	0.160	0.019	0.232
20	0.352	0.899	0.029	-0.012	0.243
20	0.058	0.504	0.852	-0.065	0.078
21	-0.123	0.114	0.949	-0.055	0.260
21	-0.068	0.960	0.125	-0.042	0.222
21	-0.117	-0.077	0.150	-0.174	0.946
21	0.238	0.767	0.154	-0.100	0.560
21	0.530	0.724	0.399	-0.011	0.166
21	0.592	0.772	0.055	0.219	0.048
22	0.737	0.254	0.244	0.559	0.085
22	0.000	0.978	0.146	-0.023	0.111
22	0.555	0.326	0.265	-0.089	0.707
25	-0.310	0.302	0.051	-0.213	0.866
27	0.050	0.795	0.539	-0.084	0.238
28	0.640	0.100	-0.043	0.754	0.078
29	0.154	0.869	0.186	-0.081	0.422
29	0.660	0.179	-0.092	0.710	0.031
29	0.602	0.483	0.066	0.477	0.408
29	0.491	0.697	0.436	0.165	0.050
29	-0.054	0.993	0.050	-0.050	0.044
29	0.258	0.526	0.804	-0.047	0.070
31	0.222	0.386	-0.026	0.381	0.806
31	0.550	0.176	-0.073	0.793	0.033
31	0.423	-0.061	0.071	0.892	0.038
32	0.243	0.943	0.184	0.038	0.071
32	0.530	0.366	0.161	0.221	0.713
33	0.422	-0.006	0.081	0.891	0.042
34	0.385	0.873	0.238	0.071	0.054
34	0.058	0.825	-0.165	0.517	0.029
35	0.468	0.518	-0.108	0.706	-0.043
35	0.419	-0.051	0.007	0.902	0.018
35	0.071	0.953	0.276	-0.050	0.046

Water depth (m)	PC1	PC2	PC3	PC4	PC5
37	0.259	0.915	0.114	0.278	-0.034
38	0.639	0.533	-0.102	0.536	0.058
38	0.421	0.552	-0.127	0.628	0.289
40	0.642	0.706	0.273	0.001	0.100
40	0.317	0.934	0.038	0.137	-0.065
41	0.515	0.819	0.222	0.061	0.055
42	0.382	0.889	-0.040	0.224	-0.017
42	0.540	0.070	0.067	0.834	0.014
42	0.218	0.195	0.079	0.846	-0.319
43	0.668	0.558	0.158	0.458	-0.022
44	0.767	0.594	0.229	-0.011	0.069
45	0.711	0.537	0.351	-0.008	0.286
46	0.299	0.577	0.739	-0.030	0.154
47	0.811	0.376	0.192	0.395	-0.032
48	0.204	-0.175	-0.131	0.940	-0.155
49	0.601	0.576	0.540	0.002	0.105
49	0.486	0.844	0.082	0.158	-0.055
50	0.527	0.752	0.384	-0.020	0.007
50	0.735	0.118	-0.088	0.613	-0.146
50	0.807	0.244	0.174	0.490	-0.038
50	0.394	0.038	0.064	0.872	-0.226
50	0.790	0.173	-0.083	0.488	-0.170
51	0.559	0.823	0.077	0.003	0.042
52	0.572	0.366	0.722	-0.016	0.107
52	0.796	0.307	0.393	0.309	-0.036
52	0.500	0.673	0.092	0.522	-0.087
52	0.027	-0.061	-0.179	0.953	-0.216
53	0.817	0.562	0.057	0.032	0.002
53	0.204	0.976	-0.017	-0.039	-0.036
55	0.217	0.504	0.194	-0.042	-0.498
55	0.773	0.342	0.223	0.448	-0.102
56	0.780	0.118	-0.035	0.589	-0.112
59	0.904	0.281	0.084	0.255	-0.022
59	0.879	0.118	0.046	0.442	-0.066
60	0.817	0.547	0.106	0.062	0.014
61	0.797	0.033	-0.087	0.593	-0.050
63	0.611	0.525	-0.063	0.567	-0.090
63	0.851	0.036	0.138	0.498	-0.044
63	0.897	0.100	0.000	0.401	-0.045
64	0.222	0.257	-0.124	0.887	-0.252
65	0.059	0.783	0.304	0.394	-0.179
65	0.531	0.136	-0.098	0.802	-0.135
65	0.739	0.409	-0.148	0.384	-0.074
66	0.509	0.826	0.212	-0.010	0.083
67	0.911	0.109	0.205	0.339	0.008
67	0.668	-0.002	-0.032	0.735	-0.076
68	0.924	0.189	0.047	0.309	0.092
70	0.878	0.220	0.272	0.325	0.002
70	0.849	0.072	0.263	0.449	0.042
73	0.899	0.243	0.070	0.341	0.047
73	0.885	0.222	0.033	0.404	0.016
74	0.827	0.048	0.313	0.463	0.018
75	0.852	0.393	0.066	0.340	0.025

Water depth (m)	PC1	PC2	PC3	PC4	PC5
77	0.855	0.076	0.009	0.476	-0.020
77	0.897	0.334	0.117	0.228	0.113
79	0.916	0.179	-0.047	0.315	-0.013
80	0.855	0.463	0.165	0.090	0.125
82	0.857	0.084	0.152	0.475	0.068
82	0.310	-0.228	-0.196	0.800	-0.190
82	0.971	0.160	-0.092	0.038	0.003
83	0.765	0.616	0.069	0.159	0.064
83	0.828	0.225	-0.070	0.491	0.013
85	0.737	-0.035	-0.105	0.624	-0.041
89	0.943	0.219	0.105	0.199	0.097
90	0.946	0.192	-0.036	0.242	0.070
92	0.951	0.246	0.004	0.149	0.048
94	0.790	0.062	-0.046	0.595	0.020
98	0.901	0.143	0.101	0.374	0.102
99	0.971	0.183	0.068	0.085	0.105

A.2 PLATES

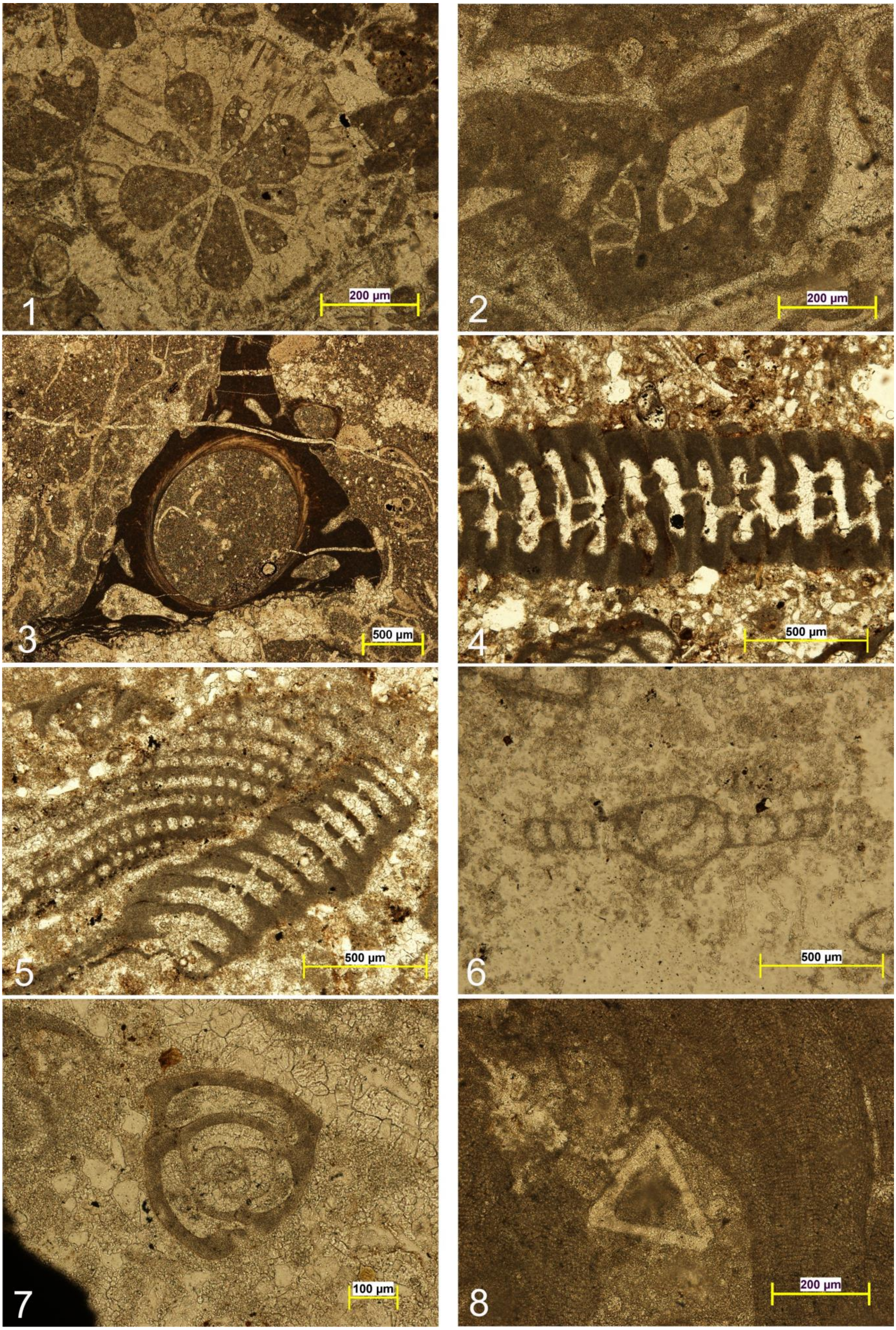
1
200 µm
2
200 µm
3
500 µm
4
500 µm
5
500 µm
6
500 µm
7
100 µm
8
200 µm

Plate 1:

Selected Foraminifera and other Fossils of the Qom Formation from the Molkabad section:

Fig. 1: Tubocellaria sp., sample no. 555.

Fig. 2: *Ammonia* sp., sample no. 561.

Fig. 3: *Kuphus arenarius* Lamarck, 1818; sample no. 621.

Fig. 4: *Meandropsina iranica* Henson, 1950; sample no. 664.

Fig. 5: *Meandropsina iranica* Henson, 1950; sample no. 664.

Fig. 6: *Peneroplis* cf. *tomasi* Henson, 1950; sample no. 664.

Fig. 7: *Triloculina tricarinata* d'Orbigny, 1826; sample no. 664.

Fig. 8: *Reussella* sp., sample no. 553.

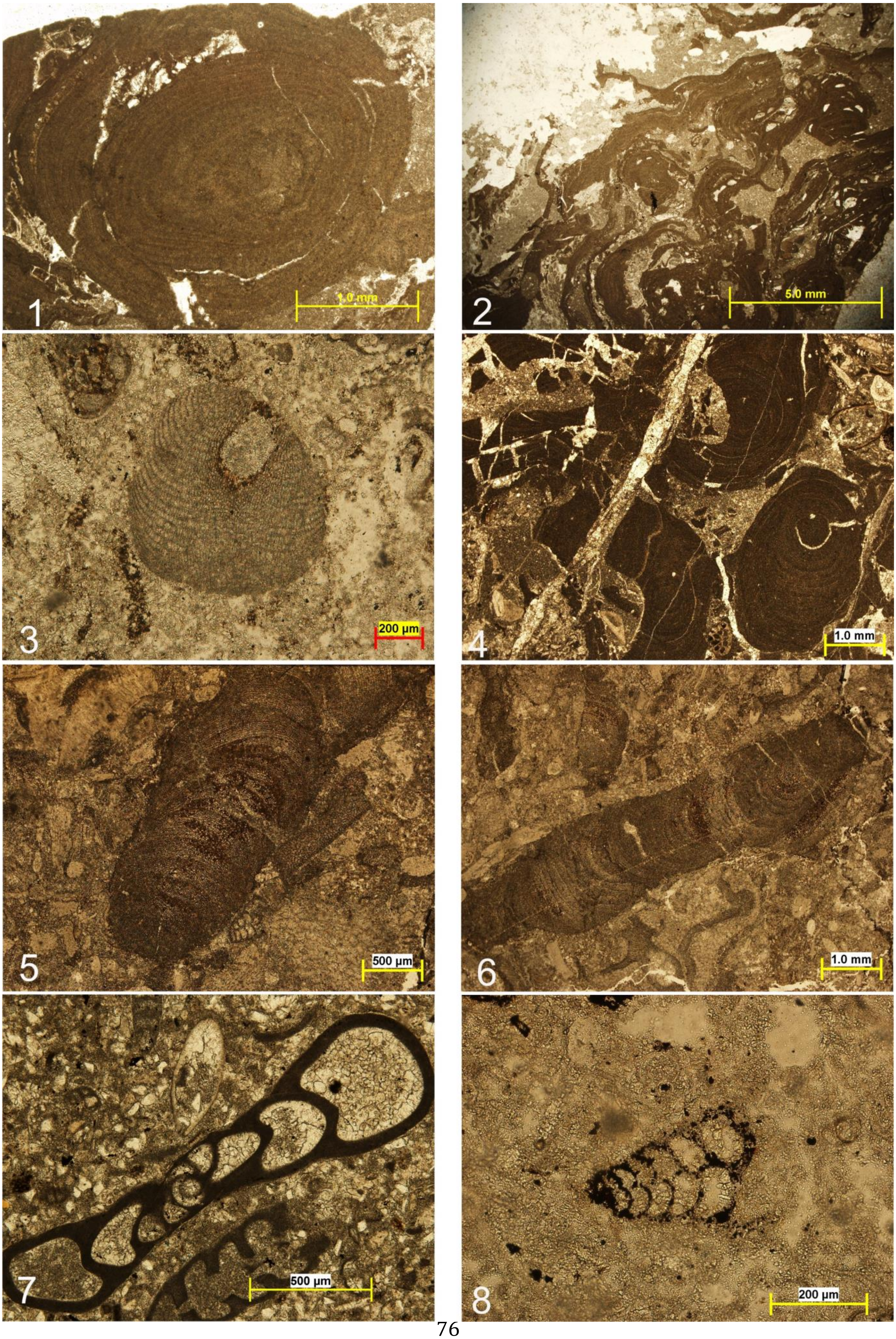
1
1.0 mm
2
5.0 mm
3
200 µm
4
1.0 mm
5
500 µm
6
1.0 mm
7
500 µm
8
200 µm

Plate 2

Selected Foraminifera of the Qom Formation from the Molkabad section

Fig. 1: *Lithotamnium* algae, sample no. 553.

Fig. 2: *Lithotamnium* algae, sample no. 553.

Fig. 3: Red algae, sample no.609.

Fig. 4: *Lithotamnium* algae, sample no. 563.

Fig. 5: Red algae, sample no.599.

Fig. 6: Red algae, sample no.612.

Fig. 7: *Spiroloculina* sp., sample no. 661.

Fig. 8: *Textularia* sp., sample no. 572.

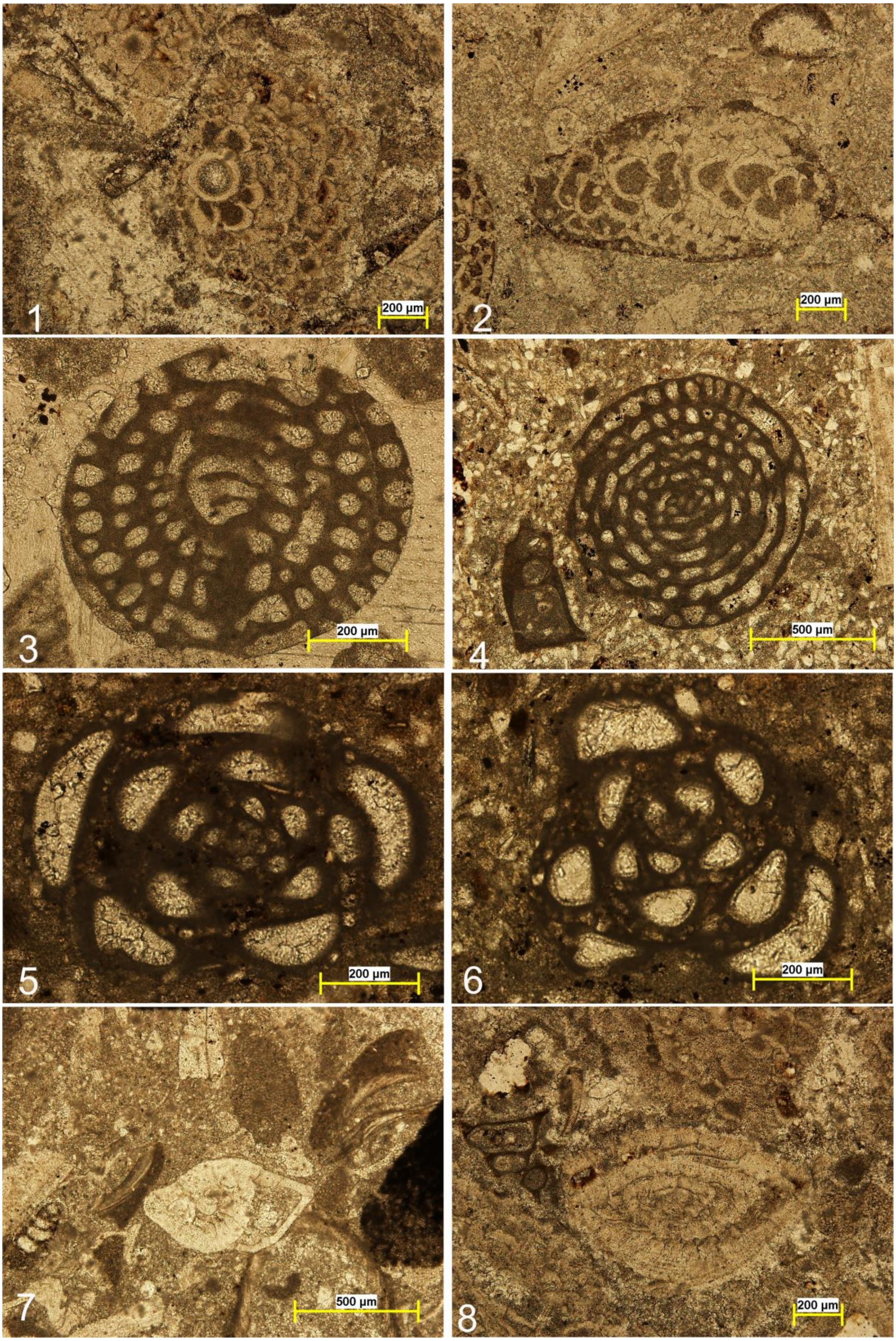

1
200 µm
2
200 µm
3
200 µm
4
500 µm
5
200 µm
6
200 µm
7
500 µm
8
200 µm

Plate 3

Selected Foraminifera of the Qom Formation from the Molkabad section:

Figs. 1: *Miogypsina* sp., sample no. 571.

Fig. 2: *Miogypsina* sp., sample no. 564.

Fig. 3: *Borelis melo curdica* Reichel, 1937; sample no. 573.

Fig. 4: *Borelis melo curdica* Reichel, 1937; sample no. 661.

Fig. 5: *Schlumbergerina* sp., sample no. 659.

Fig. 6: *Schlumbergerina* sp., sample no. 659.

Fig. 7: *Rotalia* sp., sample no. 563.

Fig. 8: *Amphistegina* sp., sample no. 571.

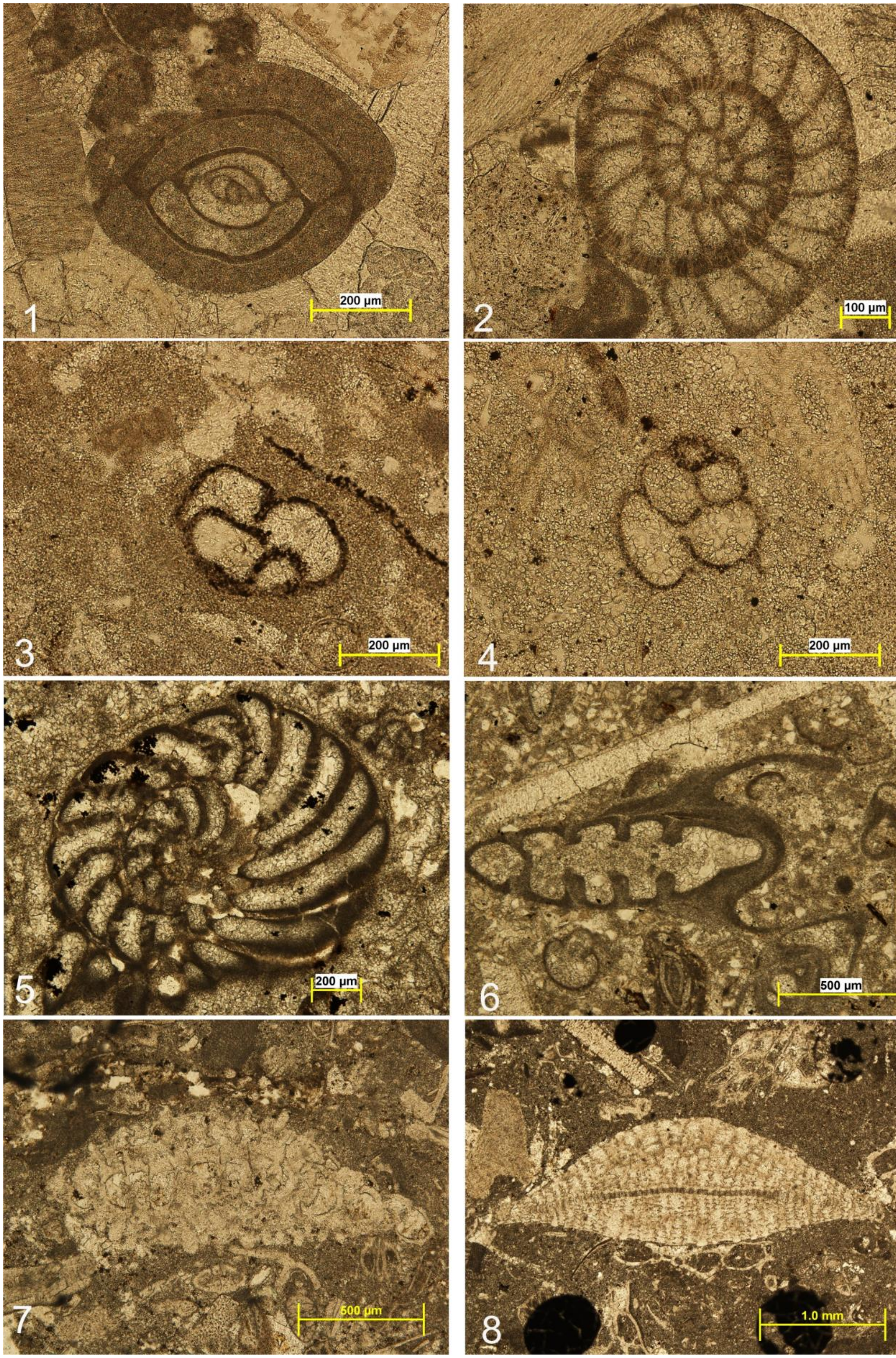

200 µm
1
100 µm
2
200 µm
3
200 µm
4
200 µm
5
500 µm
6
500 µm
7
1.0 mm
8

Plate 4:

Selected Foraminifera of the Qom Formation from the Molkabad section:

Fig. 1: *Pyrgo* sp., sample no. 573.

Fig. 2: *Elphidium* sp., sample no. 573.

Fig. 3: *Valvulina* sp., sample no. 575.

Fig. 4: *Valvulina* sp., sample no. 648.

Fig 5: *Dendritina rangi* d'Orbigny, 1826; sample no. 666.

Fig. 6: *Dendritina rangi* d'Orbigny, 1826; sample no. 661.

Fig. 7: *Miogypsina* sp., sample no. 554.

Fig. 8: *Nephrolepidina* sp., sample no. 445.

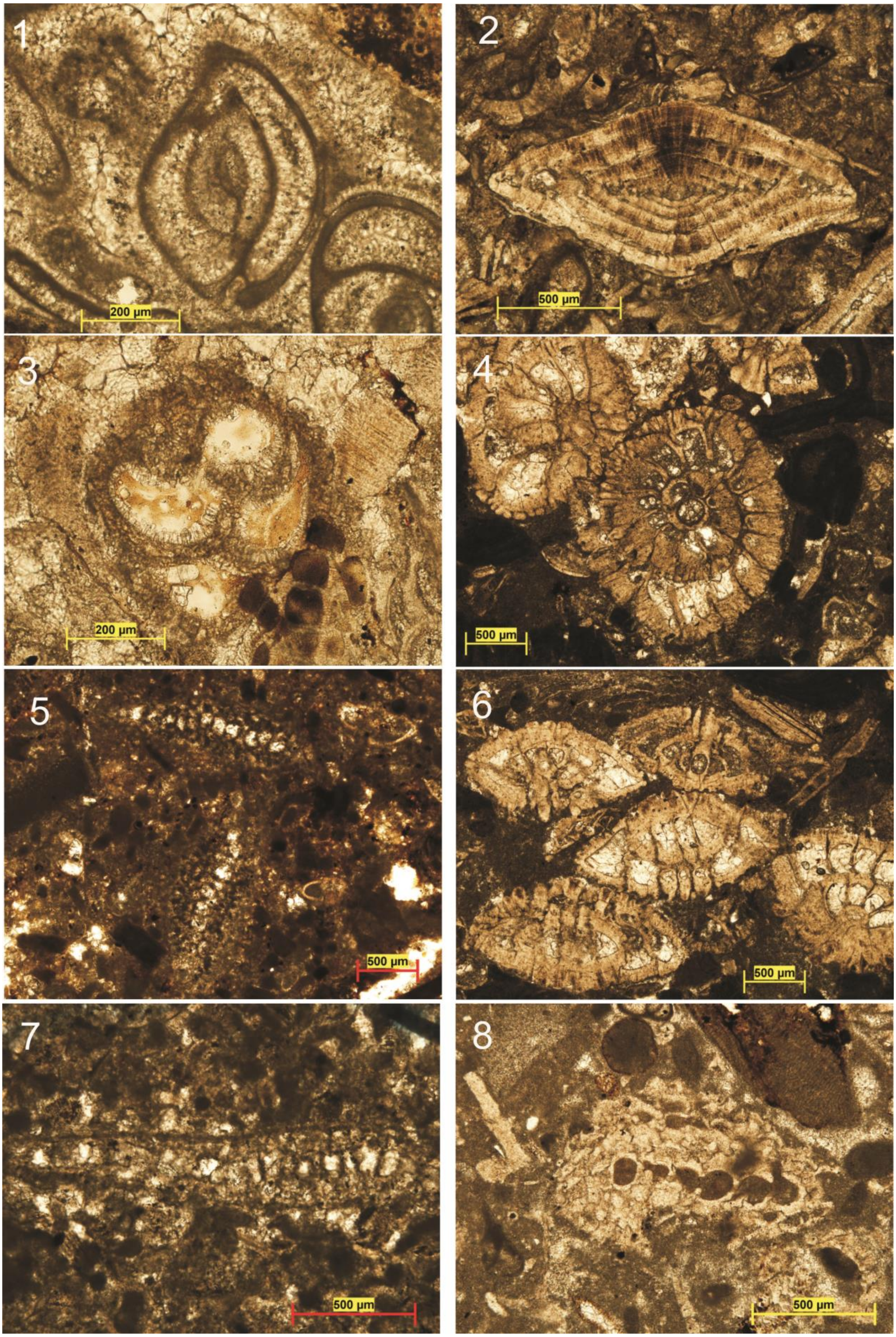
1
200 µm
2
500 µm
3
200 µm
4
500 µm
5
500 µm
6
500 µm
7
500 µm
8
500 µm

Plate 5:

Selected Foraminifera and other fossils of the Qom Formation from the Navab section:

Fig. 1: *Spiroloculina* sp., sample no. 352.

Fig. 2: *Tubocellaria* sp., sample no. 387.

Fig. 3: *Valvulina* sp., sample no. 365.

Fig. 4: *Rotalia viennoti* Greig, 1935; sample no. 373.

Fig. 5: *Miogypsina* sp., Sample no. 400.

Fig. 6: *Rotalia viennoti* Greig, 1935; Ssample no. 373.

Fig. 7: Red algae, sample no. 373.

Fig. 8: *Miogypsina* sp., sample no. 409.

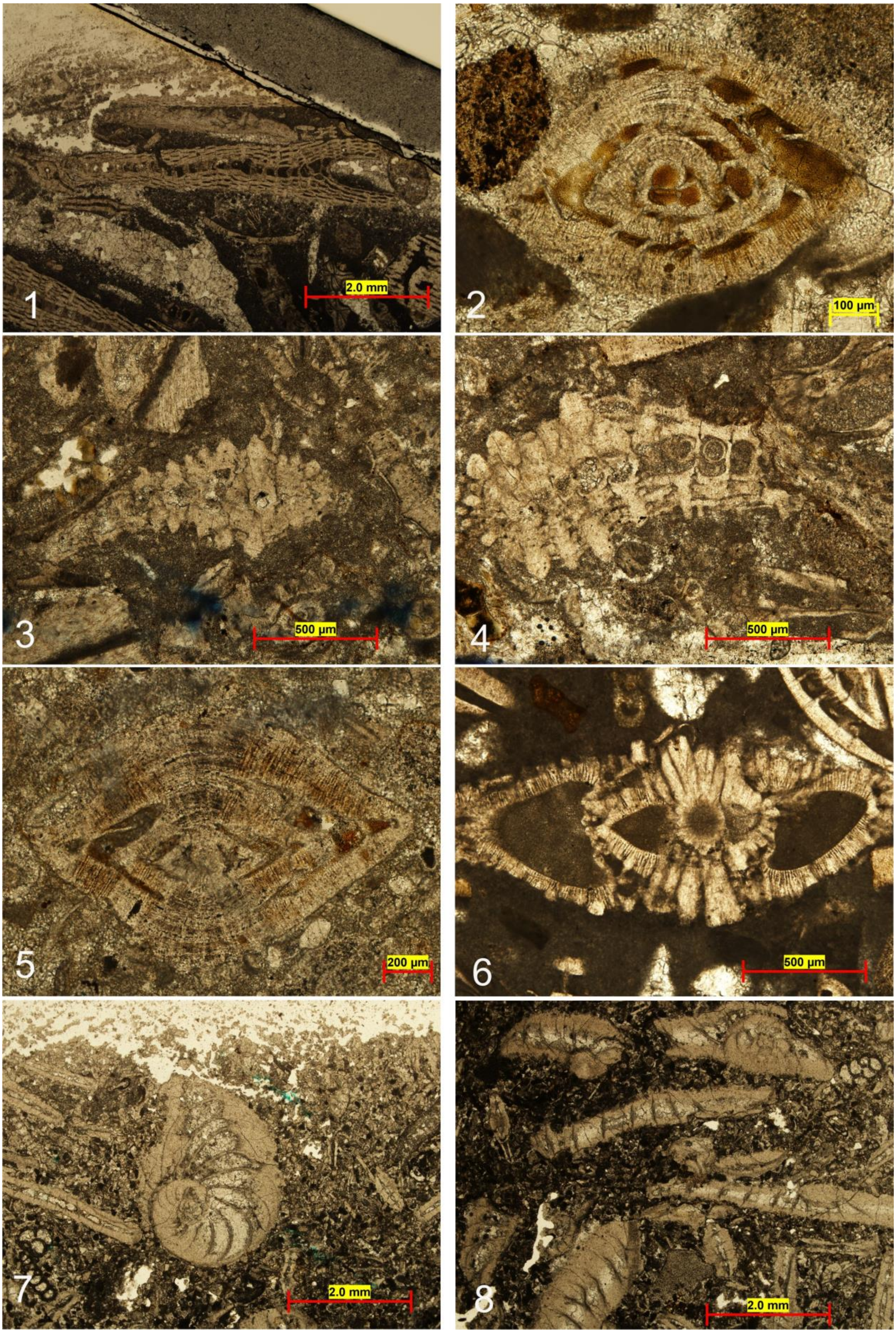
1
2.0 mm
2
100 µm
3
500 µm
4
500 µm
5
200 µm
6
500 µm
7
2.0 mm
8
2.0 mm

Plate 6:

Selected Foraminifera of the Qom Formation in Navab section:

Fig. 1: *Eulepidina* sp., sample no. 366.

Fig. 2: *Asterigerina* sp., sample no. 356.

Fig. 3: *Miogypsinoides* sp., sample no. 375.

Fig. 4: *Miogypsinoides* sp., sample no. 375.

Fig. 5: *Amphistegina* sp., sample no. 404.

Fig. 6: *Rotalia* sp., sample no. 366.

Fig. 7: *Operculina* sp., sample no. 408.

Fig. 8: *Operculina* sp., sample no. 408.

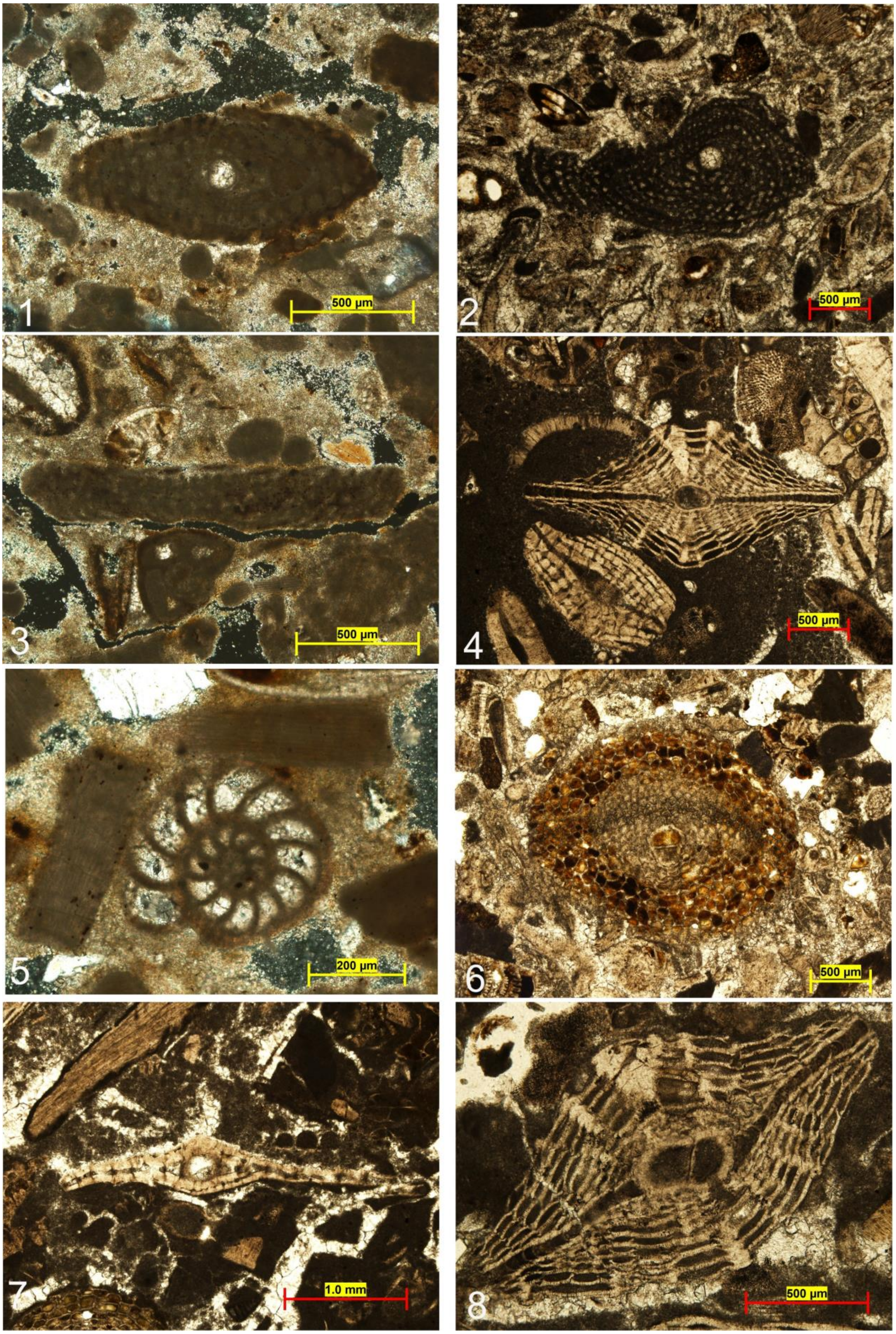
1
500 µm
2
500 µm
3
500 µm
4
500 µm
5
200 µm
6
500 µm
7
1.0 mm
8
500 µm

Plate 7:

Selected Foraminifera of the Qom Formation from the Navab section:

Fig. 1: *Archaias kirkukensis* Henson 1950; sample no. 399.

Fig. 2: *Archaias kirkukensis* Henson 1950; sample no. 386.

Fig. 3: *Archaias kirkukensis* Henson 1950; sample no. 388.

Fig. 4: *Eulepidina dilatata* Michelloti, 1861; sample no. 366.

Fig. 5: *Elphidium* sp., sample no. 388.

Fig. 6: *Nephrolepidina* sp., sample no. 356.

Fig. 7: *Heterostegina* sp., sample no. 371.

Fig. 8: *Nephrolepidina* sp., sample no. 366.

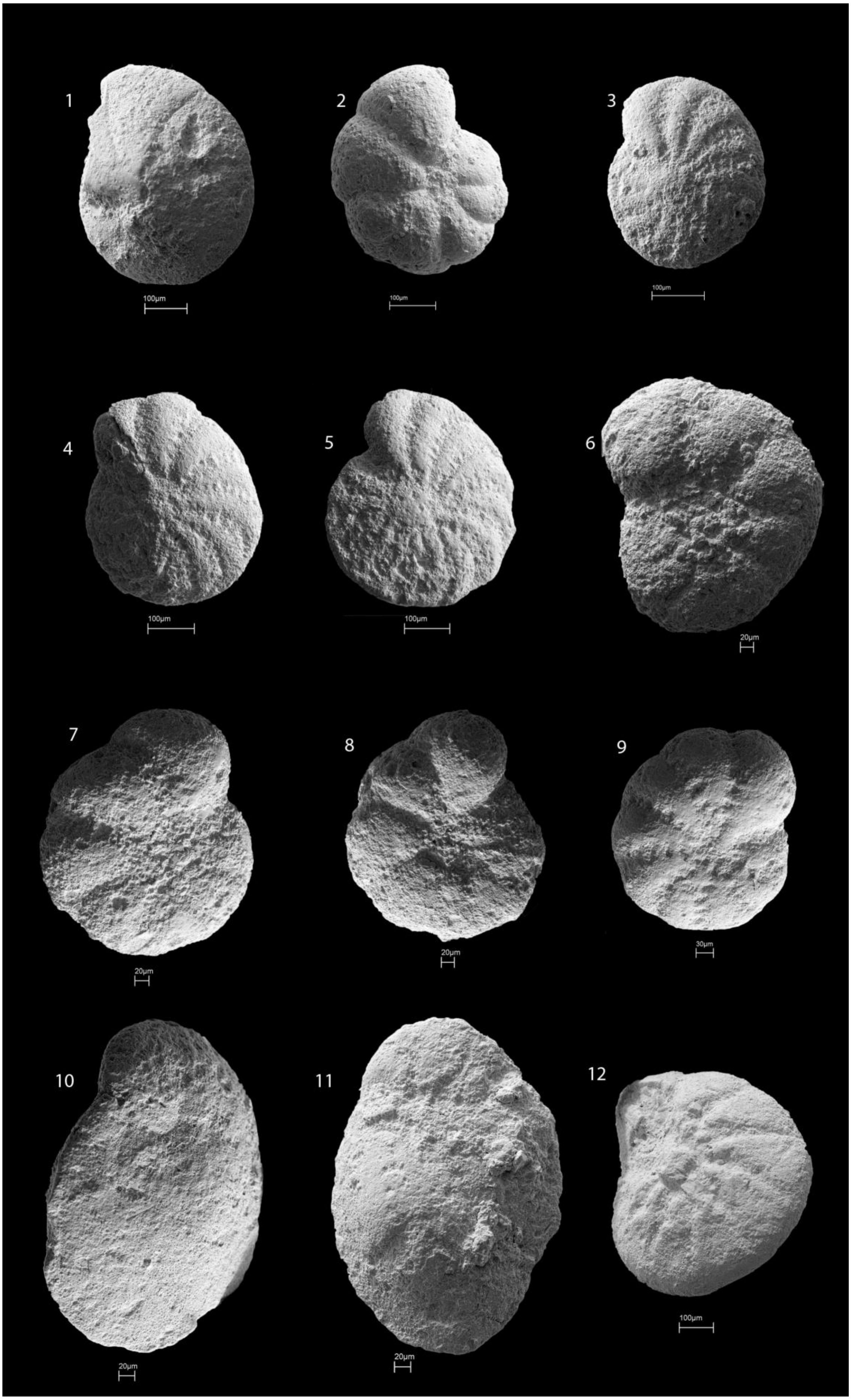
1
2
3
100µm
100µm
100µm
4
5
6
100µm
100µm
20µm
7
8
9
20µm
20µm
30µm
10
11
12
20µm
20µm
100µm

Plate 8

Small benthic foraminifera from the Molkabad section.

Figs. 1,2: *Heterolepa* sp.

Figs. 3,4,5: *Elphidum advenum* Cushman, 1922.

Fig. 6: *Elphidium granosum* d'Orbigny, 1846.

Figs. 7,8: Elphidium sp.

Fig. 9: *Elphidium hauerinum* d'Orbigny, 1846.

Figs. 10,11: Cancris sp.

Fig. 12: Ammonia *beccarii* Linné, 1758.

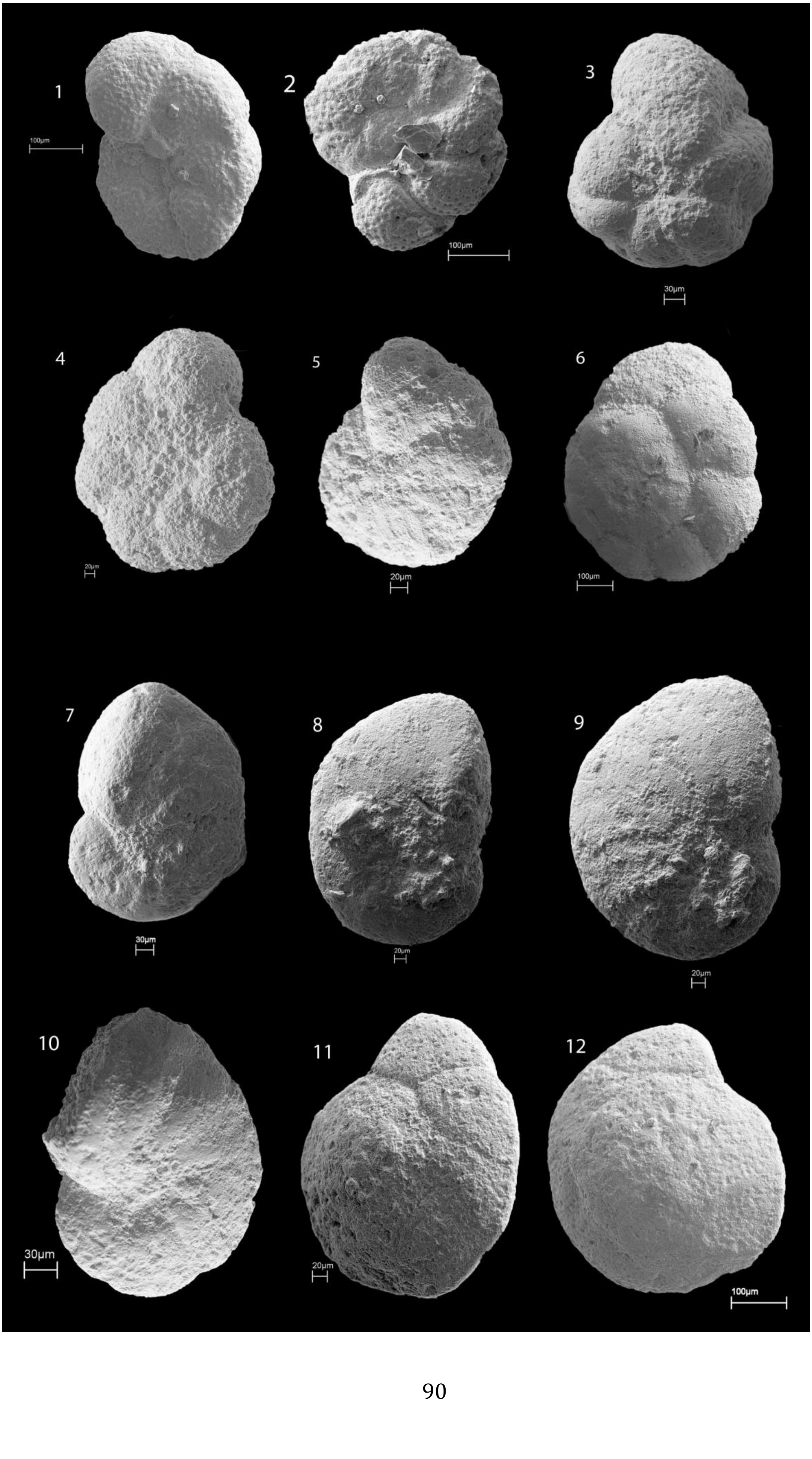
1
100µm
2
100µm
3
30µm
4
20µm
5
20µm
6
100µm
7
30µm
8
20µm
9
20µm
10
30µm
11
20µm
12
100µm

Plate 9

Small benthic foraminifera from the Molkabad section.

Figs. 1,2: Cibicides *lobatulus* Walker & Jacob, 1798.

Fig. 3: Cibicides *lobatulus* Walker & Jacob, 1798.

Figs. 4,5: Elphidium sp.

Fig. 6: Ammonia *beccari* Linné, 1758.

Figs. 7,8,9: Nonion *asterizans* Fichtel & Moll, 1798.

Fig. 10: Cancris sp.

Figs. 11,12: Heterolepa sp.,

REFERENCES

Abreu, V.S., Anderson, J.B., 1998; Glacial Eustasy during the Cenozoic: Sequence Stratigraphic Implications. AAPG Bulletin. v. 82, p.1385-1400.

Adams, T.D., Bourgeois, F., 1967; Asmari Formation Biostratigraphy. IOOC Report No.1074, Teheran (Unpubl.).

AGIP, 1982; Foraminiferi Padani. Atlante Iconografico E Distribuzione Stratigrafica, Milan, 52 pl., 134 p.

Aghanabati, A., 2000; Iran's geology, Geological Survey of Iran, Teheran

Aghanabati, A., 2004; Geology of Iran. Ministry of Industry and Mines, Geological Survey of Iran

Amirshahkarami, M., Vaziri Moghaddam, H., Taheri, A., 2007; Sedimentary facies and sequence stratigraphy of the Asmari Formation at Chaman-Bolbol, Zagros Basin, Iran. Journal of Asian Earth Science 29, 947-959.

Amirshahkarami, M., Taheri, A., 2010; Biostratigraphy characterization of the Rupelian-Burdigalian carbonates succession at the Chaman-Bolbol area in the Zagros Basin. Stratigraphy and Sedimentology Researches, Isfahan University, Iran 40, 119-136.

Amirshahkarami, M., 2013; Microfacies correlation analysis of the Oligocene-Miocene Asmari Formation, in the central part of the Rag-e-Safid anticlinal oil field, Zagros Basin, south-west Iran. Turkish Journal of Earth Science 22, 204-219.

Amirshahkarami, M., Karavan, M., 2014; Microfacies models and sequence stratigraphic architecture of the Oligocene–Miocene Qom Formation, South of Qom city, Iran. Geoscience Frontiers 6, 593-604.

Anjomshoa, A., Amirshahkarami, M., 2014; Biostratigraphy and paleoenvironmental model of the Late Oligocene depositions of the Tanbour section (SW Kerman, Central Iran). Sedimentary Facies 6, 130–149 (in Persian).

Barattolo, F., Bassi, D., Romero, R., 2007; Upper Eocene larger foraminiferal-coralline algal facies from the Klokova Mountain (south continental Greece). Facies 53, 361–375.

Bassi, D., Hottinger, L., Nebelsick, H., 2007; Larger foraminifera from the Upper Oligocene of the Venetian area, Northeast Italy. Palaeontology 50, 845–868.

Bassi, D., 2005; Larger foraminifera and coralline algal facies in an Upper Eocene storm-influenced, shallow-water carbonate platform (Colli Berici, north-eastern Italy). Palaeogeography, Palaeoclimotology, Palaeoecology 226, 17-35.

Beavington-Penny, S.J., Racey, A., 2004; Ecology of extant Nummulitids and other larger benthic forminifera, application in palaeoenvironmental analysis. Earth Science 67, 219-265.

Behforouzi, E., Safari, A., 2011; Biostratigraphy and paleoecology of the Qom Formation in Chenar area (northwestern Kashan), Iran. Revista Mexicana de Ciencias Geológicas 28, 555–565.

Bernard, J.M. Sen Gupta, B.K., 1999; Foraminifera of oxygen depleted environments. in Modern Foraminifera, edited by B.K. Sen Gupta, (Kluwer, London) pp. 201-216.

Bernaus, J. M., Josep, M., Arnaud-Vanneau, A. Caus, E., 2003; Carbonate platform sequence stratigraphy in a rapidly subsiding area; the late Barremian- early Aptian of the Organya Basin, Spanish Pyrenees. Sedimentary Geology 159, 177–201.

Betzler, C., Brachert, T.C., Braga, J.C. & Martín, J.M. 1997; Nearshore, temperate, carbonate depositional systems (lower Tortonian, Agua Amarga Basin, southern Spain): implications for carbonate sequence stratigraphy. Sedimentary Geology 113, 27–53.

Biolzi, M., Iaccarino, S.M., Turco, E., Rettori, R., 2005; Practical manual of Oligocene to Middle Miocene planktonic foraminfera. IV course, dalla Tipografia Pontefelcino-Perugia.

Boltovskoy, E. Wright, R., 1976; Recent Foraminifera. xvii + 515 pp., Junk, The Hague. Price Dutch Guilders 125.00.

ISBN 90 6193 030 8. - Volume 114 Issue 2 - J. W. M.

Bosellini, F.R., Perrin, C., 2008; Estimating Mediterranean Oligocene–Miocene sea-surface temperatures: an approach based on coral taxonomic richness. Palaeogeography, Palaeoclimatology, Palaeoecology 258,71–88.

Boudagher-Fadel, M.K., Lokier, S.W., 2005; Significant Miocene larger foraminifera from south central Java. Revue de Micropaléontologie 24, 291-309.

Brasier, M.D., 1975; The ecology and distribution of Recent foraminifera from the reefs and shoals around Barbuda, West Indies. Journal of Foraminiferal Research 5, 193–210.

Brandano, M., Corda, L., 2002; Nutrients, sea level and tectonics constraints for the facies architecture of a Miocene carbonate ramp in central Italy. Terra Nova 14, 257–262.

Brandano, M., Tomassetti, L., Bosellini, F.R., Mazzucchi, A., 2010; Depositional model and paleo-depth reconstruction of a coral-rich, mixed siliciclastic-carbonate system: the Burdigalian of Capo Testa (northern Sardinia, Italy). Facies 56, 434-444.

Burchette, T.P., Wright, V.P., 1992; Carbonate ramp depositional systems. Sedimentary Geology 79, 3-57.

Buxton, M.W.N., Pedley H.M., 1989; Short paper: a standardised model for Tethyan Tertiary carbonates ramps. Journal of the Geological Society 146, 746–748.

Buzas, M.A., Gibson., T.G., 1969; Species Diversity: Benthonic Foraminifera in Western North Atlantic. Science 163(3862), 72-75.

Cahuzac, B. Poignant, A., 1997; Essai de biozonation de l'Oligo–Miocene dans les basins européens à l'aide des grands foraminifères néretiques. Bulletin de la Société Géologique de France 168, 155–169.

Corda, L., Brandano, M., 2003; Aphotic zone carbonate production on a Miocene ramp, Central Apennines, Italy. Sedimentary Geology 161, 55–70.

Culver, S.J., Woo, H.J., Oertel, G.F., Buzas, M.A., 1996; Foraminifera of coastal depositional environments, Virginia, U.S.A.: distribution and taphonomy. Palaios 11, 459–456.

Daneshian, J., Ramezani Dana, L., 2007; Early Miocene benthic foraminifera and biostratigraphy of the Qom Formation, Deh Namak, Central Iran. Journal of Asian Earth Sciences 29, 844–858.

Dill, M.A., Seyrafian A., Vaziri-Moghaddam, H., 2010; The Asmari Formation, north of the Gachsaran (Dill anticline), southwest Iran: facies analysis, depositional environments and sequence stratigraphy. Carbonates Evaporites 25, 145–160.

Dodd, J.R, Stanton, R.J., 1990; Paleoecology: concepts and applications. Wiley, New York,528 pp.

Drinia, H., Antonarakou, A., Tsaparas, N., Dermitzakis, M.D., 2007; Foraminiferal stratigraphy and palaeoecological implications in turbidite-like deposits from the Early Tortonian (Late Miocene) of Greece. Journal of Micropaleontology 26, 145–158.

Dunham, R.J., 1962; Classification of carbonate rocks according to their depositional texture. AAPG Memoir 1, 108–121.

Faiz-Nia, S., Mosafi, H.R., 1998; Microfacies and depositional environment of the Qom Formation in Semnan region. Geoscience 27–28 (in Persian).

Flügel, E., 1982; Microfacies analysis of limestone. Springer, Berlin Heidelberg New York, 633 pp.

Flügel, E., 2004; Microfacies analysis of limestones, analysis interpretation and application. Berlin: Springer. 976 pp.

Furrer, M.A., Soder, P.A., 1955; The Oligo-Miocene marine formation in the Qom region (Central Iran). Proceedings of the 4th World Petroleum Congress, Rome, 267–277

Geological Survey of Iran, 1995; Geological maps of Iran no. G6 (Kuh-e Gugerd), Scale 1:1250000 .

Geological Survey of Iran, Geological maps of Iran (Natanz), series 6457, Scale 1:1000000.

Geel, T., 2000; Recognition of stratigraphic sequence in carbonate platform and slope: empirical models based on microfacies analysis of Paleogene deposits in southeastern Spain. Palaeogeography, Palaeoclimatology, Palaeoecology 155, 211–238.

Gosling, E., 2015; Marine Bivalve Molluscs. 536 p.

Hammer, Ø., Harper, D.A.T., Ryan, P. D., 2001; PAST: Paleontological Statistics Software Package for Education and Data Analysis. Palaeontologia Electronica 4, 9 p.

Hardenbol, J., Thierry, J., Farley, M.B., Jacquin, T., de Graciansky, P.C., Vail, P.R., 1998; Mesozoic and Cenozoic sequence chronostratigraphic framework of European basins. in: Graciansky, P.C. de, Hardenbol, J., Jacquin, T., Vail, P.R., eds., Mesozoic and Cenozoic sequence stratigraphy of European basins. Society for Sedimentary Geology (SEPM) Special Publication 60, Charts 1-8, 3-13.

Haq, B.U., Hardenbol, J., Vail, P., 1987; Chronology of fluctuating sea levels since the Triassic. Science 235, 1156-1167.

Halfar, J., Mutti, M., 2005; Global dominance of coralline red-algal facies: A response to Miocene oceanographic events. Geology 33, 481-484.

Hallock P., 1985; why are larger foraminifera large? Paleobiology 11, 195–208.

Hallock P., Glenn E.C., 1986; Larger foraminifera: a tool for paleoenvironmental analysis of Cenozoic carbonate depositional facies. Palaios 1, 44–64.

Hallock, P., Schlager, W., 1986; Nutrient excess and the demise of coral reefs and carbonate platforms. Palaios 1, 389–398.

Heydari, E., Hassanzadeh, J., Wade, W.J., Ghazi, A.M., 2003; Permian–Triassic boundary interval in the Abadeh section of Iran with implications for mass extinction: Part 1–Sedimentology. Paleogeography, Paleoclimatology, Paleoecology 193, 405–423.

Holcová, K., Zágoršek, K. 2008; Bryozoa, foraminifera and calcareous nannoplankton as environmental proxies of the “bryozoan event” in the Middle Miocene of the Central Paratethys (Czech Republic). Palaeogeography, Palaeoclimatology, Palaeoecology 267, 216–234.

Hohenegger, J., 1996; Remarks on the distribution of larger foraminifera (Protozoa) from Palau (western Carolines). in: Aoyama, T. (Ed.), The Progress Report of the 1995 Survey of the Research Project, Man and the Environment in Micronesia, vol. 32. Kagoshima University Research Center for the Pacific Islands, Occasional Papers, Kagoshima, Japan, pp. 19-45.

Hohenegger, J., Yordanova, E., Tatzreiter, Y., 1999; Habitats of larger foraminifera on the upper reef slope of Sesko Island, Okinawa. Marine Micropaleontology 36, 109-168.

Hottinger, L., 1983; Processes determining the distribution of larger foraminifera in space and time. Utrecht Micropaleontology Bulletin 30, 239-253.

Hottinger, L., 1997; Shallow benthic foraminiferal assemblages as signals for depth of their deposition and their limitations. Bulletin de la Société Géologique de France 168, 491-505.

Karavan, M., Mahboubi, A., Vaziri-Moghaddam, H., Moussavi-Harami, R., 2015; Sedimentary facies analysis and sequence stratigraphy of Qom Formation deposits in NE Delijan-NW Central Iran. Geosciences Journal 24 (94), 237-248 (in Persian).

Khaksar, K., Maghfouri Moghadam, I., 2007; Paleontological study of the echinoderms in the Qom Formation (Central Iran). Earth Science Research Journal 11, 57–79.

Lee, J.J., Mcenery, M.E., Kahn, E.G., 1979; Symbiosis and the evolution of larger Foraminifera. Micropaleontology 25,118–140.

Leutenegger, S., 1984; Symbiosis in benthic foraminifera, specificity and host adaptations. Journal of Foraminiferal Research 14, 16–35.

Loeblich, A.R., Tappan, J.H. 1987; Foraminiferal Genera and their Classification. Van Nostrand Reinhold Co., NewYork, NY, 2 volumes, 869 p., 847 pls.

Loeblich, A.R., Tappan, J.H., 1988. Foraminiferal genera and their classification. Van Nostrand Reinhold Company, New York.

Loftus, W.K., 1855; On the geology of the Turko-Persian Frontier and of the districts adjoining, The Quarterly Journal of the Geological Society of London, 11, 247–34.

Lutze, G., 1965; Zur Foraminiferen-Fauna der Ostsee. Meyniana 15 75–147.

Lutze, G., 1974; Benthische Foraminiferen in Oberflächen-Sedimenten des Persischen Golfes. Teil 1: Arten. Meteor Forschungs Ergebnisse, Reihe C No.17, 1-66.

Magurran, A.E., 1988; Ecological Diversity and its Measurement, Princeton: Princeton University Press, 215 p.

Mandic, O., Harzhauser, M., 2003; Molluscs from the Badenian (Middle Miocene) of the Gaindorf Formation (Alpine Molasse Basin, NE Austria), Taxonomy, Paleoecology and Biostratigraphy. Annalen des Naturhistorischen Museums in Wien 104 A, 85–127.

Meulenkamp, J., Sissingh, W., 2003; Tertiary paleogeography and tectonostratigraphic evolution of the Northern and Southern Peri-Tethys platforms and the intermediate domains of the African Eurasian convergent plate boundary zone. Paleogeography, Paleoclimatology, Paleoecology 196, 209-228.

Miller, K.G., Kominz, M.A., Browning, J.V., Wright, J.D., Mountain, G.S., Katz, M.E., Sugarman, P.J., Cramer, B.S., Christie-Blick, N., Pekar, S.F., 2005; The Phanerozoic record of global sea-level change. Science, 310, 1293–1298.

Mohammadi, E., Safari, A., Vaziri-Moghaddam, H., Vaziri, M., Ghaedi, M. 2011; Microfacies analysis and paleoenviornmental interpretation of the Qom Formation, South of the Kashan, Central Iran. Carbonates Evaporites, 26, 255-271.

Mohammadi, E., Hasanzadeh-Dastgerdi, M., Ghaedi, M., Dehghan, R., Safari, A., Vaziri-Moghaddam, H., Baizidi, C., Vaziri, M., Sfidari, E., 2013; The Tethyan Seaway Iranian Plate Oligo-Miocene deposits (the Qom Formation): distribution of Rupelian (Early Oligocene) and evaporate deposits as evidences for timing and trending of opening and closure of the Tethyan Seaway. Carbonates Evaporites 28, 321–345.

Momenzadeh, A., 2003; Stratigraphy of the Qom Formation in southeast of Kashan. Unpublished MSc Dissertation, Isfahan University (in Persian).

Murray, J.W., 1991; Ecology and Paleoecology of Benthic Foraminifera. London, Longman Scientific & Technical, 397 p.

Murray, J.W., Alve, E., 1999; Natural dissolution of modern shallow water benthic foraminifera: taphonomic effects on the palaeoecological record. Palaeogeography, Palaeoclimatology, Palaeoecology 146, 195–209.

Murray, J.W., 2006; Ecology and Applications of Benthic Foraminifera. Cambridge, Cambridge University Press, 422 p.

Naeije, M.R., 2000; Depositional environment of mixed carbonate–epiclastic deposits of the Qom formation in east of Tehran. in: Proceedings of the fourth symposium of the Geological Society of Iran, Tabriz University, Tabriz, Iran, p 652 (in Persian).

Naimi, M., Amirshahkarami, M., 2011; Revision in the biozonation of the Qom Formation based on the foraminifera. Abhar, Iran, 5th National Geological Conference of Payame Noor University, Abhar, pp. 658–662 (in Persian).

Nebelsick, J.H., Stingl, V., Rasser, M., 2001; Autochthonous Facies and Allochthonous Debris Flows Compared: Early Oligocene Carbonate Facies Patterns of the Lower Inn Valley (Tyrol, Austria). Facies 44, 31-46.

Okhravi, R., Amini, A., 1998; An example of mixed carbonate– pyroclastic sedimentation (Miocene, Central Basin, Iran). Sedimentary Geology 118, 37–57.

Pedley, M., 1996; Miocene reef facies of Pelagian region (Central Mediterranean region). in: Franseen E.K., Esteben M., Ward W.C., Rouchy J.M. (eds) Models for carbonate stratigraphy from Miocene Reef complexes of Mediterranean Regions. S.E.P.M. Concepts in Sedimentology and Paleontology 5, 247–259.

Pedley, M., 1998; A review of sediment distributions and processes in Oligo-Miocene ramps of southern Italy and Malta (Mediterranean Divide). Geological Society, London, Special Publications 149, 163-179.

Pippèrr, M., Reichenbacher, B., 2010; Foraminifera from the borehole Altdorf (SE Germany): proxies for Ottnangian (early Miocene) palaeoenvironments of the Central Paratethys. Palaeogeography, Palaeoclimatology, Palaeoecology 289, 62-80.

Pippèrr, M., 2011; Characterisation of Ottnangian palaeoenvironments in the North Alpine Foreland Basin using benthic foraminifera - a review on the Upper Marine Molasse of Southern Germany. Marine Micropaleontology 79, 80-99.

Pomar, L., Mateu-Vicens, G., Morsilli, M., Brandano, M., 2014; Carbonate ramp evolution during the Late Oligocene (Chattian), Salento Peninsula, Southern Italy. Palaeogeography, Palaeoclimatology, Palaeoecology 404, 109-132.

Pomar, L., 2001a; Types of carbonate platforms: a genetic approach. Basin Research 13, 313–334.

Pomar, L., 2001b; Ecological control of sedimentary accommodation: evolution from carbonate ramp to rimmed shelf, Upper Miocene. Balearic Islands". Palaeogeography, Palaeoclimatology, Palaeoecology 175.1-4, 249-272.

Rahaghi, A., 1973; Etude de quelques grands foraminiferes de la Formation de Qum (Iran Central). Revue de Micropaléontologie 16, 23–38.

Rahaghi, A., 1976; Contribution a l'étude de quelques grands foramifères de l'Iran. Société National Iranienne des Pétroles Laboratoire de Micropaléontologie 6, 1–79.

Rahaghi, A., 1980; Tertiary faunal assemblage of Qum-Kashan, Sabzewar and Jahrum area. National Iranian Oil Company, v. 8, 64 p.

Rahimzadeh, F., 1994; Iran`s Geology (Oligocene- Miocene- Pliocene), Geological Survey of Iran, Report No. 12, Teheran.

Reiss, Z., Hottinger, L., 1984; The Gulf of Aqaba, Ecological Micropaleontology. Springer, Berlin, p.

354.

Reuter, M., Piller, W., Harzhauser, M., Mandic, O., Berning, B., Rögl, F., Kroh, A., Aubry, M., Wielandt-Schuster, U., Hamedani, A., 2009; The Oligocene-Miocene Qom Formation (Iran): evidence for an early Burdigalian restriction of the Tethyan Seaway and closure of its Iranian gateways. International Journal of Earth Sciences (Geologische Rundschau) 98(3), 627-650.

Reuter, M., Piller, W.E., Brandano, M., Harzhauser, M., 2013; Correlating Mediterranean Shallow Water Deposits with Global Oligocene–Miocene Stratigraphy and Oceanic Events. Global and Planetary Change 111, 226-236.

Riegl, B., Piller W.E., 2000; Biostromal coral facies: A Miocene example from the Leitha Limestone (Austria) and its actualistic interpretation. Palaios 15, 399–413.

Rögl, F., 1998; Oligocene–Miocene palaeogeography and stratigraphy of the Circum Mediterranean region. in: Whybrow, P.J., Hill, A.: Fossil vertebrates of Arabia. 485–500. New Haven Yale University Press.

Romero, J., Caus, E., Rossel, J., 2002; A model for the paleoenvironmental distribution of larger foraminifera based on late Middle Eocene deposits on the margin of the south Pyrenean basin (NE Spain). Palaeogeography, Palaeoclimatology, Palaeoecology 179, 43–56.

Roozpeykar, A., Maghfouri Moghaddam, I., 2016; Benthic Foraminifera as Biostratigraphical and Paleoecological Indicators: An Example from Oligo-Miocene Deposits. in: The SW of Zagros Basin, Iran. Geoscience Frontiers 7, 125-140.

Sabouhi, M., Sheykh, M., Darvish, Z., Naghavi azad, M., 2010; Facies Analysis and Depositional environment of the Oligocene-Miocene Qom Formation in the Central Iran (Semnan area). Vol. 12, EGU, Wien.

Sadeghi, R., Vaziri-Moghaddam, H., Taheri, A., 2009; Biostratigraphy and paleoecology of the Oligo-Miocene succession in Fars and Khuzestan areas (Zagros Basin, SW Iran). Historical Biology 21, 17-31.

Schuster, F., Wielandt, U., 1999; Oligocene and early Miocene coral faunas from Iran: paleoecology and paleobiogeography. International Journal of Earth Sciences (Geologische Rundschau) 88, 571–581.

Sedighi, M., 2008; Biostratigraphy and sedimentary environment of the C member of the Qom Formation in south and southeast of Qom. Unpublished MSc Dissertation, Isfahan University (in Persian).

Seibold, E.,Vollbrecht, K., 1969; Die Bodengestalt des Persischen Golfs. "Meteor" Forschungsergebnisse, Reihe C, 2, 29-56.

Sen-Gupta, B.K., Machain-Castillo, M.L., 1993; Benthic foraminifera in oxygen-poor habitats. Marine Micropaleontology 20, 183–201.

Seyrafian, A., Torabi, H., 2005; Petrofacies and sequence stratigraphy of the Qom Formation (Late Oligocene-Early Miocene?), North of Nain. Southern trend of the Central Iranian Basin. Carbonates Evaporites 20, 82–90.

Seyrafian, A., Torabi, H., Shojaei, M., 2006; Microfacies and depositional environment of the Qom Formation in Natanz region (Charkha mountain). Basic Science Journal of Isfahan University 23:135–148 (in Persian).

Sinclair, H.D., Sayer, Z.R., Tucker, M.E., 1998. Carbonate sedimentation during early foreland basin subsidence: the Eocene succession of the French Alps. in: Wright, V.P., Burchette, T.P. (Eds.), Carbonate Ramps. Geological Society Special Publications 149, 205–227.

Steininger, F.F., Wessely, G., 2000; From the Tethyan Ocean to the Paratethys Sea: Oligocene to Neogene Stratigraphy, Paleogeography and Paleobiogeography of the circum-Mediterranean region and the Oligocene to Neogene basin evolution in Austria. – Mitteilungen der Österreichischen Geologischen Gesellschaft 92, 95-116.

Stöcklin, J., Setudehnia, A., 1991; Stratigraphic Lexicon of Iran. Geological Survey of Iran Publication, 3rd edn, vol 18, p 376.

Tsaparas, N., Marcopoulou-Diacantoni, A., 2005; Tortonian scleractinian corals from the island of Gavdos (South Greece). Revue de Paleobiologie 24, 629–637.

Van Der Zwaan, G.J., Jorissen F.J., De Stigter, H.C., 1990; The depth dependency of planktonic/benthic foraminiferal ratios: Constrains and applications. Marine Geology 95, 1–16.

Vaziri-Moghaddam, H., Torabi, H., 2004; Biofacies and sequence stratigraphy of the Oligocene succession, Central basin, Iran. Neues Jahrbuch für Geologie und Paläontologie 6, 321–344.

Vaziri-Moghaddam, H., Kimiagari, M. Taheri, A., 2006; Depositional environment and sequence stratigraphy of the Oligocene-Miocene Asmari Formation in SW Iran. Facies 52, 41-51.

Vaziri-Moghaddam, H., Seyrafian, A., Taheri, A., Motiei, H., 2010; Oligocene-Miocene ramp system (Asmari Formation) in the NW of the Zagros basin, Iran: microfacies, paleoenvironmental and depositional sequence. Revista Mexicana de Ciencias Geológicas 27, 56-71.

Veron, J.E.N., 1995; Corals in space and time. University of New South Wales Press, Sydney, 321 p.

Vennin, E., Rouchy, J. -M., Chaix, C., Valleron, M.M.B., Caruso, A., Rommevau, V., 2004; Paleoecological constraints on reef-coral morphologies in the Tortonian–early Messinian of the Lorca Basin, SE Spain. Palaeogeography, Palaeoclimatology, Palaeoecology 213, 163–185.

Vicens, M., Hallock, P., Brandano, M., 2008; A depositional model and paleoecological reconstruction of the Lower Tortonian distally steepened ramp of Menorca (Balearic Islands, Spain). Palaios 23, 465–481.

Wilson, B., 2003; Foraminifera and Paleodepths in a section of the Early to Middle Miocene Brasso Formation, Central Trinidad. Caribbean Journal of Science 39, 209–214.

Wilson, J.L., 1975; Carbonate facies in geological history. Springer, Heidelberg, p. 471.

Wood, R., 1993; Nutrients, predation and the history of reef building. Palaios 8, 526–543.

Wynd, J.G. , 1965; Biofacies of the Iranian Oil Consortium Agreement Area. IOOC Report No.1082, Teheran.

Yazdi, M., Parvanenejad Shirazi, M., Rahiminejad, A.H., Motavalipoor, R., 2012; Paleobathymetry and paleoecology of colonial corals from the Oligocene-early Miocene (?) Qom Formation (Dizlu area, central Iran). Carbonates and Evaporates 6, 395–405.

Yazdani, 2014; Biostratigraphy and Facies Distribution of The Asmari Formation in Aghajari Well # 66, Zagros Basin, SW Iran. International Research Journal of Geology and Mining 4(4), 101-115.

Zabihi Zoeram Z., Vahidinia, M., Asadolah, M., Amir Bakhtiari, H., 2013; Facies Analysis and Sequence Stratigraphy of the Asmari Formation in the Northern Area of Dezful Embayment, South-West Iran. Studia Universitatis Babes-Bolyai, Geologia 58.1, 45-56.

Zachos, J.C., Pagani, M., Sloan, L., Thomas, E., Billups, K., 2001; Trends, Rhythms, and Aberrations in Global Climate 65 Ma to Present. Science 292(5517), 686-693.

Zachos, J.C., Shackleton, N.J., Revenaugh, J.S., Pälike, H., Flower, B.P., 2001b; Climate response to orbital forcing across the Oligocene–Miocene boundary. Science 292 (5515), 274–278.

Zachos, J.C., Dickens, G.R., Zeebe, R.E., 2008; An early Cenozoic perspective on greenhouse warming and carbon cycle dynamics. Nature 451, 279-283.